SU-SEL-66-124

A Correlation Study of the Diurnal Variation of Upper Atmospheric Phenomena in the Southern Auroral Zone

by

H. M. Morozumi and R. A. Helliwell

December 1966

Scientific Report No. 2

Prepared under
National Science Foundation
Office of Antarctic Programs
Grants NSF G23817, GA-56, and GA-144

RADIOSCIENCE LABORATORY

STANFORD ELECTRONICS LABORATORIES

STANFORD UNIVERSITY · STANFORD, CALIFORNIA

SEL-66-124

A CORRELATION STUDY OF THE DIURNAL VARIATION OF UPPER ATMOSPHERIC GEOPHYSICAL PHENOMENA IN THE SOUTHERN AURORAL ZONE

by

H. M. Morozumi and R. A. Helliwell

December 1966

Scientific Report No. 2

Prepared under

National Science Foundation
Office of Antarctic Programs
Grants NSF G23817, GA-56, and GA-144

Radioscience Laboratory
Stanford Electronics Laboratories
Stanford University Stanford, California

ABSTRACT

As a part of a high-latitude study of vlf emissions, the temporal relationships among eight upper atmosphere phenomena were investigated. The following quantities were recorded at Byrd Station during the austral winter and spring of 1963: 1) vlf noise (1-25 kc broadband); 2) aurora (5577A and white light); 3) ionospheric absorption (30 Mc/s riometer); 4) vlf noise (1 kc/s narrowband); 5) elf (2-30 cps); 6) ulf (0.001-5 cps); 7) variations in the earth's magnetic field (standard magnetometer); and 8) ionospheric phenomena (C-3 ionosonde).

The correlation charts exhibited a clear relationship with planetary magnetic activity. On quiet days, few prominent events were detected. On days of moderate disturbance ($10 < \Sigma K_p < 30$), two well defined peaks of activity appeared, one near magnetic midnight and the other near magnetic noon. On disturbed days, prominent events were observed, but they did not conform to the semidiurnal pattern of the moderately disturbed day.

The night peak on the moderately disturbed day consists of "events" of duration varying from minutes to several hours. These events usually exhibit three distinct phases, which we call N-1, N-2, and N-3. The N-1 phase precedes the breakup of the aurora, and may be called the "hiss phase," because vlf hiss appears to be an outstanding feature of the records at this time. The N-2 phase may be considered to be the breakup phase of the aurora. Phase N-3 is the post breakup phase, during which vlf chorus and ionospheric absorption are often observed.

Although the night event usually shows some element of all three phases, in many cases one or two of the phases predominate. There appears to be a correlation between the intensity and duration of a phase and the time of occurrence. Early in the evening, the N-1 phase tends to be relatively long, and dominates the other phases. In mid-evening, N-1, N-2, and N-3 frequently appear, each with good definition. In the late evening, there is a tendency for N-3 to predominate.

The day regime appears to exhibit important similarities to the sequence of night events. The most obvious similarity is to the N-3 phase. However, a hiss burst, an N-1 type phenomenon, is occasionally observed at the beginning of a D event. Ulf-associated pulsating aurora,

reminiscent of N-2, is also recorded on occasion. The main phase of the D event, broadly similar to N-3, lasts about five hours.

The temporal variations involving N-1 hiss and N-3 chorus were found to have a spatial counterpart in the transition between chorus and hiss at the 40-kev trapping boundary observed by the Injun III experimenters.

CONTENTS

CONTENTS (Cont)

TABLES

ILLUSTRATIONS

ILLUSTRATIONS (Cont)

ACKNOWLEDGMENTS

We wish to thank D. L. Carpenter for assisting in the preparation of this report, and call attention to the prominent role played by J. P. Katsufrakis in organizing the field operation at Byrd.

Comments on the manuscript by J. E. Lokken and J. A. Shand of the Pacific Naval Laboratory, Victoria, B.C., are gratefully acknowledged.

Acknowledgments are also due to C. S. Wright of the Pacific Naval Laboratory for permission to record the elf and ulf data and to the Institute for Telecommunication Sciences and Aeronomy of ESSA for making the output of their riometer available. C-3 data were provided by the ITSA World Data Center and magnetic data were made available by the U.S. Coast and Geodetic Survey of ESSA. The auroral photometer output was provided by Mr. J. H. Kinsey of the Arctic Institute of North America.

The logistic support by U.S. Navy Task Force 43 is gratefully acknowledged.

This research was supported by the Office of Antarctic Research Programs of the National Science Foundation under Grants NSF G23817, GA-56, and GA-144.

I. INTRODUCTION

This is a report on a correlation study of high-latitude geophysical phenomena made in 1963 at Byrd Station in the Antarctic. The study was based on the use of eight-channel continuous correlation records, supplemented by wideband recordings of the vlf noise spectrum. Unique features of the investigation are the large number of geophysical quantities measured and the availability of broadband vlf information. These features helped to clarify many matters of detail.

The work reported here is an extension of a vlf-aurora study made at the South Pole in 1960 [Morozumi, 1962, 1963]. In this earlier work, a strong semidiurnal pattern of occurrence in auroral zone phenomena was found, one peak of activity occurring near magnetic midnight and the other near magnetic noon. The night peak was found to be associated with vlf hiss and type B aurora, and the day peak with ray type aurora, vlf chorus and ionospheric absorption. The more extensive study reported here had as one of its purposes the investigation of the semidiurnal pattern in greater detail.

The location of Byrd Station in the southern auroral zone is shown in Fig. 1. Table 1 lists the quantities recorded on the eight-channel paper recorder during the present study. Through this report the abbreviation ulf (ultra low frequency) will be used to represent a micropulsation channel, and the abbreviation CNA (cosmic noise absorption) to represent the riometer channel. Natural signals recorded on channels a, b, and c are usually considered to be vlf hiss. Channel e was used to identify vlf chorus. An example of a 24-hour section of the correlation chart is shown in Fig. 2. The order of the channels in the charts illustrated in this report is usually kept in the sequence shown in Table 1 and Fig. 2. However, in some cases channels were interchanged during the course of the experiment. A dotted line appearing under the hour marks of the correlation charts in the text and atlas portion of this report indicates that the vlf and FM signals of the relevant channels were tape-recorded at 3-3/4 ips. Solid lines under the hour marks indicate that the broadband vlf spectrum was recorded continuously at 3-3/4 ips.

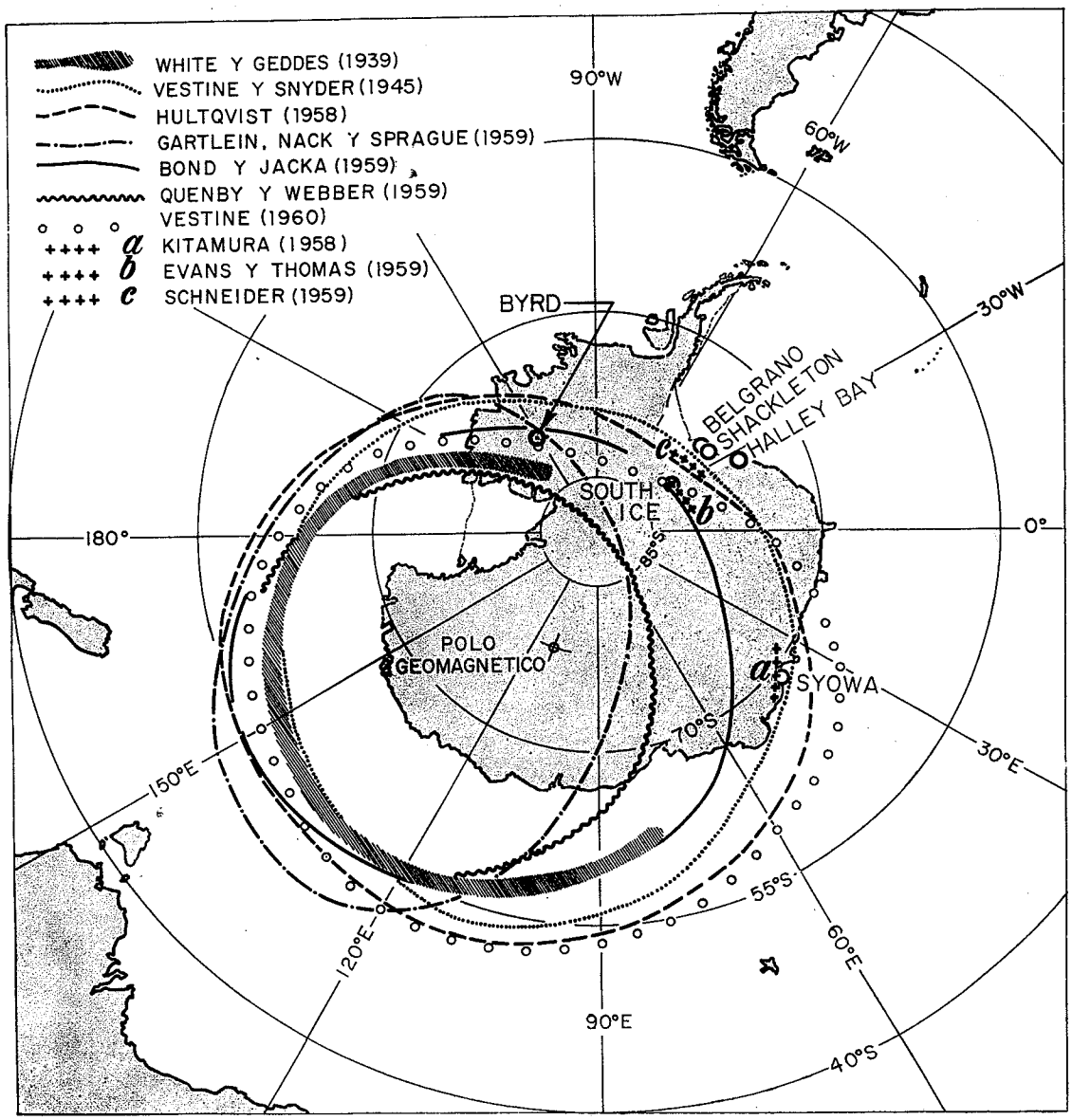

Diversas propuestas para ubicar la zona auroral del Hemisferio Sur según Bond y Jacka (1960); cuadro completado con otros datos teóricos y empíricos.

FIG. 1. AURORAL ISOCHASM (TAKEN FROM SCHNEIDER [1961]).

TABLE 1. QUANTITIES RECORDED ON THE CORRELATION RECORDER

	Input Signal
Channel a	VLF broadband (1-25 kc/s) NS (north-south loop)
Channel b	VLF broadband (1-25 kc/s) EW (east-west loop)
Channel c	VLF broadband (1-25 kc/s) V (vertical electric antenna), or VLF broadband H (horizontal loop antenna), or Aurora 5577 A
Channel d	Riometer 30 Mc/s (CNA)
Channel e	VLF 1 kc/s
Channel f	ELF Z (2-40 cps)
Channel g	Micropulsations X (0.02-5 cps)
Channel h	Micropulsations Z (0.2-5 cps; or dc-5 cps) denoted by the symbol U_{Zb}

In addition to the 8-channel charts and associated tapes, the experiment involved use of data from an 8-channel vlf spectrum analyzer. Broadband vlf tapes recorded daily on a 3-hour continuous basis and hourly on a 2-minute synoptic basis were available. Magnetic and ionosonde data were also used. The reader is referred to the appendix for details on instrumentation and calibration.

We fully recognize that many of the phenomena discussed in this report have been described in one form or another by previous workers. We hope to provide additional insights, particularly on matters of complex detail, and thus lead to a better overall view of the phenomena studied.

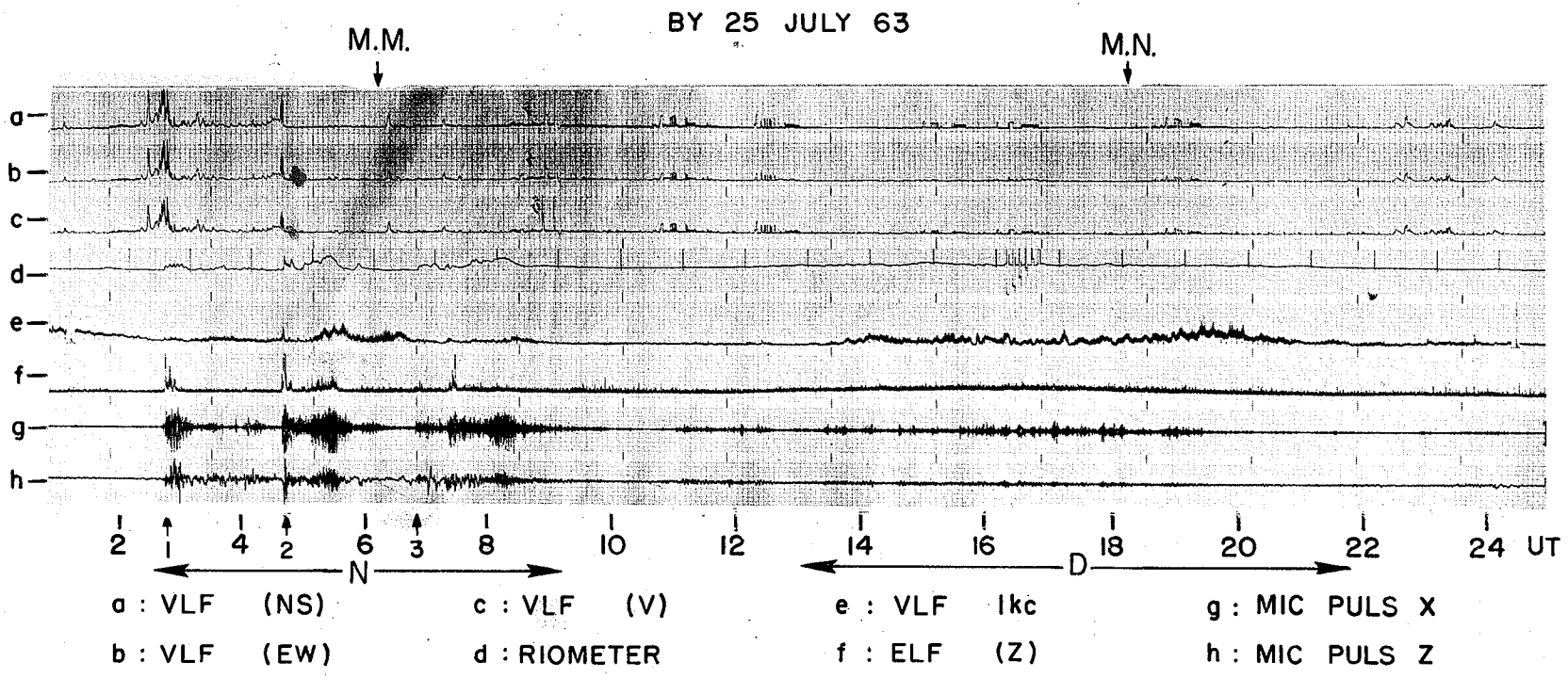

FIG. 2. CORRELATION RECORD OF JULY 25, 1963, BYRD, SHOWING CONDITIONS TYPICAL OF THE MODERATELY DISTURBED CATEGORY.

II. RESULTS OF THE CORRELATION STUDY

The purpose of this section is to present the results of the correlation study described in the introduction. In the latter part of the section, some results on the diurnal variation of individual phenomena will be presented and compared with the results from the correlation charts.

A. PERIOD OF THE CORRELATION STUDY

Correlation charts were obtained on an uninterrupted basis for 196 days from May 8 through 19 November 1963. In the following description of results, emphasis will be placed upon charts from the months of May through August, and comments on seasonal effects will be made near the end of the section. An advantage of emphasizing data from the austral winter is the availability of auroral light data, which can be obtained on a 24-hour basis during June and parts of July. The absence of sunlight also simplifies various ionospheric conditions.

B. DIVISION OF THE RECORDS ACCORDING TO PLANETARY MAGNETIC CONDITIONS

It was found that, in general, the records could be divided into three classes, corresponding to quiet, moderately disturbed, and disturbed planetary magnetic conditions. When the planetary K_p sum was ≤ 10 for 24 hours, the correlation charts exhibited smooth straight lines, interrupted only occasionally by small events. When the K_p sum was between about 10 and 30, the records showed regular types of events at specific times of the day. Since the K_p sum was in the range 10 - 30 about 80 percent of the time, this type of record may be considered the steady-state pattern of correlation events. The third class of correlation records corresponds to days when the K_p sum is above 30. In these cases, the regular pattern observed during periods of moderate agitation seems to break down. For the period May through October, of a total of 196 records, 25 are classified as quiet, 163 as moderately disturbed, and 8 as disturbed.

C. GENERAL FEATURES OF THE QUIET-DAY CORRELATION CHART

An example of a quiet-day chart is shown in Fig. 3. This record was made on 3 July 1963, when the K_p sum was 5. With the exception of vlf hiss bursts, seen between 0200 and 0600 on channels a and b, there is virtually no activity in any of the channels. The step in the photometer record (channel c) at 0630 UT indicates resumption of operation following an interval of instrumental difficulties.

D. GENERAL DESCRIPTION OF THE CORRELATION CHART ON A MODERATELY DISTURBED DAY

Approximately 80 percent of the days are in the moderately disturbed category. An example, the record of 25 July 1963, is shown in Fig. 2. On this day the K_p sum was 21. The characteristic feature of this type of record is the grouping of activity into a distinctive night regime between 0200 and 0900 UT (marked N) and a day regime (marked D) between 1300 and 2100 UT (0500 LT and 1300 LT). The letters MM and MN at the top of the chart stand for magnetic midnight and magnetic noon, respectively.

1. The Night Regime

Consider the 0200 to 0900 period in Fig. 2. There are three major events indicated by arrows numbered 1, 2, and 3. These have been identified by the onset of the elf burst (channel f) since the elf burst usually shows a particularly well defined starting time. (The term "elf burst" must be interpreted with care, since these bursts are in fact due to the high-frequency components of broadband micropulsations. Their frequencies rarely exceed 2 or 3 cycles per second.)†

From a sequential point of view, event 1 started at 0220 (preceding the arrow by 23 minutes) with large vlf bursts in channels a, b, and c, which were closely followed (at the time of the arrow) by nearly simultaneous cosmic noise absorption (riometer), elf bursts, and ulf events. Event 2 started with a weak steady hiss at 0427, and was

† J. E. Lokken, private communication.

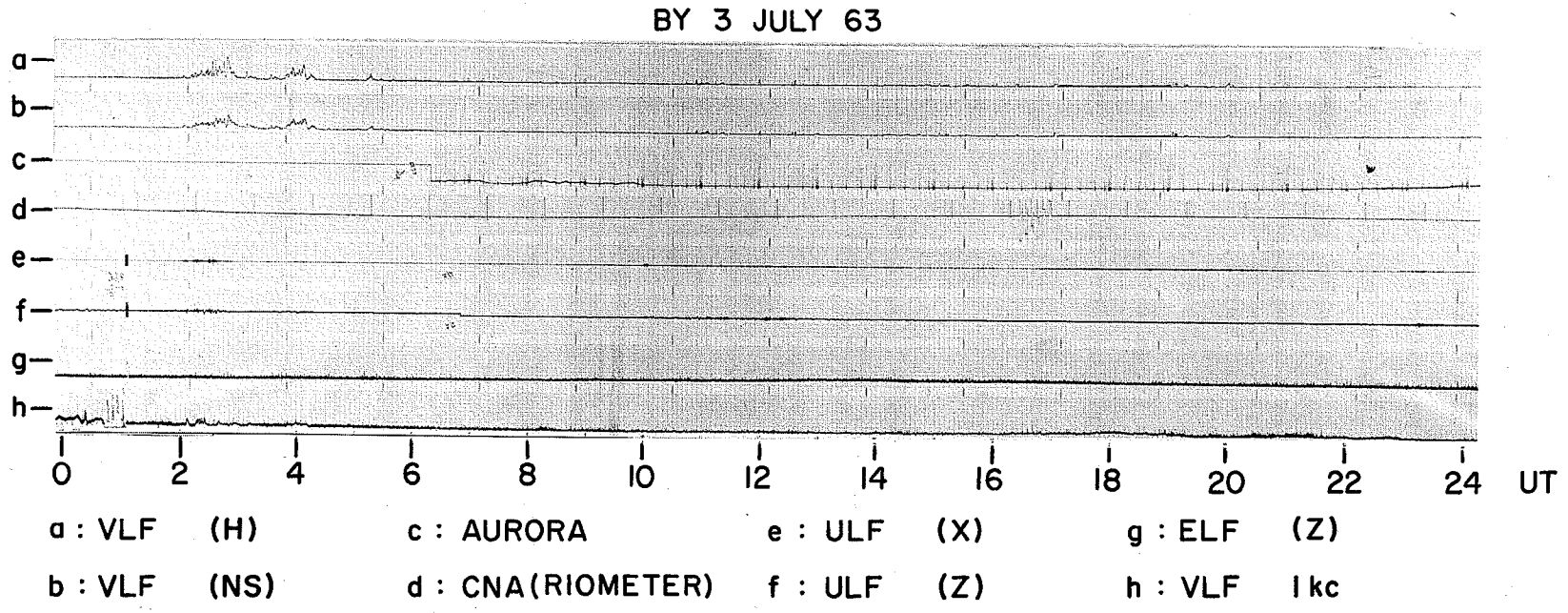

FIG. 3. CORRELATION RECORD OF JULY 3, 1963, SHOWING TYPICAL QUIET-DAY CONDITIONS AT BYRD.

followed (at the time of the arrow) by a large sudden increase in the hiss, and an extremely sudden onset of cosmic noise absorption, elf and ulf. After its sudden rise, the hiss exhibited relatively rapid fluctuations in amplitude (not evident on this record; details are discussed later). Note that vlf near 1 kc/s (channel e) followed closely upon the cessation of the hiss signal, and continued until about 0640. Event 3 began at 0650 with a sudden onset of micropulsations (especially channel g), absorption, and a very weak hiss burst. There were no conspicuous hiss bursts here. However, cosmic noise absorption and vlf 1 kc/s, elf and ulf activity were observed. The three events show in a general way much of the morphology which later will be described in terms of the phases of night events.

2. The Day Regime

On a typical moderately disturbed day, the important features of the events seen between 1300 and 2100 UT are (see Fig 2, for example): 1) very little vlf hiss activity (a, b, c); 2) long persisting riometer absorption during the entire period (d); 3) long persisting vlf 1 kc/s emissions (e); 4) a general increase in elf background level by a factor of 2.5 (f); and 5) long persisting ulf of small amplitude (evident in g), generally known as P_c, continuous pulsation.

The grouping of the active periods near magnetic midnight and magnetic noon suggests the terms "magnetic night event" and "magnetic day event." The occurrence frequency of these events usually peaks slightly before magnetic midnight and noon, respectively.

E. CORRELATION OF NIGHT EVENTS WITH K_p

We have already pointed out that the correlation charts may be categorized as quiet, moderately disturbed, or disturbed according to whether the K_p sum is less than 10, between 10 and 30, or greater than 30. As another means of studying the correlation, we counted the number of elf bursts during a night and compared this with the K_p sum for the preceding UT day. (The elf burst appears to be related to the nighttime P_i type of ulf disturbance. The latter has a high-frequency component

which may well be above the regular ulf frequency range, and which appears in the elf channel with the sudden onset of an event. Note that the three events indicated in Fig. 2 include well defined elf bursts.) The results for July 1963 are shown in Table 2. A good correlation is shown, particularly in the lower ranges of the K_p sum.

TABLE 2. OCCURRENCE OF ELF BURSTS AS A FUNCTION OF THE K_p SUM FOR THE PRECEDING UT DAY IN JULY, 1963

Number of elf bursts	$\sum K_p$ 0-10	11-20	21-30	31
4			1	1
3			2	
2	1	4	5	1
1	1	2	3	
0	7	2	1	

The relation between the night event as observed at Byrd and planetary magnetic activity is further illustrated by the sequence of night events for the period 22 July to 31 July, shown in Figs. 51 through 60 in the atlas portion of the illustrations. The K_p sums for the relevant dates are shown in Table 3. The outstanding feature of the K_p sum in this period is the drop to a value of 7 on the 29th following a period of values in the 20 to 30 range. Following the drop another period of moderate disturbance begins. This same general pattern is evident in the sequence of correlation records, with a particularly quiet period being evident on the 29th. Generally, the correlation seems highest when the night event is compared with the K_p sum for the preceding day. The drop to relatively low levels of activity on the chart for the 26th may be related to the reduction in the K_p sum between the 24th and 25th of July. Note that although the K_p sum for the 30th was relatively high with respect to the 29th, the correlation chart showed events of relatively high amplitude only on the 31st.

TABLE 3.
$\sum K_p$ FOR JULY 21 - AUGUST 1, 1963

UT Day July, 1963	$\sum K_p$
21	28
22	22
23	28
24	32
25	21
26	23
27	24
28	12
29	7
30	31
31	26

F. GENERAL DESCRIPTION OF THE CORRELATION CHART ON A DISTURBED DAY

Extremely active days with the K_p sum substantially above 30 were rare during the 1963 period of the correlation study. Figure 4 shows a case recorded on 22 September 1963 when the K_p sum was 50. The vlf 1 kc/s channel (e) shows a pronounced diurnal effect, but the ulf and elf channels (f, g, h) show repeated bursts of activity over much of the day, with no obvious grouping into day and night regimes. There seems to be little correlation between ulf and vlf chorus, in contrast to the relation indicated on the moderately disturbed record of Fig. 2. Note the complete absence of vlf hiss, usually well defined on the moderately disturbed days, and often present on the quiet charts. The sudden level changes on vlf channels a, b, c, represent keydown transmissions from a vlf station. It may be seen that the field strength of these transmissions is at a relatively high level during the night period 0100 - 1000 UT (1900 - 0400 LT).

G. DETAILED DESCRIPTION OF THE NIGHT EVENT

In the previous section it was pointed out that on moderately disturbed days, and thus on most days, the activity on the records tends to group into well defined night and day regimes. The night events generally show three distinct phases, called N-1, N-2, and N-3. We shall now describe some of the details of the night events.

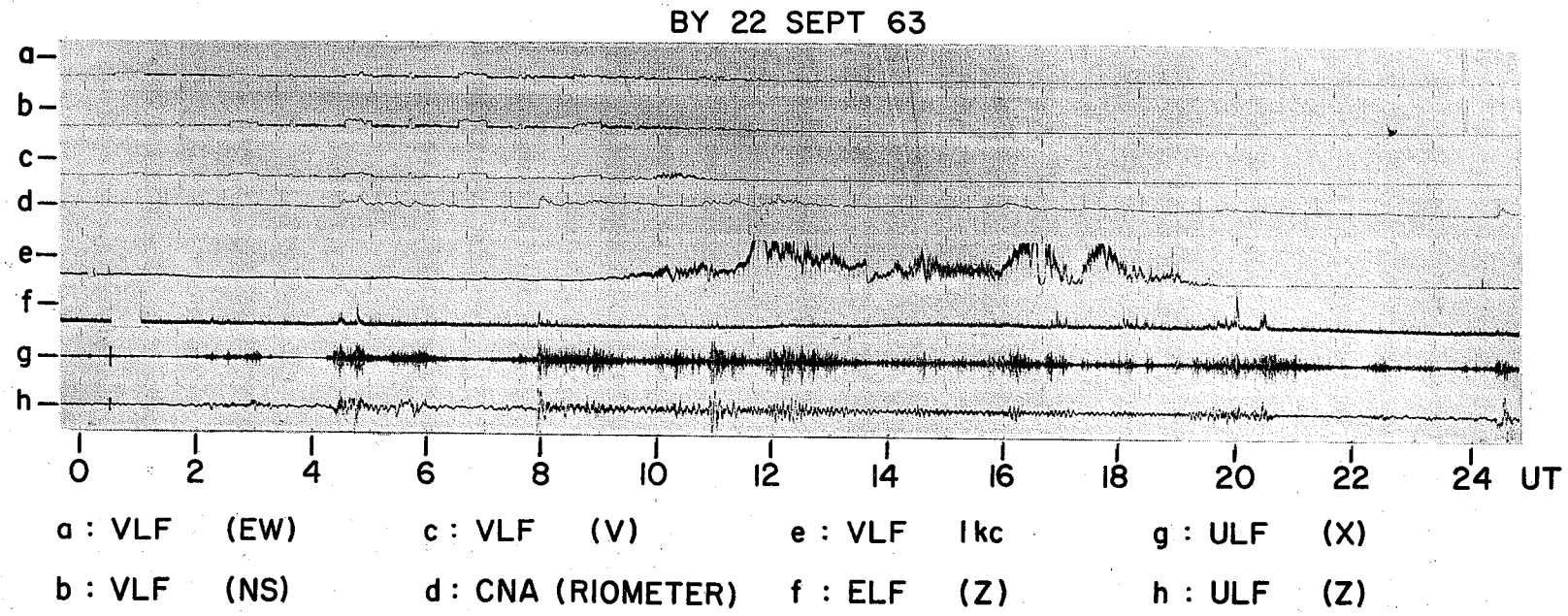

FIG. 4. CORRELATION RECORD OF SEPTEMBER 22, 1963, SHOWING TYPICAL DISTURBED-DAY CONDITIONS AT BYRD.

The various phases have been observed over a wide range of hours during the night regime. The time sequence of the phases is always the same (i.e., N-1, N-2, N-3), although there is a strong tendency for one phase or another to dominate the record, depending on the time. Figure 5 shows an example in which all three phases are prominent. N-1 appears between 0427 and 0510 (see arrows at bottom), N-2 between 0519 and 0530, and N-3 between 0531 and 0700.

1. Phase N-1

The N-1 phase occurs in the latter part of a quiet period that precedes large impulsive events characteristic of the N-2 phase. During the N-1 phase, aurora, vlf hiss, ionospheric absorption, and ulf are usually observed simultaneously. (The simultaneous presence of these phenomena does not mean that their amplitudes are correlated on a fine scale.) During N-1, the amplitudes of absorption, ulf and elf events are small in comparison to corresponding events observed later during N-2. Riometer events rarely exceed 1 db. Ulf amplitude is usually less than 2γ peak to peak (referred to 0.5 c/s calibration frequency). Most outstanding in terms of amplitude is the broadband hiss, with amplitude that sometimes exceeds 1/2 mv/m. The vlf hiss channel is the most sensitive indicator of the N-1 phase, and often serves as a means of determining its duration, which may range from 10 to 200 minutes.

Examples of N-1 are shown in Figs. 5 and 6. In Fig. 6 only the N-1 phase is clearly evident. It started on 19 June at 2334 and lasted about 4 hours, until 20 June at 0323. In this event there was coincident auroral activity, vlf noise, riometer absorption, and ulf activity.

Note in Fig. 6, and in later figures, that the 6γ/sec peak to peak range on the micropulsation channels represents a calibration at 0.5 c/s. For the chart of Fig. 6, this calibration is shown twice within the time period 2330 - 0000. Note also in Fig. 6 and later figures that E_z is used to denote the elf Z component of the magnetic field.

Consider now the N-1 phase in Fig. 5. This event lasted from 0427 to about 0510. Although the riometer record appears to show a decrease in absorption during N-1, this is the result of the normal decrease for a quiet day. A spectrum of the N-1 hiss at time A in Fig. 5 is shown on line A in Fig. 7. This hiss is characterized by a

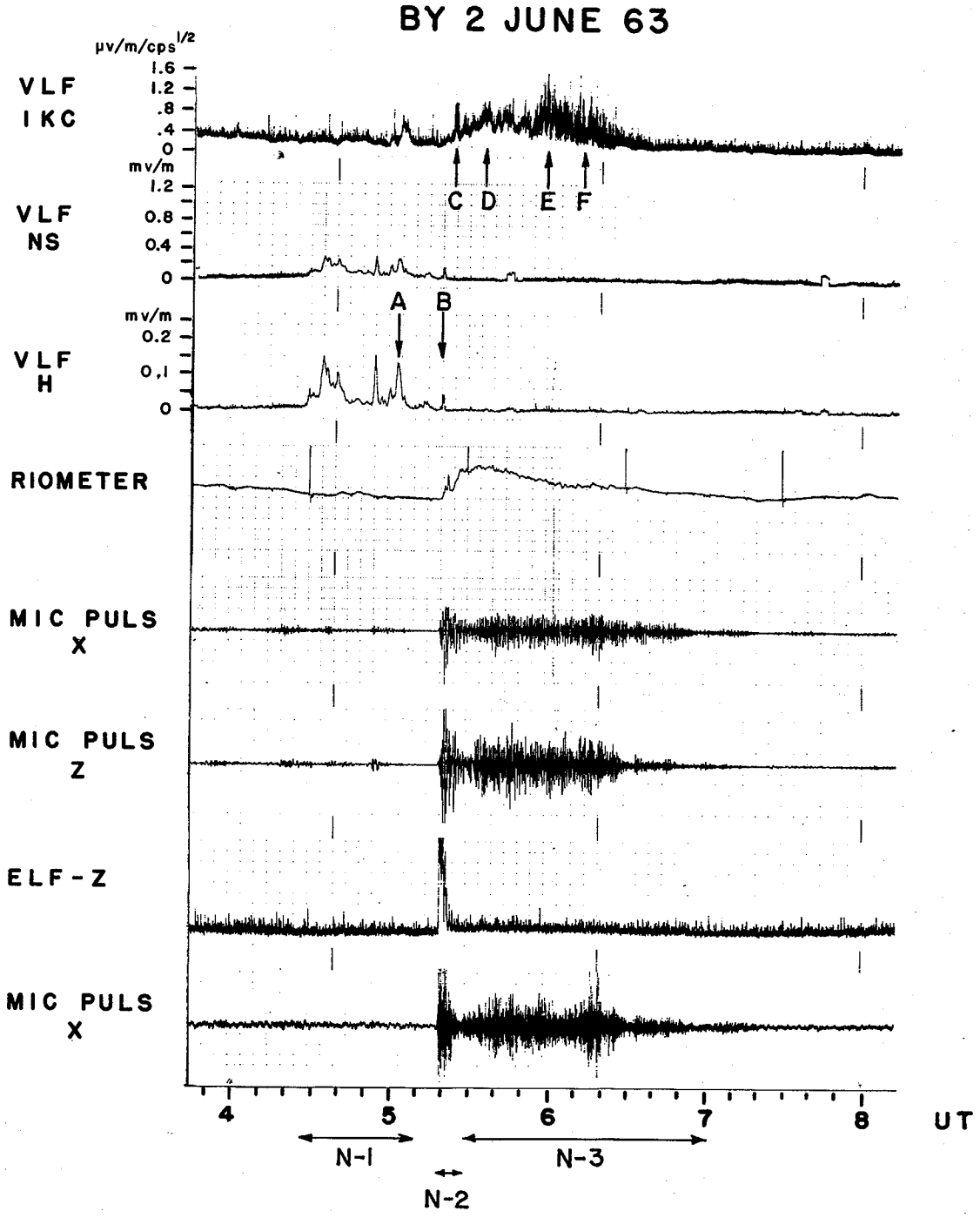

FIG. 5. CORRELATION RECORD OF JUNE 2, 1963, SHOWING ALL THREE PHASES, N-1, N-2, AND N-3, OF A NIGHT EVENT AT BYRD.

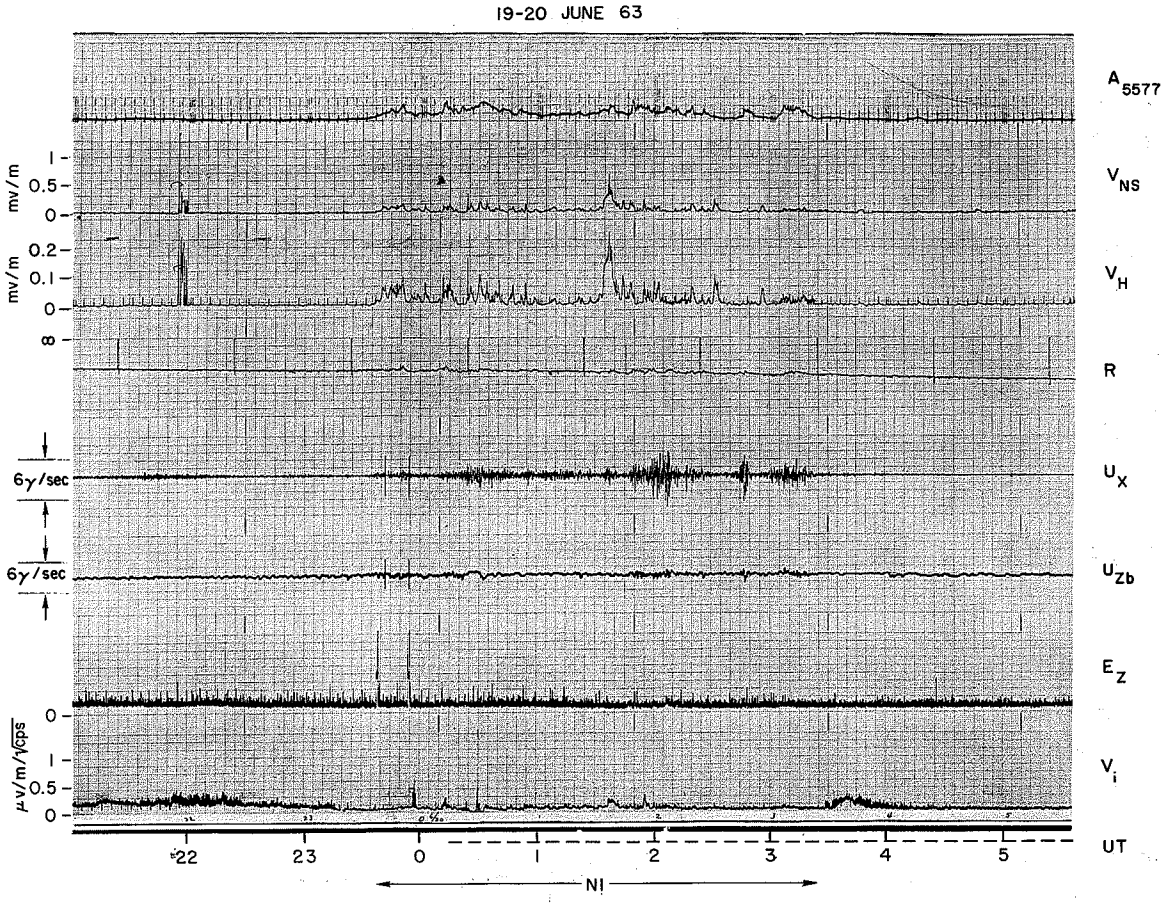

FIG. 6. EXAMPLE OF N-1 EVENT, JUNE 19 - 20, 1963, BYRD. The entire event between 2330 and 0330 appears to belong to N-1. Note the simultaneous presence of auroral light (A5577), vlf hiss (V_{NS},V_H) cosmic noise absorption (R) and ulf (U_X,U_{Zb}).

smooth variation of amplitude, no faster than 6 db in 30 seconds. Its lower cutoff frequency is 2 kc/sec, while the upper cutoff frequency exceeded the equipment limit of 10 kc/sec. (On some occasions during N-1, we noted a periodic dispersive type of hiss whose frequency changed from about 8 kc/sec to 4 kc/sec in about 4 sec. The duration was several minutes. This is not the "impulsive" hiss described later as occurring in phase N-2.)

In summary, the distinguishing feature of the N-1 phase is vlf hiss of relatively high amplitude, accompanied by simultaneous occurrence of aurora, ionospheric absorption and ulf, all having relatively low

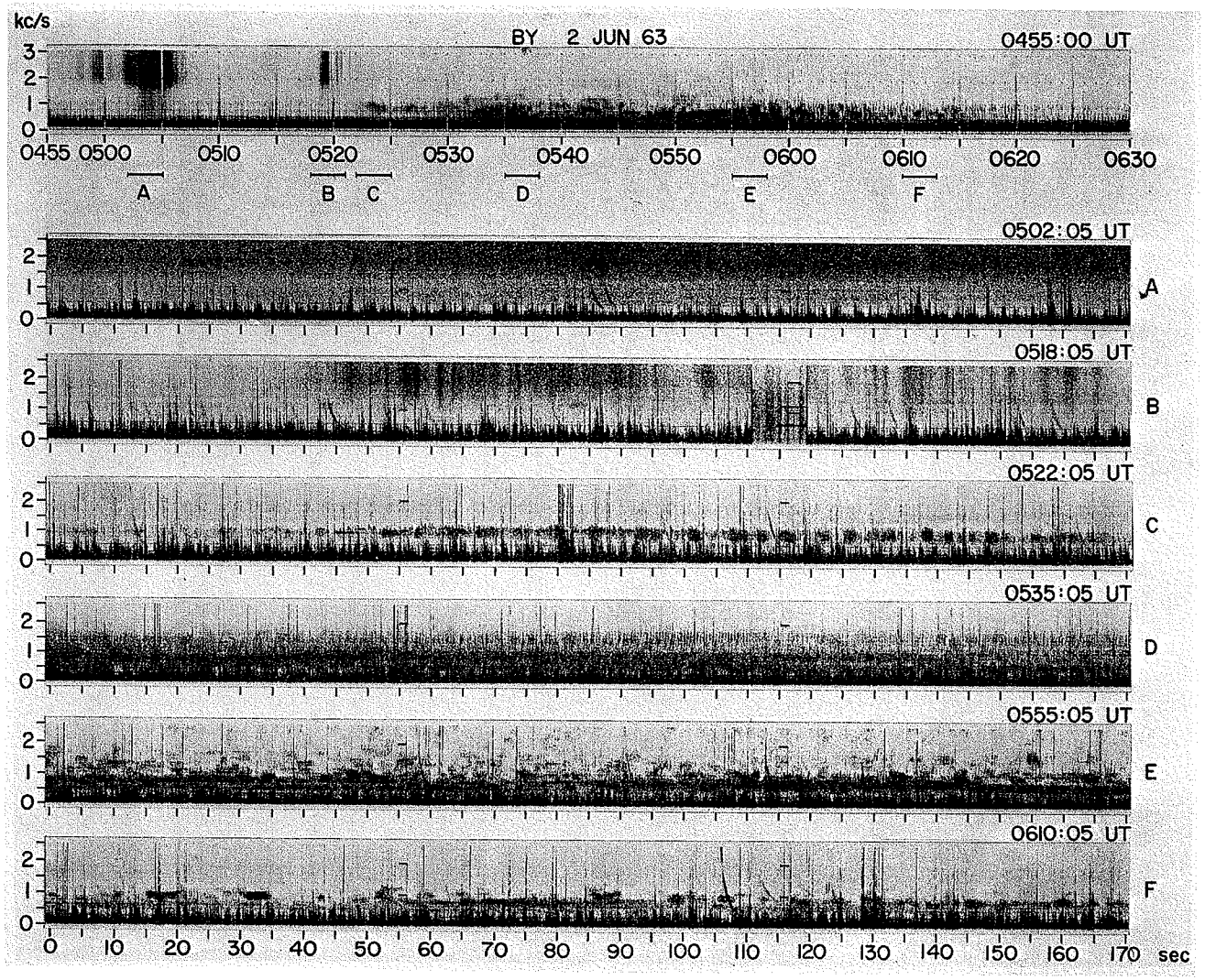

FIG. 7. SPECTRUMS OF VLF HISS AND NIGHT CHORUS, RECORDED DURING THE EVENT OF JUNE 2, 1963, ILLUSTRATED IN FIG. 5.

amplitude. Because of the prominent role of hiss in N-1, this phase will be called the "hiss" phase.

2. Phase N-2

Phase N-2 is commonly known as the breakup phase of the aurora, and will be so designated. A distinguishing feature of this phase is an essentially simultaneous sudden onset in all channels. Maximum amplitude is often reached within 100 seconds, and this amplitude is often larger than that of the other phases. Vlf hiss amplitude may exceed 1/2 mv/m, and auroral intensity often reaches IBC II or III (IBC: International Brightness Coefficient). The ulf peak-to-peak amplitude (of dH/dt) often exceeds 10 gamma/sec, while riometer absorption often reaches several db. In duration N-2 is the shortest of all the phases, usually lasting less than 15 minutes. In Fig. 5, N-2 starts at 0519 and ends by 0530. There is a simultaneous sudden onset of riometer, ulf and elf events at 0519. Vlf hiss also started at 0519 and lasted about 1 minute. The spectrum of this hiss at the time marked B in Fig. 5 is shown on line B in Fig. 7. A comparison of lines A and B in expanded time scale in Fig. 7 shows that the vlf hiss during phase N-2 exhibits rapid variations in amplitude; about 6 db in 1/2 second is shown here. Note that the variation in amplitude is not a function of frequency.

Another important feature of N-2 is the presence of active auroras. Figure 8 shows the all-sky photographs of an aurora during the N-2 event of Fig. 5. The top of the frame is geographic west and the right is geographic north. A dark circle in the north is the result of moonlight. During the impulsive hiss around 0519, auroral bands in the direction of magnetic north brightened (this is a negative). The aurora approached the zenith at 0520. The impulsive hiss shown in Fig. 7 lasted only about 1 minute, while the aurora remained active until 0529, some 8 minutes after cessation of the hiss. On these records, phase N-2 is considered to end with the disappearance of the auroral band. Following 0519, there was a large increase in absorption and ulf activity, but from Fig. 8 it may be seen that there was no discrete aurora after 0530. After 0530 (and prior to 0519), there was a glow-like aurora all over

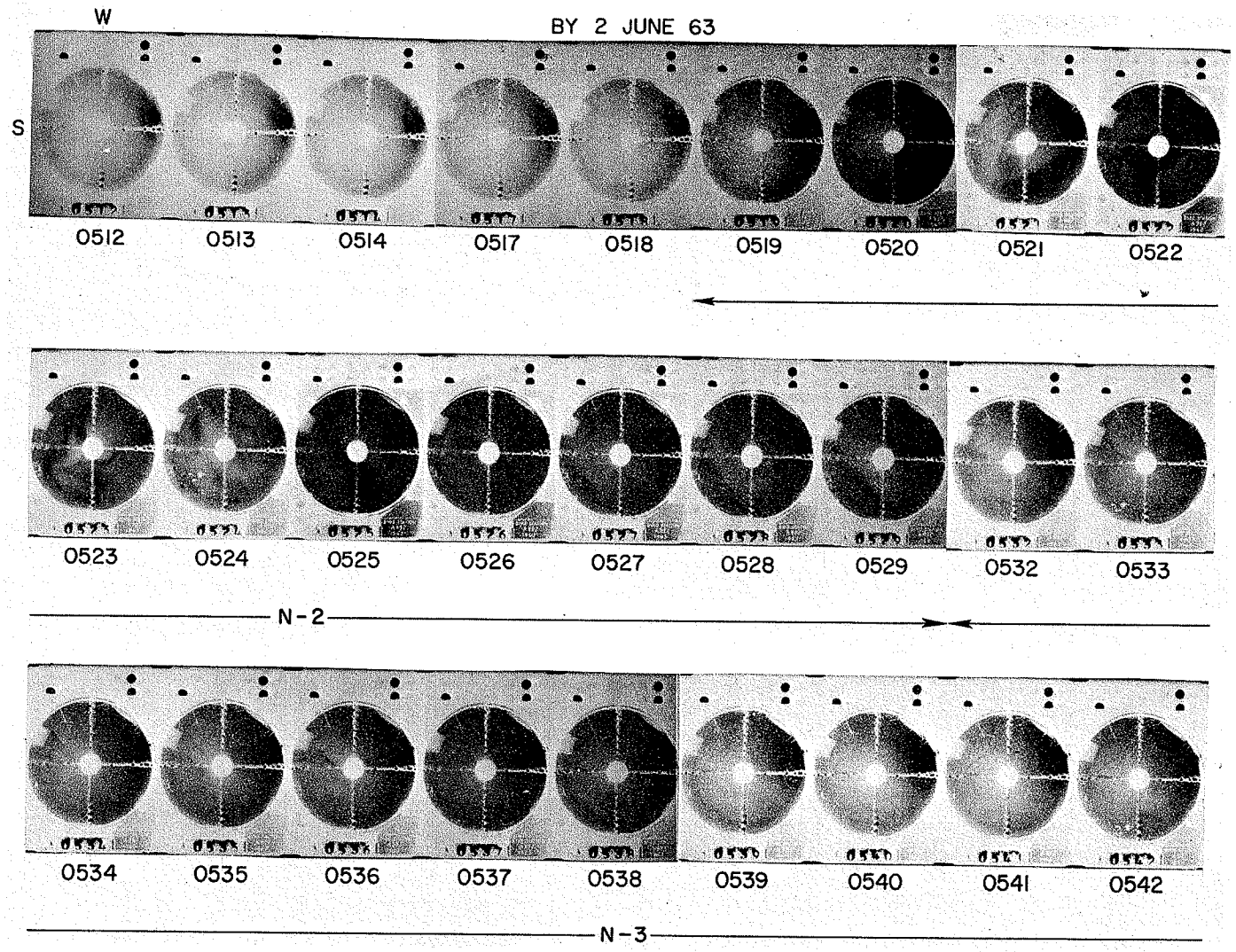

FIG. 8. ALL-SKY PHOTOGRAPHS OF AURORA DURING THE EVENT OF JUNE 2, 1963, ILLUSTRATED IN FIG. 5.

the sky (see, for example, 0512 and 0532 in Fig. 8). Therefore 0530 is taken as the transition between the N-2 and N-3 phases.

Before discussing N-3, we shall examine the onset of N-2 events in greater detail.

3. Detailed Features of N-2 Onset

The N-2 examples chosen for study of onset details were required to fulfill two criteria: 1) isolation in time, to avoid confusion with other events; and 2) a ulf Z amplitude (dH_z/dt) of more than 6 gamma/sec peak-to-peak. On the basis of these criteria, 24 well-defined N-2 events from the months of July, August, and September, 1963 were selected for study. It was found that certain characteristic times, such as the times of sudden increase or decrease and of first maximum or minimum, were part of a well defined sequence involving several of the channels. To study this sequence, three characteristic times t_o, t_1, and t_2, were identified with specific features of the ulf channel, and a variety of measurements were made involving both these times and certain corresponding times in other channels. Examples of the data are shown in Figs. 9 and 10.

In Fig. 10, t_o marks the (gradual) onset of ulf. In Figs. 9 and 10, t_1 on the ulf channel marks the first sudden reversal of the slope of dH_z/dt, while t_2 marks the second reversal (positive dH_z/dt is measured upward on the chart). On the CNA channel, t_1 marks the onset of absorption and t_2 the first peak. It is immediately clear from Figs. 9 and 10 that t_1, t_2 of CNA and t_1, t_2 of ulf (Z) are almost simultaneous. In other words, the sign of dH_z/dt changes at the onset and the first maximum in CNA. Figure 11 shows the statistical results from the 24 events. To obtain these results, t_1 of ulf was identified and t_2-t_1 and t_1-t_o were scaled. Zero time was not taken to be at t_o, but at the time of the smallest detectable onset of the event, as observed on either the vlf hiss channel or the ulf Z channel. There is a large amount of uncertainty in the determination of zero time, and thus the absolute values of the time scale in Fig. 11 must be considered approximate. The statistics of the variation in t_1 with respect to zero time are not shown. Rather t_1 is taken as the reference, and the range of t_2 and t_o with respect to t_1 are shown.

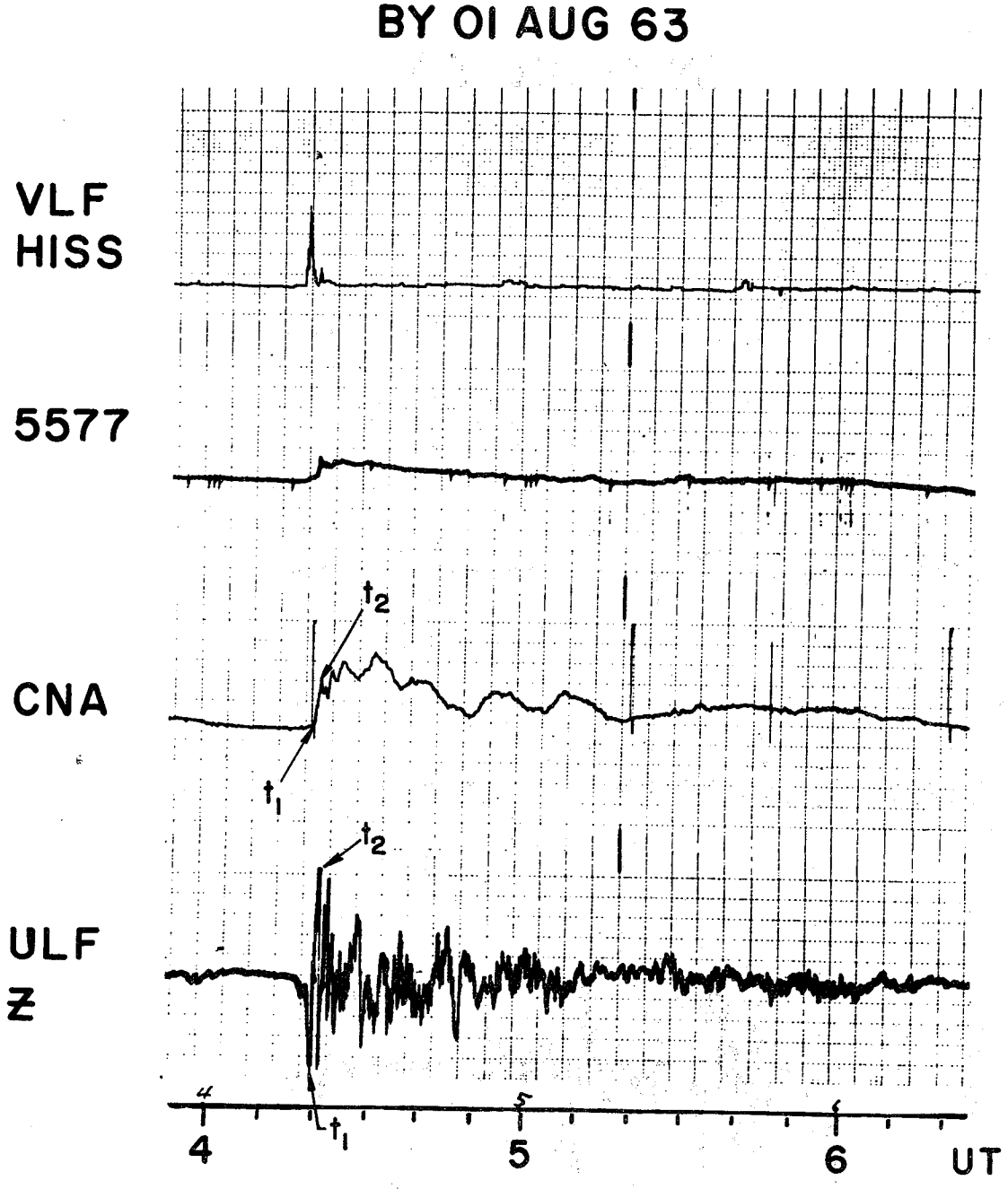

FIG. 9. N-2 EVENT OF AUGUST 1, 1963, SHOWING ONSET DETAILS.

The statistics of the CNA, 5577 and vlf hiss channel were measured for each event with respect to the times for that event already identified in the ulf Z channel. Thus the interval $t_1 - t_o$ and $t_2 - t_1$ for ulf may vary over a range of about 100 sec, while the variation of the onset time of CNA with respect to the first reversal of the sign of

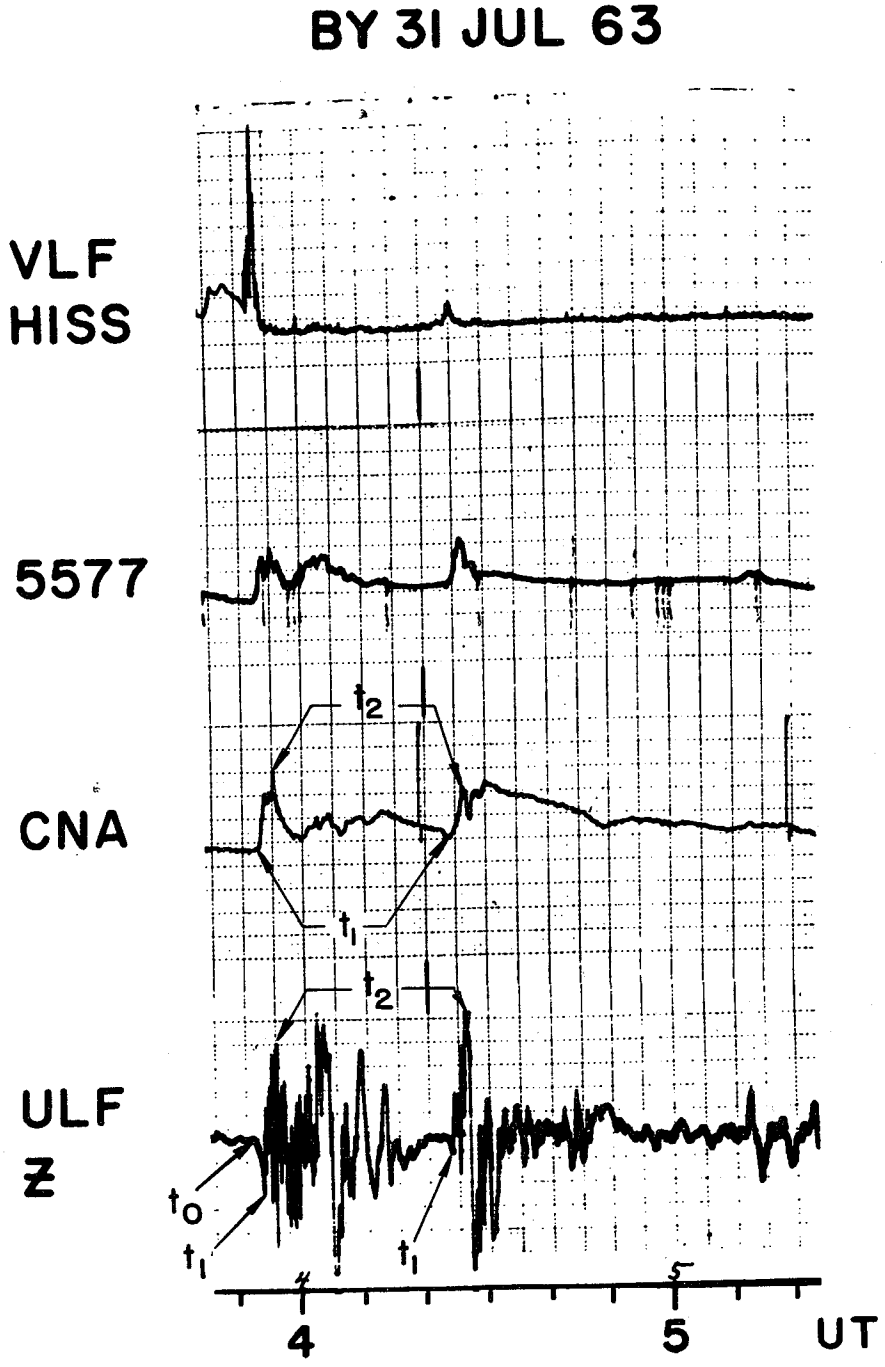

FIG. 10. N-2 EVENT OF JULY 31, 1963, SHOWING ONSET DETAILS

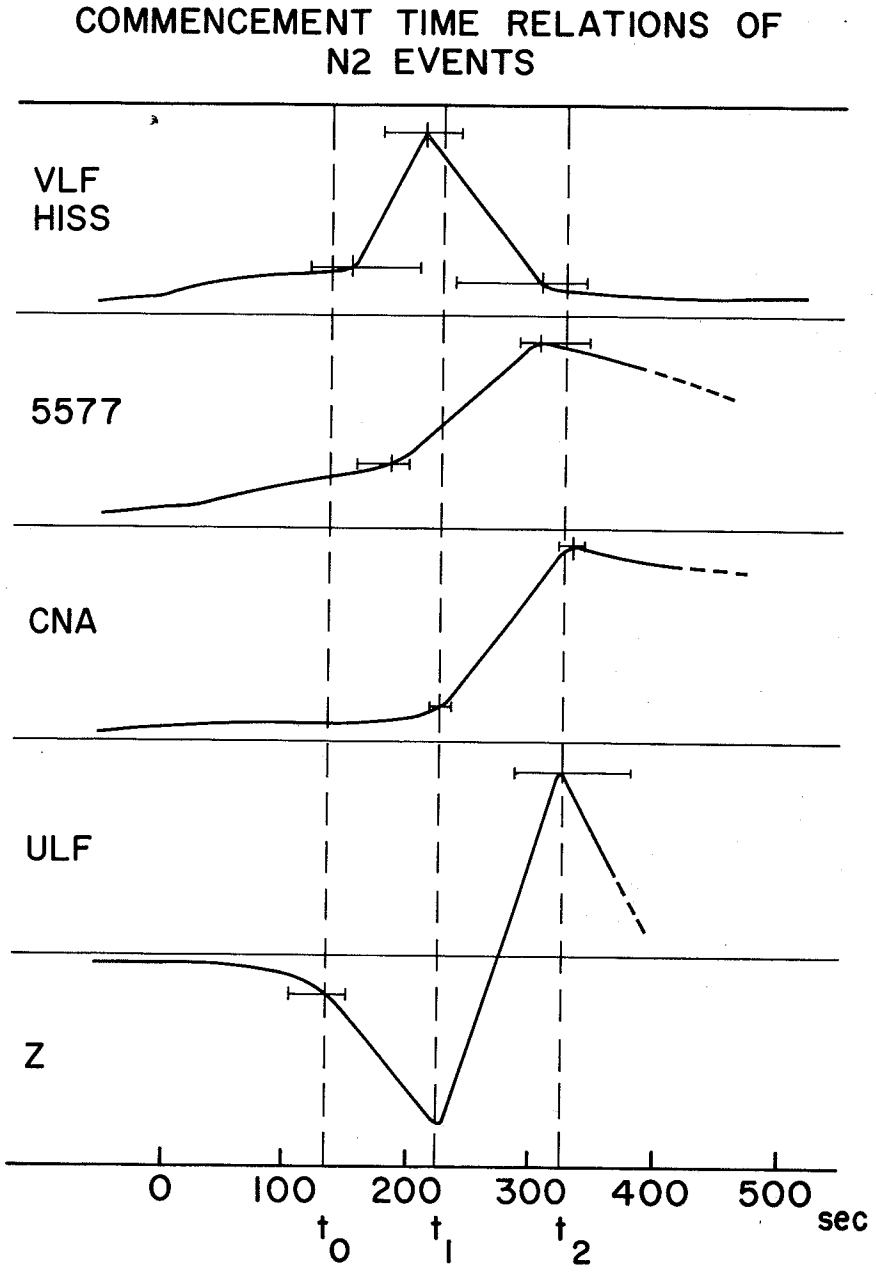

FIG. 11. COMMENCEMENT TIME RELATIONS OF N-2 EVENTS.

dH_Z/dt on the same record fluctuates over a range of about 20 sec at most. (Twenty seconds is the limit of the time resolution of the chart records.) Certainly an outstanding feature of Fig. 11 is this close relation between CNA and ulf.

4. Phase N-3

This phase comes after the breakup of the aurora and is characterized by a large increase in ionospheric absorption without a corresponding increase in auroral light. A special type of vlf chorus near 1 kc/s is usually observable. Therefore we shall call N-3 the "chorus-phase." In N-3, the amplitude of events tends to be smaller than during the N-2 phase.

An example of the N-3 phase is shown in Fig. 5, starting at 0530 and ending at 0700. Note in Fig. 8 the absence of a bright discrete aurora during this phase. Vlf near 1 kc/s was observable throughout the 0530 - 0700 period. The spectrum of corresponding vlf emissions is shown in Fig. 7, lines C, D, E and F. Another example of the N-3 phase is shown in Fig. 12. Only the N-3 phase is observed in this case, but there

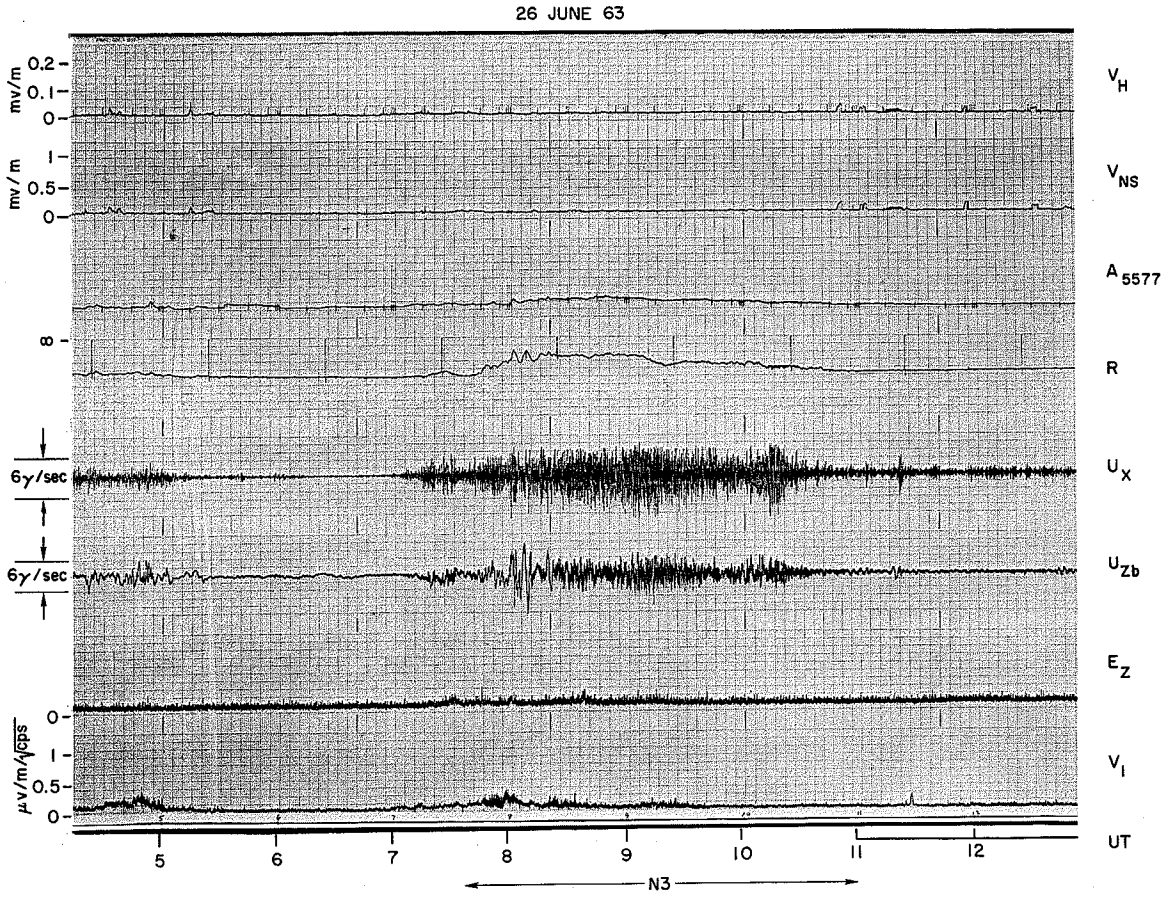

FIG. 12. EXAMPLE OF THE N-3 PHASE, JUNE 26, 1963, BYRD. This is a typical N-3 event in which vlf hiss is not prominent, but there is an indication of a small hiss burst at 0715.

is some indication of N-2 at the beginning of the event (hiss burst at 0714). Such a "small" N-2 is frequently observed at the beginning of an N-3 event. To summarize, the distinguishing features of the N-3 phase are the absence of a bright, band type aurora and the presence of vlf chorus and ionospheric absorption.

5. Variation in Phase Intensity with Time during the Night Regime

There appears to be a correlation between the intensity and duration of a phase and the time of its occurrence. Early in the evening between about 1900 and 2300 UT, the N-1 phase tends to dominate the records. Events observed between 0000 and 0200 UT tend to exhibit both N-1 and N-2, while between 0300 and 0700 UT, a combination of N-1, N-2 and N-3 tends to be present (see Fig. 5). After 0600, N-1 is rarely observed in a night event, and events occurring between 0800 and 1400 UT usually exhibit N-3 only. This temporal variation in the predominance of the phases is illustrated on a statistical basis in a later section. An actual case study of the phase relation is shown in Fig. 13. The dominant phases of the period are indicated by arrows at the bottom of the record. The night events occurring between 0052 and 0308 UT show strong N-1 and relatively weak N-2. Weak N-2 phases are seen at 0204 and 0242 UT (note at these times small ulf onsets in channel U_X). The event between 0427 and 0440 indicated by arrow N2 shows predominantly N-2 characteristics. However, N-1 and N-3 are also present in the usual sequence. The event observed between 0530 and 0820 UT and indicated at the bottom by arrow N3 shows predominantly characteristics of N-3. However, a small N-1 is present at 0510 to 0528 UT, and N-2 is seen at about 0532 UT.

H. DETAILED DESCRIPTION OF THE DAY EVENT

Events observed near magnetic noon are presently called "D" (day) events. Subdivisions of this phase into two or more subclasses may follow as a result of further study. It is already evident that vlf chorus and ulf do not peak at the same time, the difference in time of peak being on occasion as large as two hours.

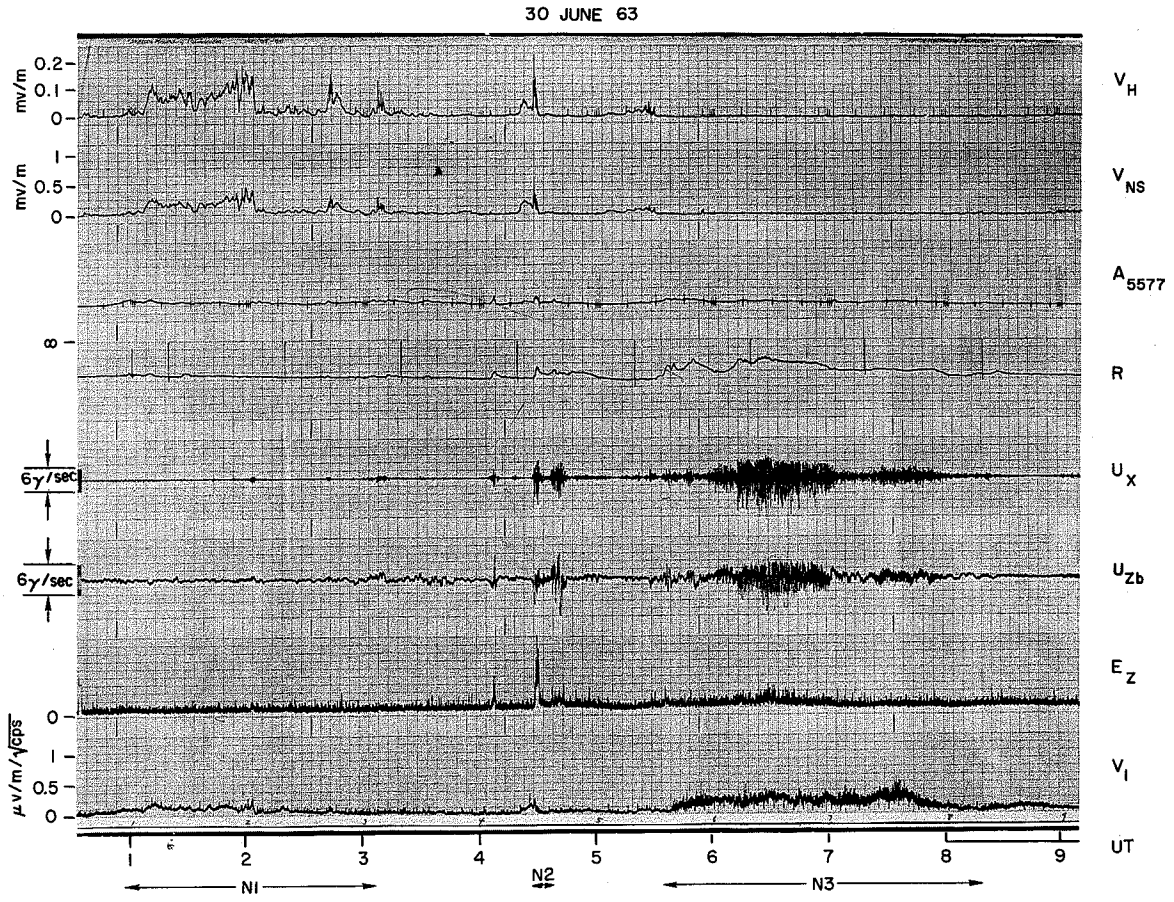

FIG. 13. CORRELATION RECORD OF JUNE 30, 1963, ILLUSTRATING VARIATIONS IN PHASE INTENSITY WITH TIME DURING THE NIGHT REGIME. (See text for details.)

An example of the day event is shown in Fig. 14. The difference in duration between day and night events can be seen by comparing Fig. 14 with the night events shown in Fig. 15. A night event typically lasts one to two hours, the day event more than five hours. Note that in both figures, the events were preceded by hiss bursts.

The vlf spectrum of Fig. 14 is shown in Fig. 16. It can be broadly classified as chorus, except in the case of the top record, which shows hiss (above 1.8 kc/s). The spectrum of this chorus is somewhat similar to that observed at night following the appearance of vlf hiss.

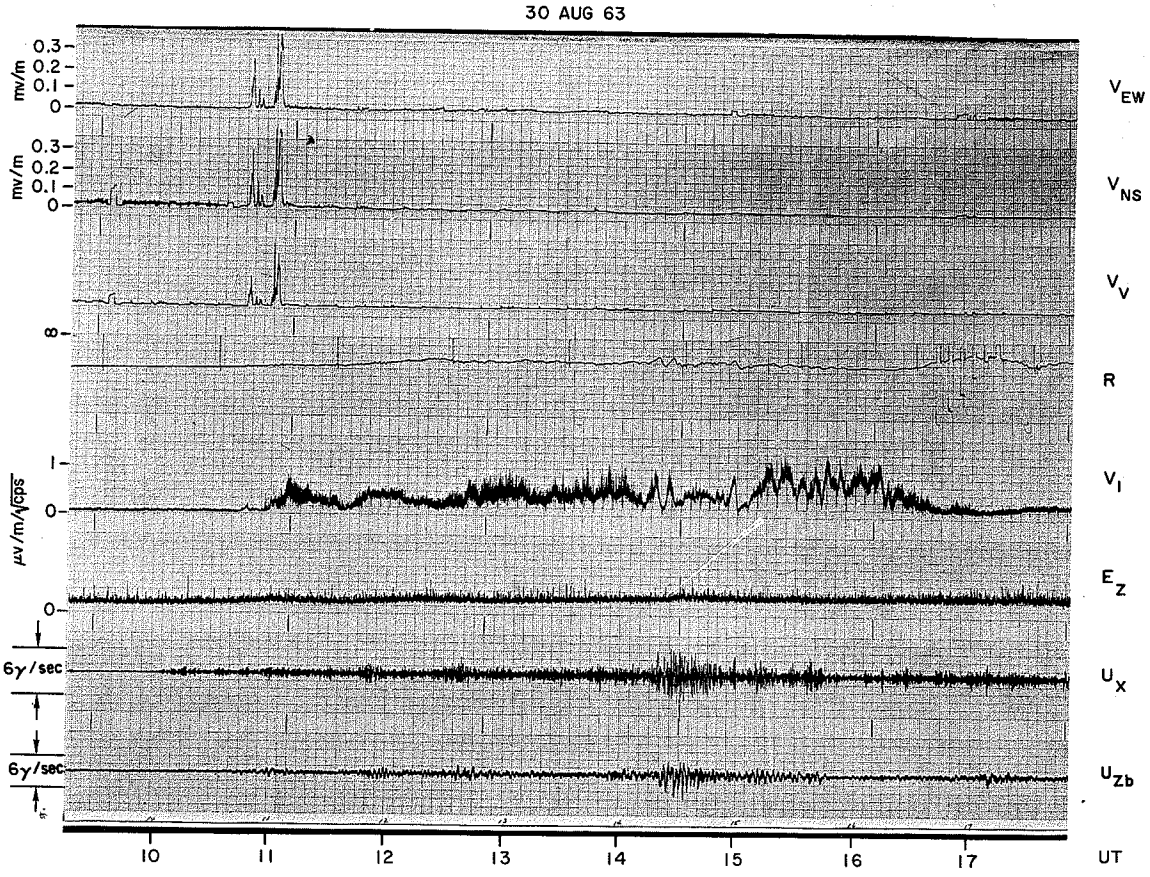

FIG. 14. DAY (D) EVENT, AUGUST 30, 1963, BYRD. The observations of vlf hiss before the onset of vlf chorus suggests an analogy to the sequence of the night event.

The similarity is in a thin rising structure seen in Fig. 16 (day) at 1250:10 UT and in Fig. 7 (night) at 0535:05 UT. Further, a close examination of Figs. 14, 17, and 18 shows that amplitude variations of vlf 1 kc/s are at times in phase with riometer absorption. Thus in both spectral properties and in a tendency to be correlated with riometer absorption we find the 1 kc/s chorus in the day regime to be similar to that observed after the hiss at night.

During the day regime, visual auroral activity is quite low, in spite of the high level of ionospheric absorption, and of ulf and of vlf chorus activity. An example of low daytime auroral level is shown in

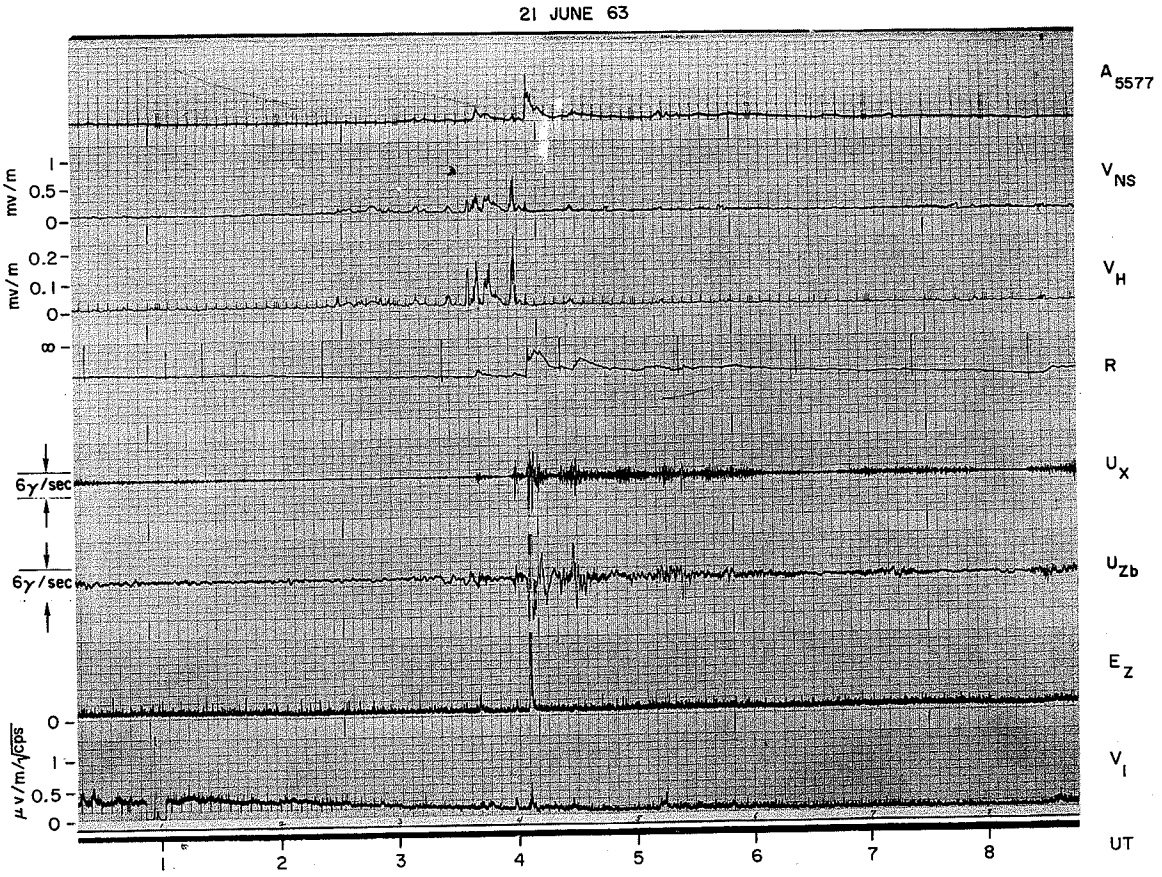

FIG. 15. CORRELATION RECORD OF JUNE 21, 1963, SHOWING A TYPICAL NIGHT EVENT. Note the occurrence of N-1 hiss from about 0228 to 0400.

Fig. 19, where the aurora record (c) exhibits practically no activity between 1100 and 2200 UT.

I. SUMMARY OF EVENT CHARACTERISTICS

The characteristics of the three night phases and the day phase are summarized in Table 4 on page 31.

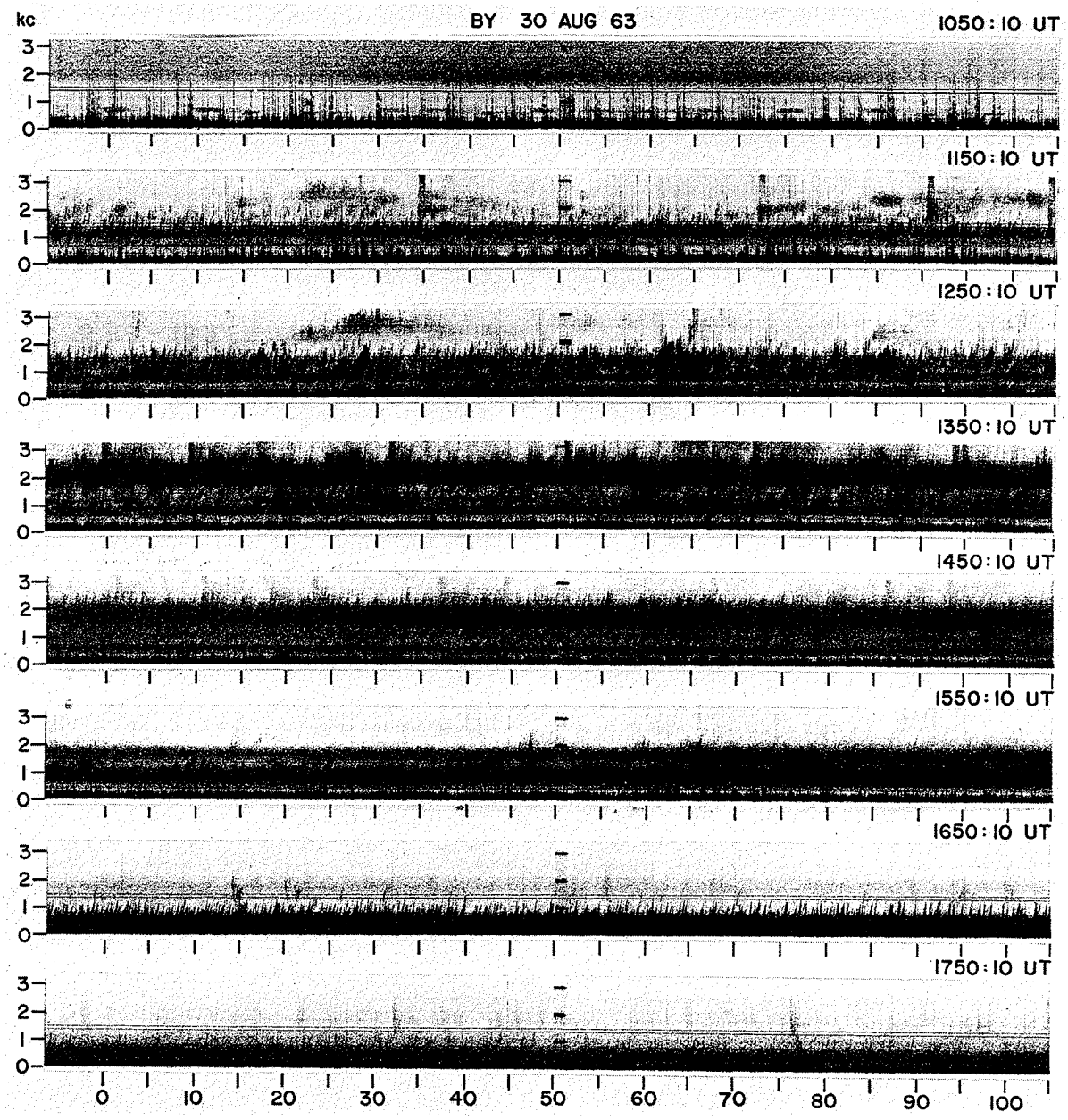

FIG. 16. SPECTRUMS OF VLF CHORUS RECORDED DURING THE DAY EVENT ILLUSTRATED IN FIG. 14.

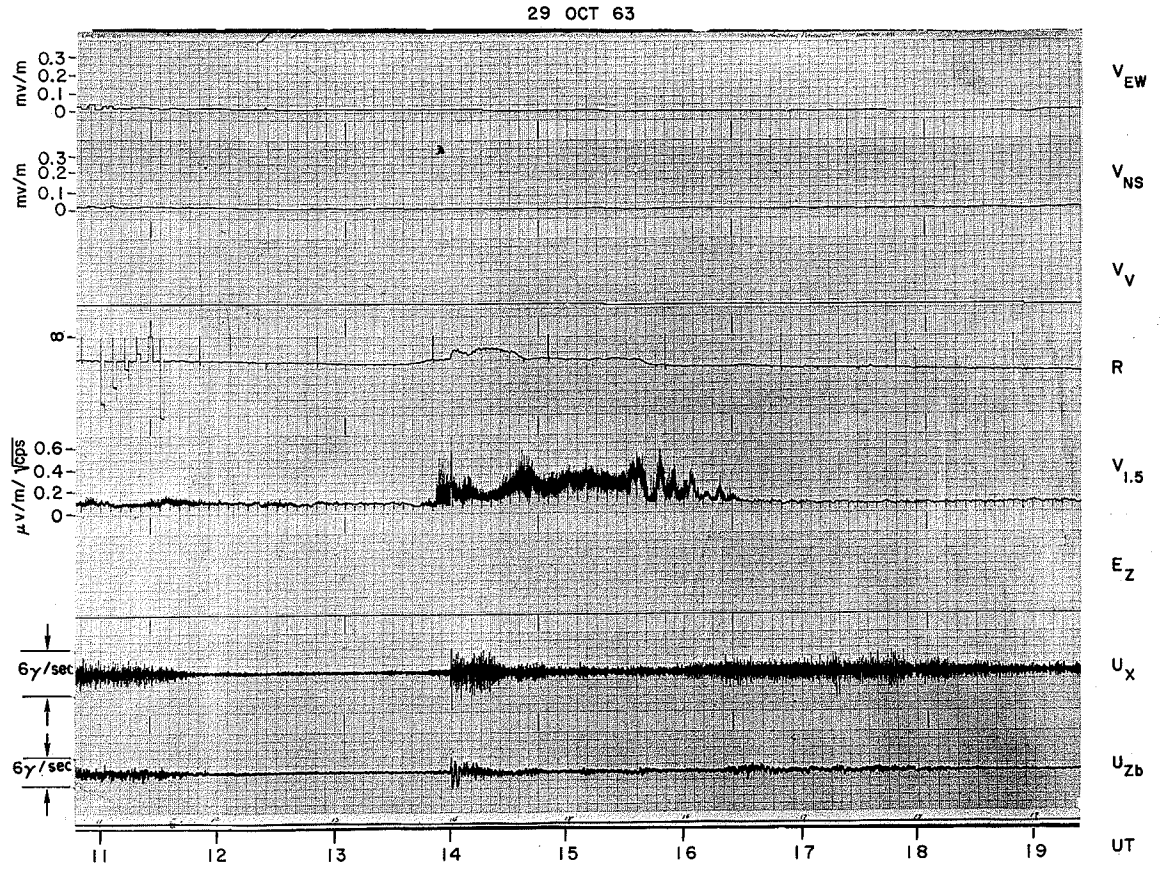

FIG. 17. DAY (D) EVENT OF OCTOBER 29, 1963, BYRD, ILLUSTRATING A POSITIVE CORRELATION BETWEEN IONOSPHERE ABSORPTION AND VLF 1.5 KC/S NOISE. The sudden onset of ulf at 1400 UT represents an SC. The elf channel was not in operation at this time.

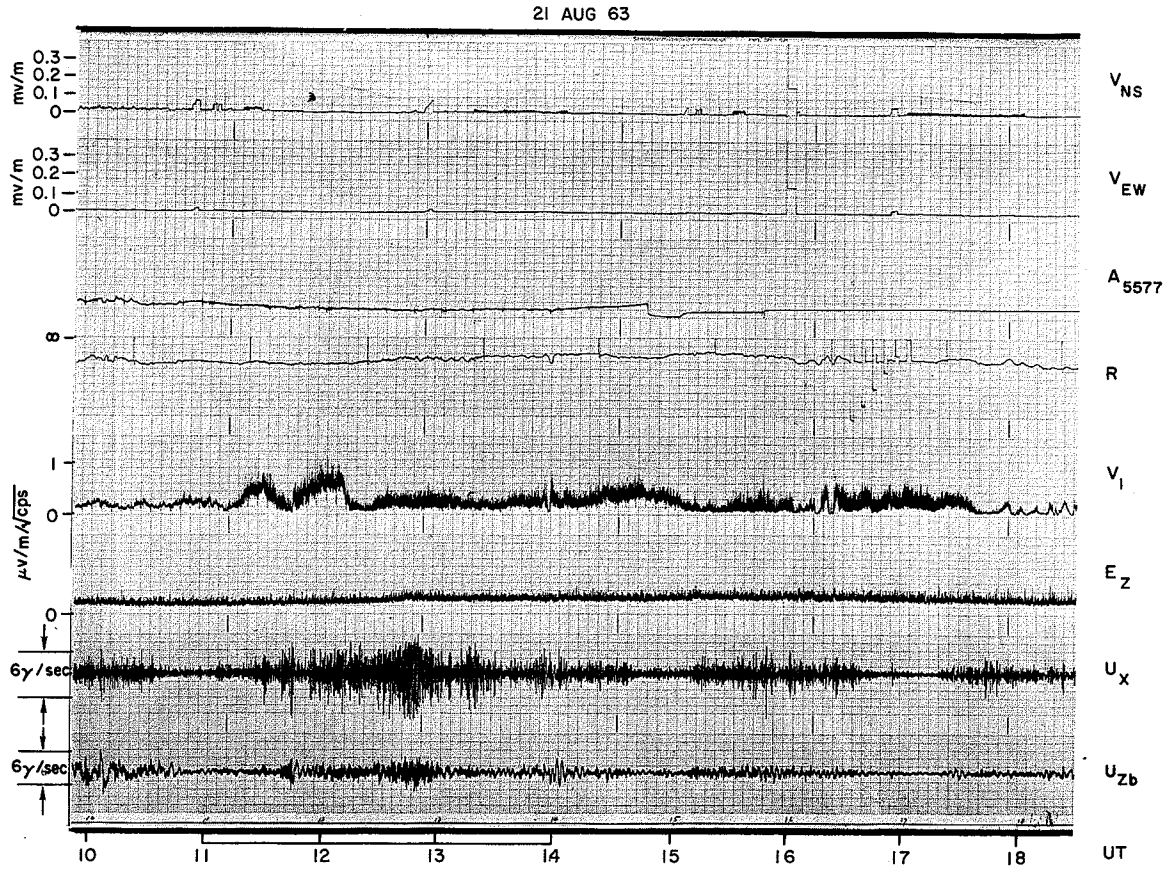

FIG. 18. DAY (D) EVENT OF AUGUST 21, 1963, BYRD. Many auroral pulsations are seen here (period 30 sec ~ 60 sec). Some of the pulsations are accompanied by similar variations on the riometer channel, e.g., at about 1130 and from 1210 to 1330. The photometer observation was discontinued at 1445 due to the increased solar illumination. A notable feature of the record is the simultaneous variation of 1 kc/s vlf, riometer, and photometer at 1355. The riometer and 1 kc/s vlf show almost one-to-one amplitude variations on several occasions.

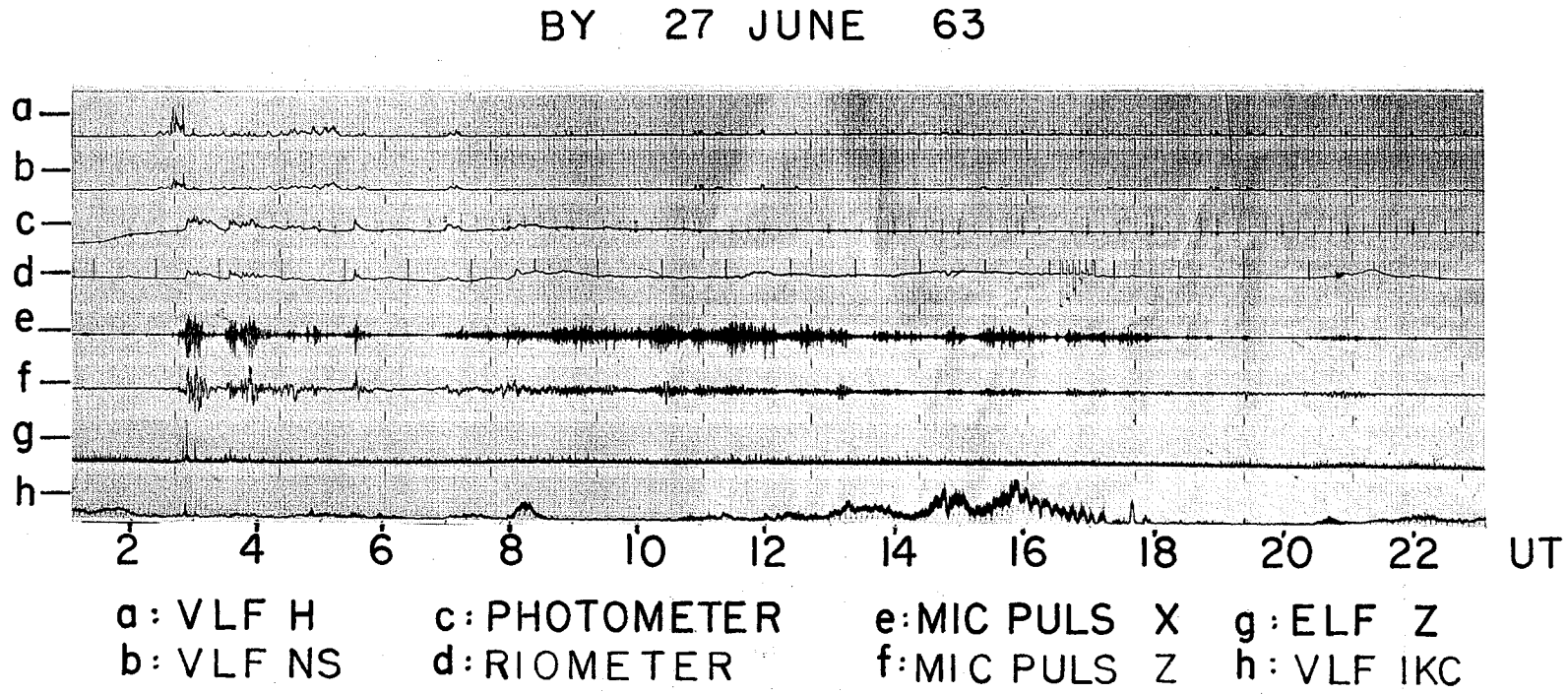

FIG. 19. CORRELATION RECORD OF JUNE 27, 1963, BYRD.

TABLE 4. SUMMARY OF CHARACTERISTICS OF THE NIGHT AND DAY EVENTS

	Night			Day
	N-1	N-2	N-3	D
Steady Hiss	H	0	0	0*
Impulsive Hiss	0	H	0	0*
Aurora	L	H	L	?(0)
Riometer	L	H	H	H
Elf	0	H	0	0
Micropulsations (P_i)**	0	H	0	0
Micropulsations (P_c)**	L	0	H	H
Vlf Chorus (1 kc/s)	0	0	H	H

H Present with a high amplitude, more than 1/2 full scale

L Present with a low amplitude, less than 1/3 full scale

0 Not present

*Vlf hiss is occasionally observed at the beginning of a D event, as shown in Fig. 13.

**Micropulsations are divided into two classes, a continuous type called P_c and an impulsive type called P_i. For further details see Jacobs, et al [1964].

J. STATISTICS

1. Diurnal Variation of Phases

The records for June 1963 were scaled for occurrence of the phases described above. Figure 20 shows the results, the ordinate of the graph being the percentage occurrence of events and the abscissa universal time. The letters AM and AN stand for auroral midnight and auroral noon [Brice and Ungstrup, 1963]. Shaded areas indicate that the observer is on the nightside of the magnetic hemisphere. The figure shows on a statistical basis the tendency discussed above for N-1 to dominate the early nighttime records and for N-3 to be predominant after midnight.

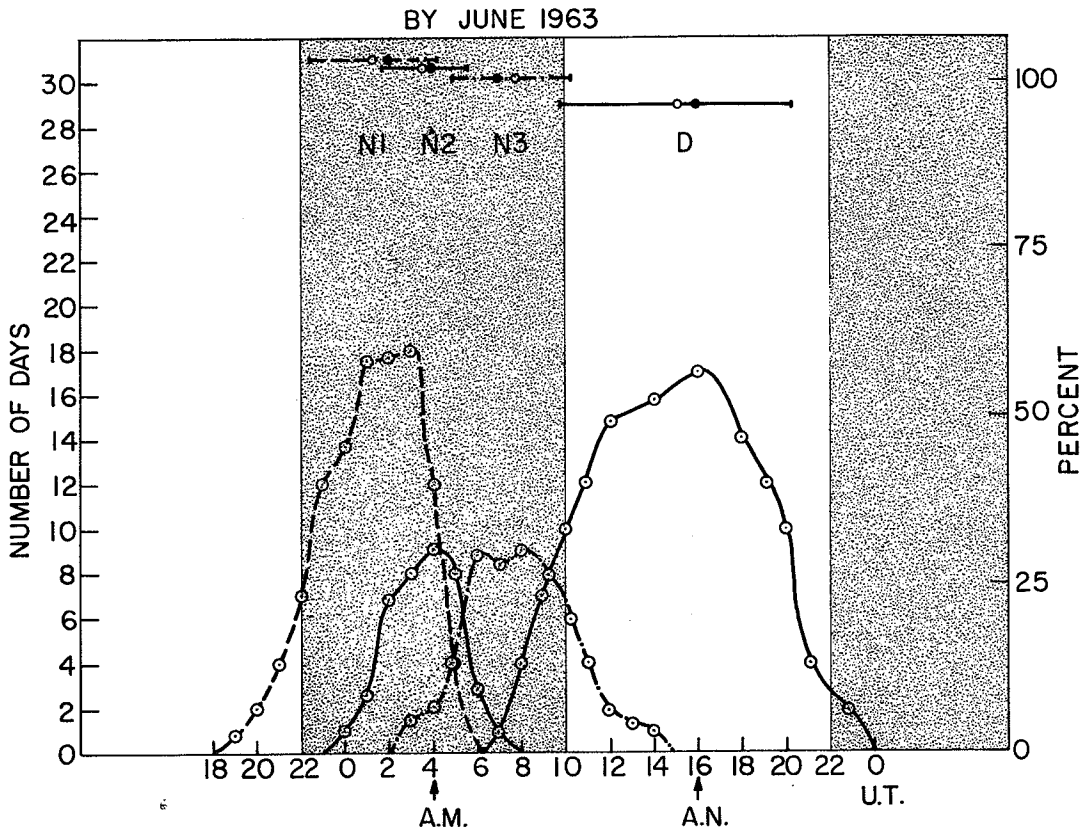

FIG. 20. DIURNAL VARIATION OF OCCURRENCE OF PHASES FOR JUNE, 1963, BYRD.

2. Seasonal Variation of Phases

Although this study did not cover the entire year, it is possible to make a number of comments on seasonal effects. For example, a seasonal variation was noted in the time of highest frequency of occurrence of the N-1, N-2, and N-3 phases. This effect is shown in Fig. 21 for the months May through October, 1963. The letters WS and SE along the abscissa stand for the winter solstice and the spring equinox. During the austral winter months, the universal time of highest frequency of occurrence of each phase tends to be relatively late. It is not clear whether these variations are due to seasonal effects or to variations in the solar wind (as manifested by the K_p sum). A plot of the K_p sum exhibited a similar trend, showing a September maximum. More data will be required before this question can be answered.

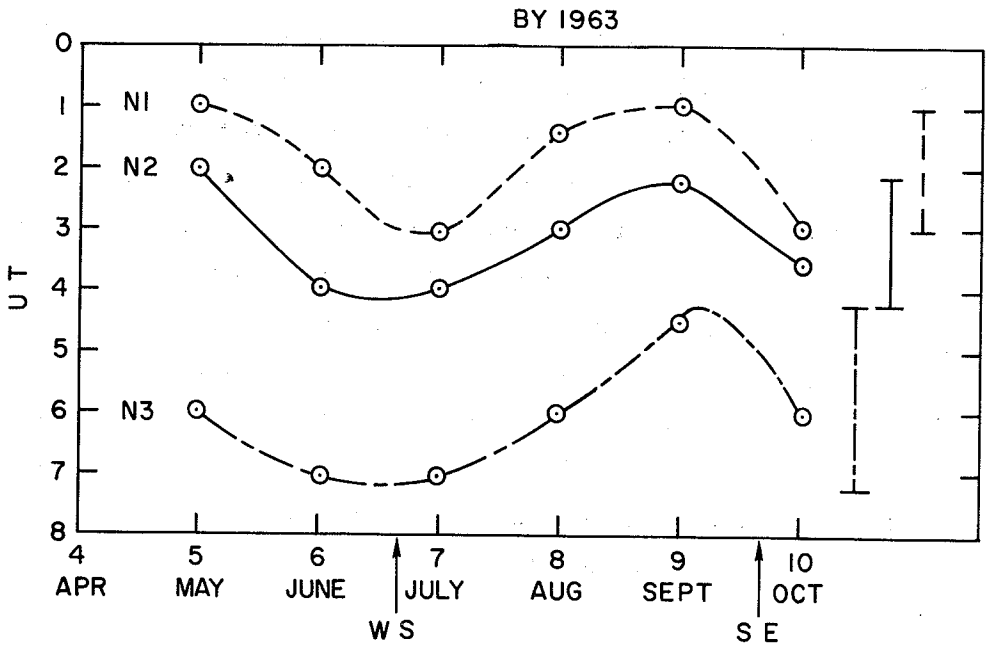

FIG. 21. SEASONAL VARIATION OF TIME OF OCCURRENCE OF NIGHT PHASES AT BYRD.

The maximum occurrence of each phase should not be confused with the occurrence time of the first night event as indicated by the onset of a negative bay. For example, Jacobs and Wright [1965] concluded from magnetograms that the time of the first onset of a negative bay tends to come earlier during the winter months and later during the summer months.

The percentage occurrence of certain phases also demonstrated a large seasonal effect. The N-1 phase tended to occur more frequently during the winter months. The maximum frequency of occurrence of N-1 in any one-hour period in June and July was 61 and 72 percent, respectively. For September and October these numbers were 42 and 43 percent, respectively. The N-2 and N-3 phases tended to exhibit the same maximum frequency of occurrence all the time, about 35 percent. The D event occurred about 60 percent of the time in winter (June), increased to almost 90 percent in September, then dropped to 68 percent in October.

Because we customarily used vlf hiss to identify N-1 and vlf chorus to identify D, it was possible to examine the seasonal variations of N-1 and D by simply using the seasonal variation of hiss and chorus. Vlf power spectral density data are available from Byrd for the year 1962. In Fig. 22 the average power spectral density of vlf emissions is plotted. These data were obtained from photographic records made with a panoramic sonic analyzer sweeping from 40 to 22,500 cps. Records were scaled for the peak value (chosen because of good definition) at half-hourly intervals. An example of an original record is shown in Fig. 23. This is an unusual case in which there were strong emissions observed in the range 2-3 kc/s. Numbers 1 through 8 in Fig. 23 are values measured from an eight-channel minimum reading hiss recorder. Note that there is a difference of about 10 db between these values and the peak values on the panoramic display.

Numbers on the contours of Fig. 22 show decibels above 10^{-18} w/m^2/cps. Note that in all four cases, there exist deep valleys in power spectral density in the 3 kc/s region. These valleys separate a higher-frequency (4 kc/s to above 20 kc/s) region and a lower frequency region (roughly 200 cps to nearly 2 kc/s). The higher-frequency region consists mainly of hiss.

Hiss intensity at 20 kc/s for the winter month (June) is 15 db higher than that for summer (December). This may explain the more frequent occurrence of N-1 during winter months. Chorus intensity at 1 kc/s shows relatively minor seasonal variations. However emissions at 600 ~ 700 cps show a summer intensity about 15 db higher than that of winter.

The decrease in hiss intensity could be explained by absorption. The estimated absorption at 20 kc/s and 70° geomagnetic latitude is about 18 db greater in daytime than at night [Helliwell, 1965]. Assuming that these figures correspond approximately to summer and winter at Byrd, much of the observed change of 15 db may then be accounted for in terms of absorption. On the other hand, the 15 db increase of chorus in summer must occur in spite of absorption, which in summer is estimated to increase 5 db in the 600 ~ 700 cps band. In these terms there is a total

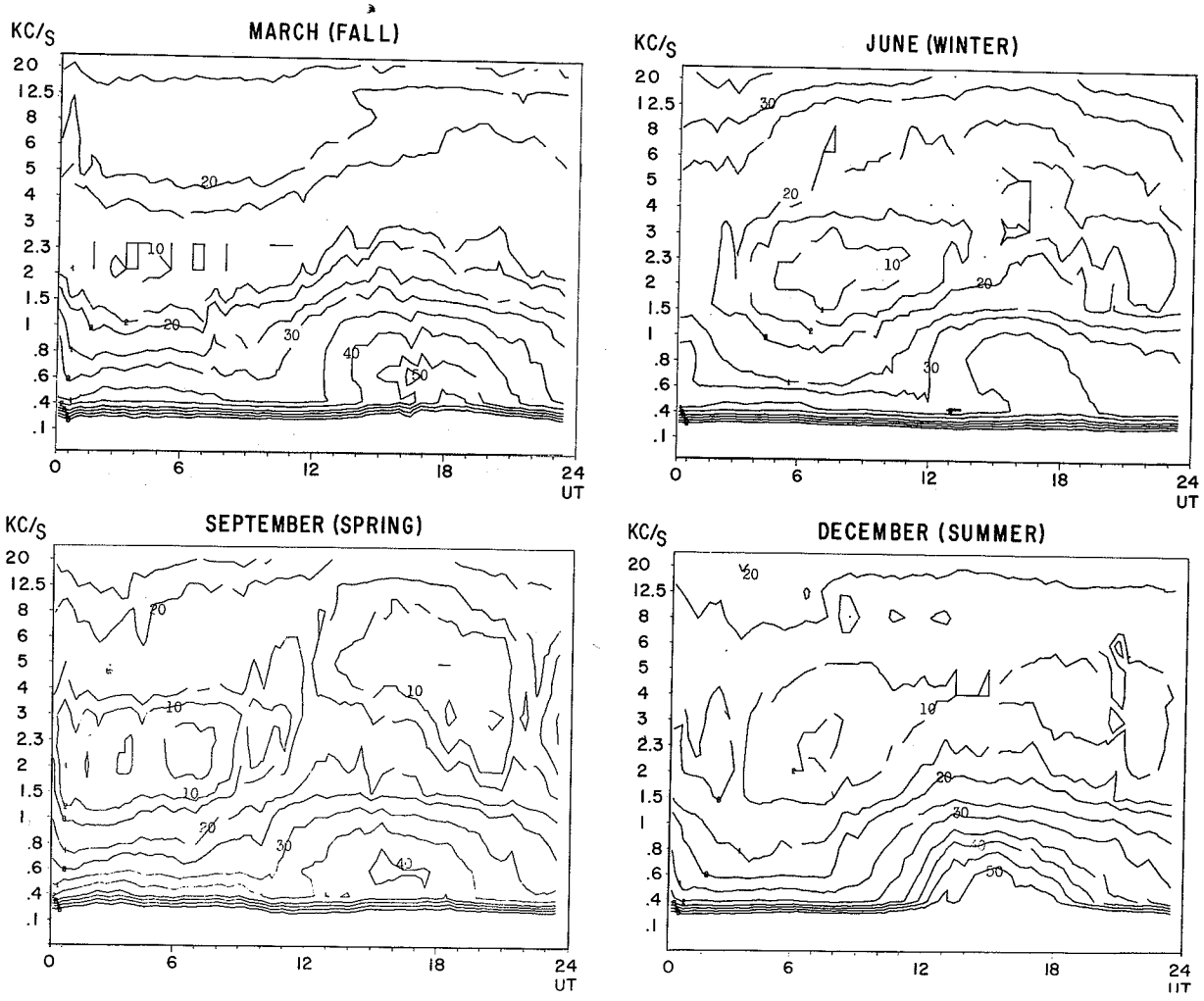

FIG. 22. VLF AVERAGE POWER SPECTRAL DENSITY FOR DIFFERENT SEASONS IN 1962 AT BYRD, VERSUS FREQUENCY AND TIME.

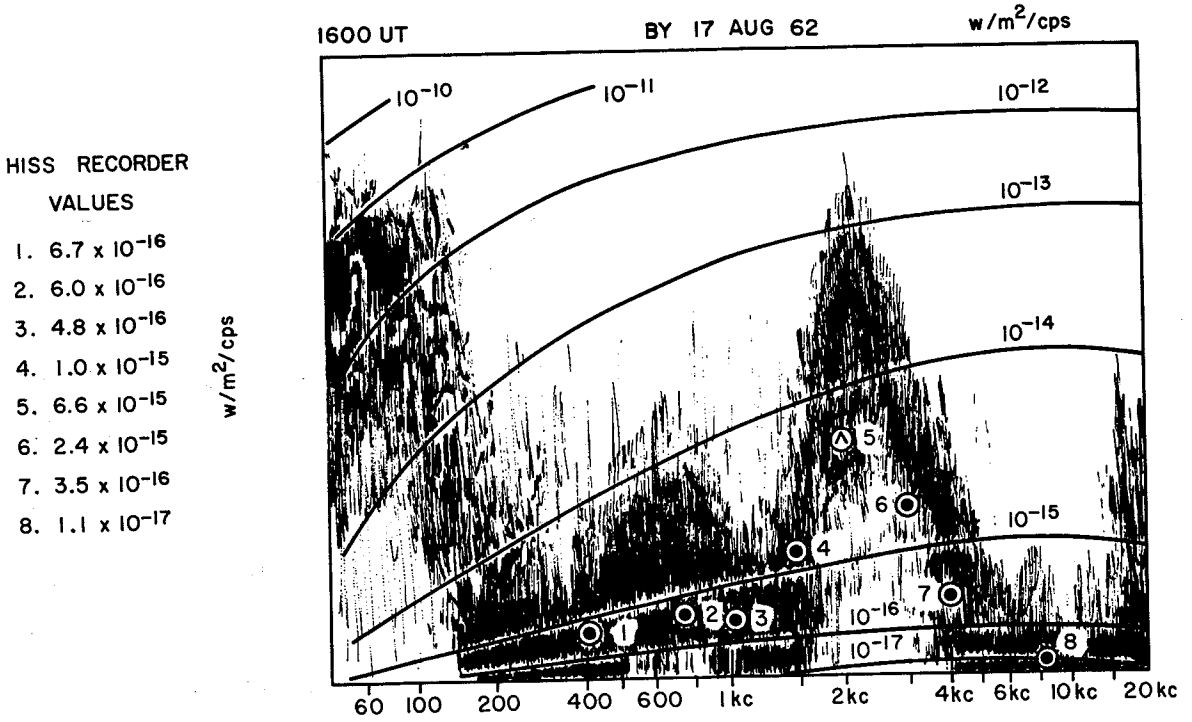

FIG. 23. EXAMPLE OF PANORAMIC RECORD OF VLF SPECTRUM, 1600 UT, AUGUST 17, 1962, BYRD.

change of about 20 db (a factor of 100 in power) during the summer months over winter months.

Although the 1962 data do not show an appreciable change in 1 kc/s emission strength between June and September, in 1963 a large increase in "D" activity after sunrise was seen during September, a month in which K_p showed a substantial increase from previous levels.

A comparison was made of 1 kc/s and 8 kc/s data scaled from a chart recorder in 1963 for the months of June and September. It was found that the hiss intensity measured at 8 kc/s decreased about 6 db in September. A similar decrease is seen from the 1962 contour map of Fig. 22. In 1963, the 1 kc/s emissions increased in September by 4 db, in keeping with the increased occurrence of "D" events as identified from the correlation charts. From these results we conclude that the decrease in 1 kc/s intensity during the summer months of 1962 is a characteristic of that year, and cannot be compared with the 1963 correlation data.

More analysis is needed to explain the September increase in the occurrence of D events.

K. DIURNAL VARIATION OF GEOPHYSICAL PARAMETERS TAKEN FROM OTHER THAN CORRELATION CHARTS

Data on auroral occurrence, magnetic K local, sporadic E of type "a," ionospheric absorption, vlf hiss and vlf chorus are plotted in Fig. 24 to give further insight into the correlation study.

The percentage occurrence of auroras was provided by J. H. Kinsey of the Arctic Institute of North America. The data were scaled from the all-sky camera film every hour. The average of the local magnetic K figure was taken from the USCGS record. The time resolution for these data is 3 hours. Data for the ionospheric parameters were scaled from F plots.

In Fig. 24, the measure of absorption based on ionosonde data is the occurrence of blackout (solid line). A single case was said to occur if one or more of the 15-minute samples in the hour showed blackout. Thus the number should be 30 for 100 percent blackout for that hour for the month. The unit of absorption based on the riometer is 0.1 db. The continuous riometer records were scaled for peak absorption on an hourly basis and then the data were averaged over 30 days (dashed line).

Vlf hiss and chorus data were scaled from the 8-channel spectrum analyzer. The average power density above the reference level of $2.46 \times 10^{-17} w/m^2/cps$ for hiss and $1.41 \times 10^{-16} w/m^2/cps$ for chorus were scaled. The numbers on the ordinates are in db above the reference level. Hiss data are based on hourly scalings of the maximum pen deflection of the hiss recorder. An average of the 4-kc/s and 8-kc/s channels was taken to represent the hiss. An average of the 750-cps, 1-kc/s, 1.5-kc/s, and 2-kc/s channels was taken to represent chorus.

In Fig. 24 it may be seen that aurora, sporadic E of type "a," vlf hiss, K local, and ionospheric absorption (riometer) exhibit peaks during the night regime, whereas ionospheric blackout (ionosonde and riometer) and vlf chorus peak during the day regime. These statistics clearly support the existence of two well-defined but significantly different regimes.

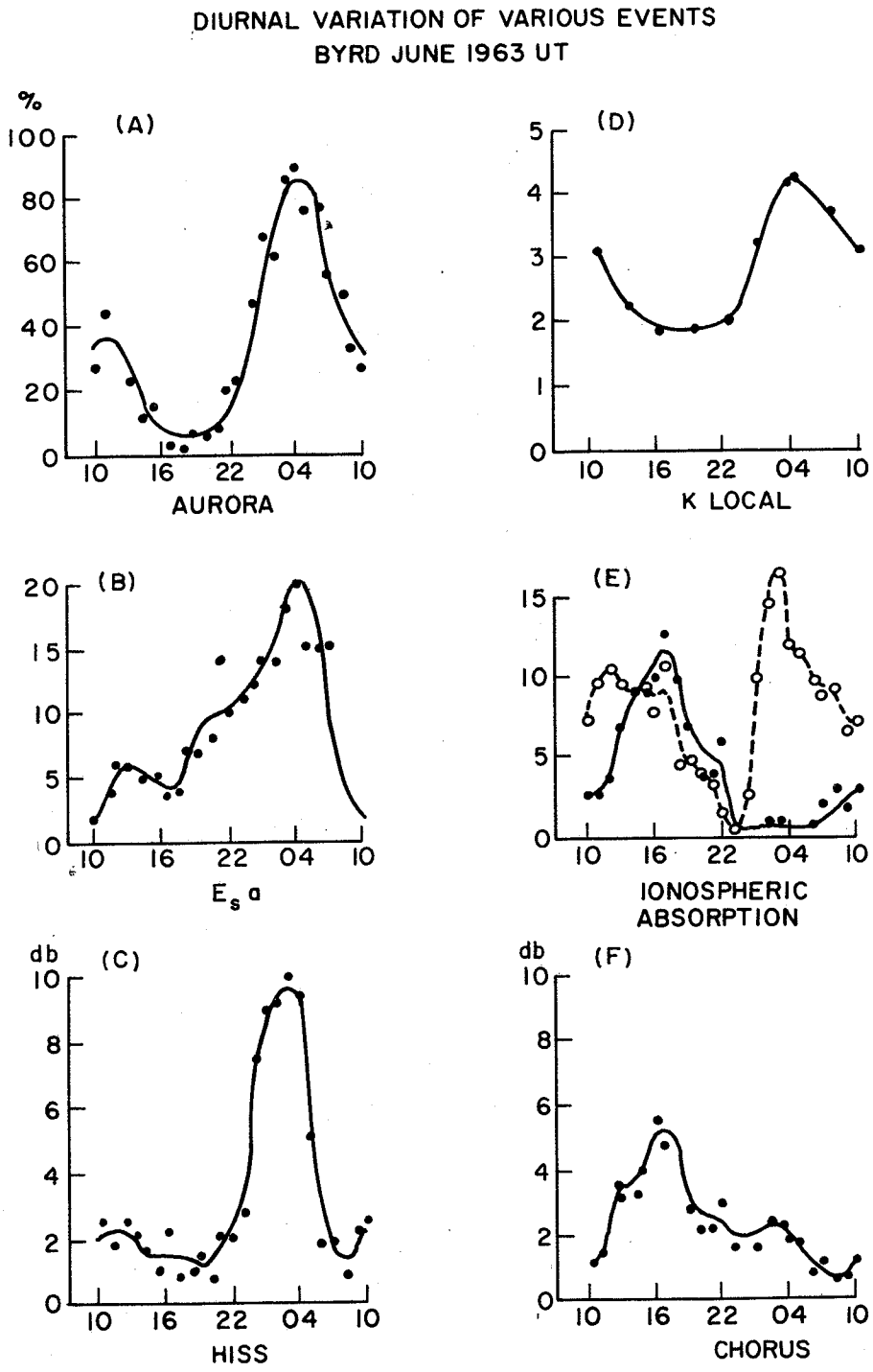

FIG. 24. DIURNAL VARIATION OF VARIOUS PHENOMENA AT BYRD FOR JUNE 1963.

L. COMPARISON WITH OTHER STATIONS

In order to obtain some understanding of the geographic extent of the phenomena observed at Byrd, a preliminary comparison was made with data from other stations, principally Eights. It was found that Byrd (71° S dipole latitude) receives more hiss than Eights (64° S dipole latitude). The reverse situation was true for vlf chorus. Figure 25 shows a comparison of a typical example of a hiss event observed at five different stations: Great Whale, Quebec City, Eights, Byrd, and South Pole. Great

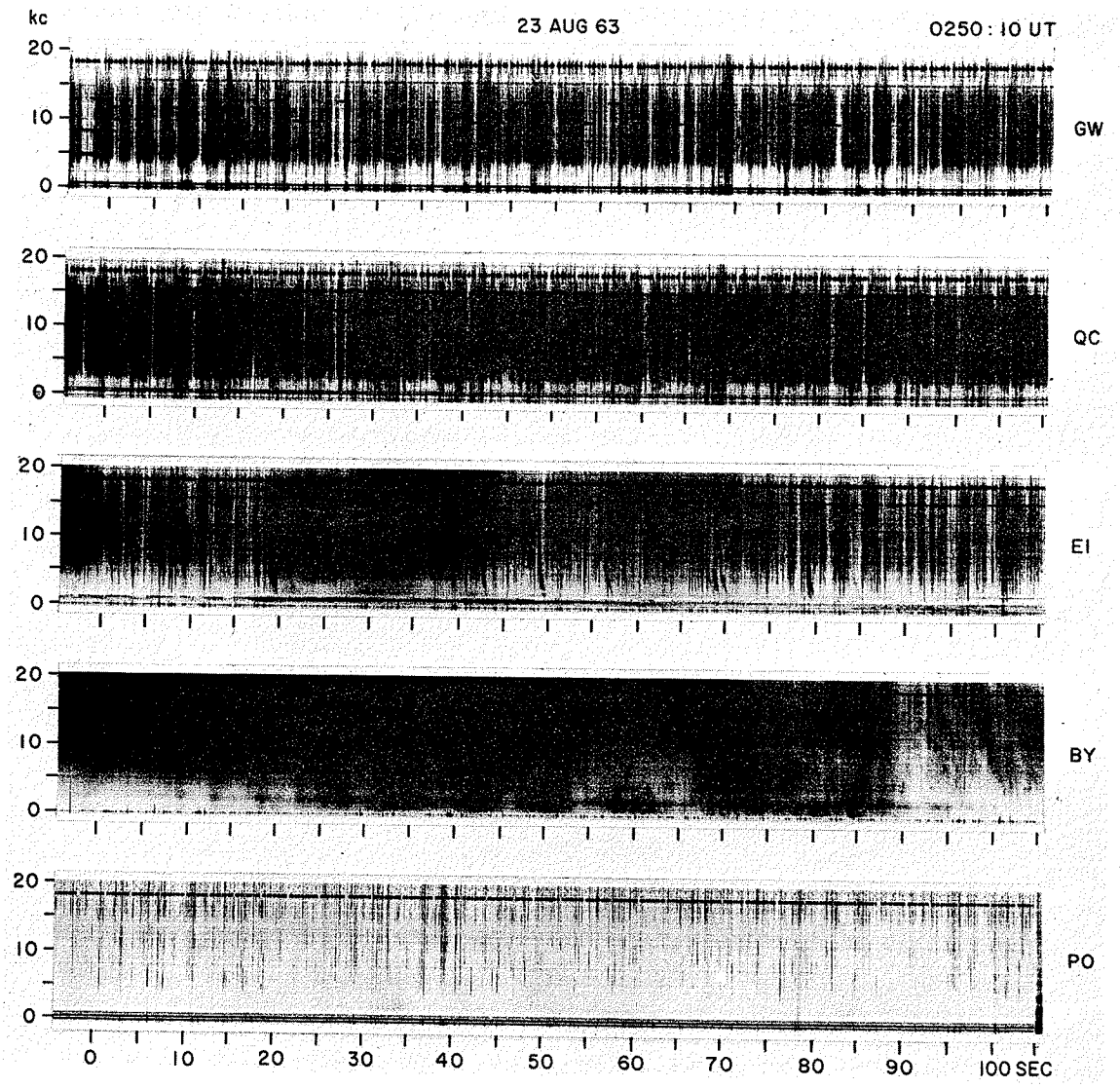

FIG. 25. SPECTRA OF A HISS EVENT ON AUGUST 23, 1963, OBSERVED AT FIVE STATIONS.

Whale - Byrd and Quebec City - Eights are conjugate pairs. No conjugate record for Pole Station is available. Note the complete absence of hiss at Pole Station. Dark lines on the Great Whale and Quebec City records are caused by sferics; however, the short periods of low noise between sferics indicated no evidence of hiss at these northern hemisphere stations. The hiss is strong at Byrd, but only the peaks are evident at Eights (e.g., the period 20 - 40 secs). In most cases studied, the hiss was much stronger at Byrd than at Eights.

Chorus, on the other hand, was observed more frequently at Eights than at Byrd. This difference was most marked when N-1, N-2, and N-3 phases were present at Byrd, and only the N-2 and N-3 phases were observed at Eights. Eights data for 2 June are shown in Fig. 26 for comparison with the corresponding data from Byrd shown in Fig. 5. Note the complete lack of hiss at Eights. However, an elf burst was observed at Eights and at Byrd at 0519, indicating the beginning of the N-2 phase. The subsequent N-3 phase at Eights lasted for about the same length of time as at Byrd, but the details of the chorus spectrum clearly differed between the two stations.

In general, it was found that when events of a broadly similar type were recognizable at both Byrd and Eights, magnitudes differed but commencements were essentially simultaneous.

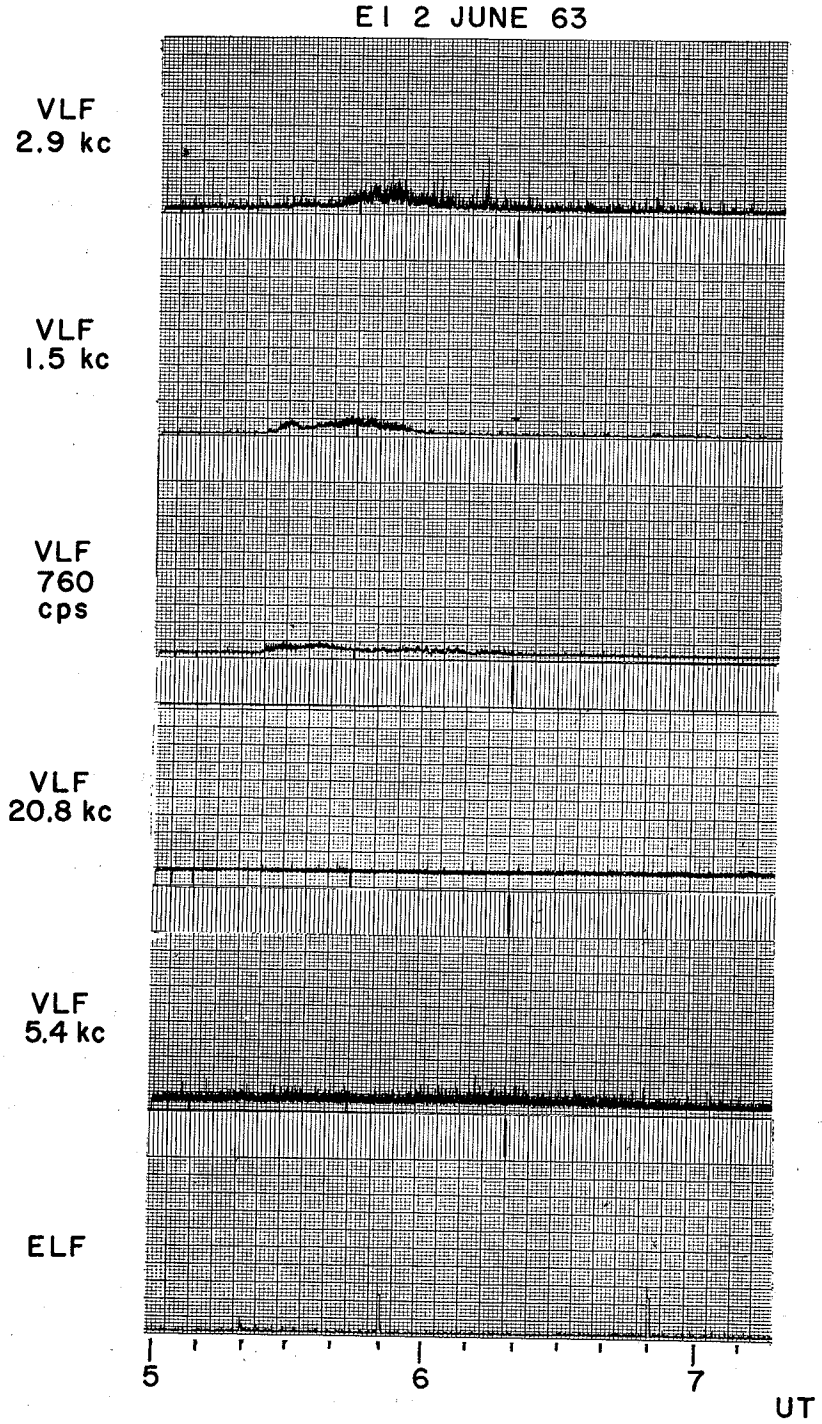

FIG. 26. VLF AND ELF RECORD FROM EIGHTS FOR JUNE 2, 1963.

III. SUMMARY AND DISCUSSION

We have reported a diurnal variation pattern of high latitude geophysical phenomena. Heppner [1954], from his studies of the aurora, concluded that results from the observations made at one station may safely be generalized to apply to other locations of the same geomagnetic latitude. Since Byrd is located in the auroral zone, we believe that results from the present study may be treated as typical of the auroral zone.

In view of the broad scope of the present research both in quantities compared and recording period, we have presented the results without detailed reference to previous work. As might be expected, however, there is a close relation between the results reported here and much that is already known about specific correlations of particular phenomena. For example, Morozumi [1962] reported that vlf hiss was associated with arcs and band types of aurora, but not with rays. Vlf-associated arcs and bands often exhibited a pink lower border (type B). Two classes of arcs and band type aurora were reported, one (class one) which is not followed by breakups, and the other (class two) which is followed by breakups. A one-to-one correlation showed that for class one displays, auroral light and hiss intensities tend to change simultaneously. In class two displays, the initial stage is similar to that of class one, but hiss intensity drops almost to zero after the breakup. Morozumi also noted that the maximum occurrence frequency of class one aurora preceded that of class two aurora by a few hours. These two types of aurora are now recognized from the present work as corresponding to the N-1 (class one) and N-2 (class two) phases.

Ungstrup [1964] reported a close connection between chorus-like vlf emissions and flickering aurora. This aurora appears to have properties similar to the aurora of N-3. Harang and Larsen [1964] at Tromsø compared vlf 8 kc/s and riometer records. He found a positive correlation between vlf hiss intensity and riometer records when the magnitude of absorption was $\sim$0.3 - 0.9 db. For a large riometer event of 5 - 9 db, he found the correlation to be negative. These two types of event appear to correspond to our N-1 and N-2 phases. Morozumi [1962]

noted a peak in geophysical disturbances on the dayside of the magnetic hemisphere. The day peak was characterized by faint aurora and high ionospheric absorption. This peak is now recognized as phase "D," according to our definition. Hargreaves, et al [1964] made an extensive study of South Pole riometer data. They found two different types of absorption peaks, analogous to our N and D peaks. Investigations by Jacobs and Wright [1965] revealed that morning and evening peaks of micropulsation events are observed at high latitude conjugate stations.

Ansari [1964] compared narrow beam riometer and all-sky camera records and found four phases for typical nighttime events. His phase 1 corresponds closely to the authors' N-1. The N-2 event reported in this work and Ansari's phase 2 are the same, but we did not observe Ansari's phase 3. The N-3 phase described in this paper is somewhat similar to Ansari's phase 4.

Nearly all of the observational results presented above were analyzed from records taken at one station, so that the spatial extent of the semidiurnal pattern was not well defined. Recently, Sandford [1964] analyzed spectrographic records taken from several Antarctic stations and deduced the contours of a semidiurnal auroral luminosity pattern. On this and the foregoing evidence, the existence of morning and evening peaks (in this note called day and night peaks) is now established beyond doubt.

The present work provided a basis for dividing the night peak into three distinct phases, each with special properties. We found that a night event usually consists of elements of all three phases N-1, N-2, and N-3. However, the N-1 characteristic tends to dominate early in the evening, all three are often well defined in mid-evening, and in the late evening, the magnitude of N-3 tends to exceed those of N-1 and N-2.

During the N-1 phase, we observed vlf hiss and arc and band type aurora [Morozumi, 1962]. N-2 is the breakup phase of the aurora, while N-3 is the post breakup phase, in which vlf chorus and absorption were often observed without a corresponding increase in auroral luminosity.

The spatial extent of events occurring in the night and day regimes has not yet been investigated. However, we briefly compared records obtained from South Pole, Byrd, and Eights Stations. It was found that

at Byrd Station, the N-1 phase occurs more frequently than at Eights Station. Vlf chorus was recorded more frequently at Eights. When an event was recognizable at both Eights and Byrd, there was no time lag between the respective times of onset.

Further evidence of the spatial distribution of vlf emissions is found in the satellite vlf data obtained from Injun III [Gurnett and O'Brien, 1964]. An example of the satellite data is given in Fig. 27, which shows the relation between trapped electrons and vlf emissions. As the satellite moved poleward, the trapped electron count started to increase at about $L = 3.5$, and continued to increase until $L = 5.7$. Note that vlf chorus was observed below a frequency of about 4 kc/s and between $L = 3.7$ and $L = 5.3$. This type of chorus was compared aurally with that observed at the N-3 phase in Fig. 5, and the two were found to be virtually identical. The spectrum of the chorus of Fig. 5 is shown in Figs. 7c and 7d and may be seen to exhibit some evidence of periodicity. Studies of periodic emissions [Helliwell, 1965] suggest a closed field line configuration for the generation of such emissions, which is again consistent with the trapping of particles.

At $L = 5.7$ (Fig. 27) there is an abrupt decrease in the counting rate of trapped electrons by a factor of 1000 or more. Gurnett (private communication) observed precipitation of low energy electrons beyond this trapping boundary. Note that hiss begins suddenly at the boundary. At the time of this writing, it is not clear that the type of hiss observed on the ground is always the same as that observed on the satellite. However, there is an analogy between the trapping boundary and our N-2 phase. Beyond $L = 5.7$, auroral hiss is observable with decreasing amplitude. This region appears to be related to our N-1.

Gurnett (private communication) finds that the regions described exist almost all the time in a certain sector of the magnetic hemisphere. In order to reconcile the temporal sequence of phases on the ground with a fixed spatial pattern observed in satellites, it is convenient to postulate that some process sequentially excites or enhances the spatial pattern every hour or two. This causes the three phases to be observed in sequence on the ground. The observation of impulsive effects is nearly simultaneous over distances of several hundred km, due to the

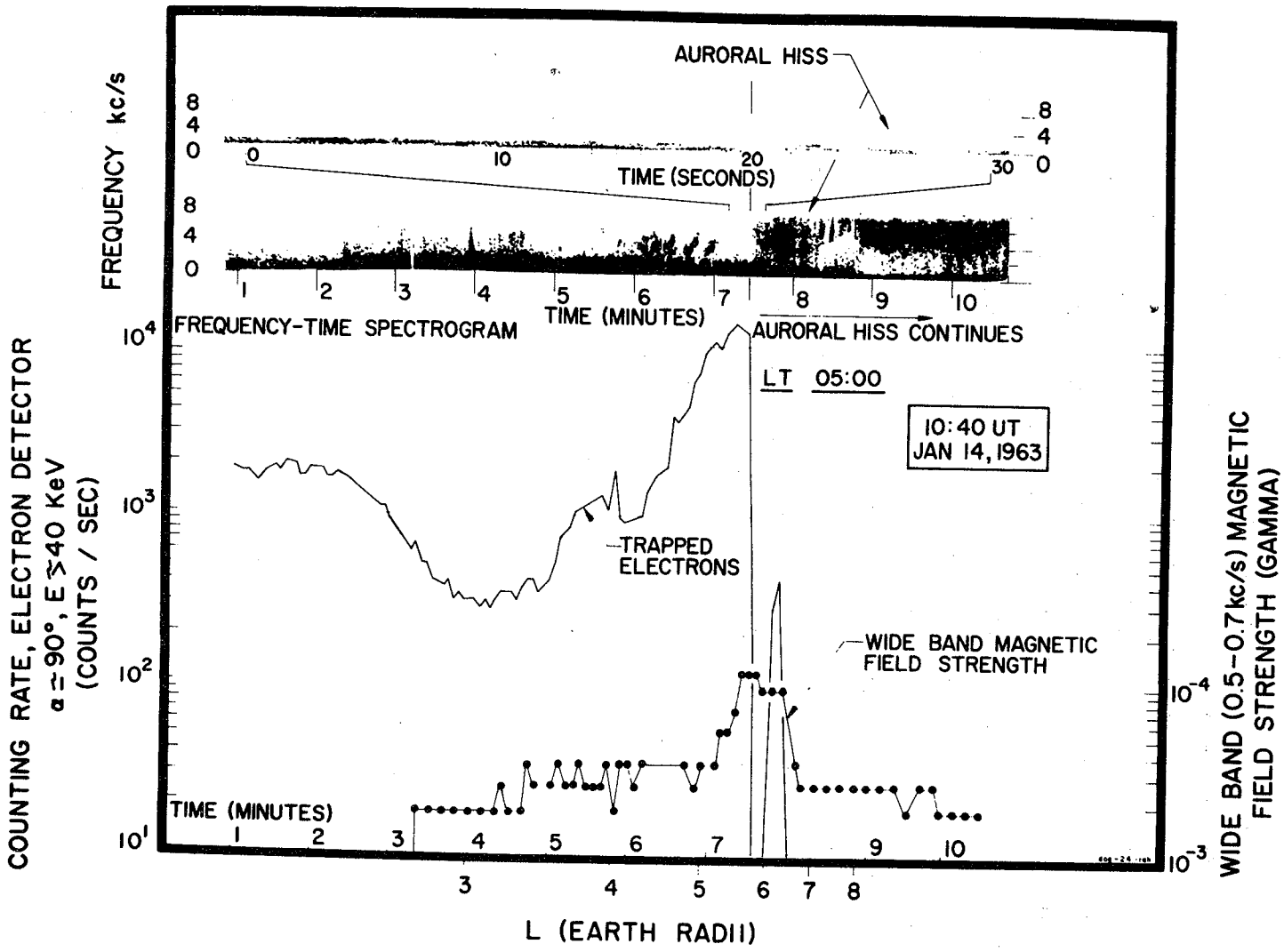

FIG. 27. RELATION BETWEEN TRAPPED ELECTRONS AND VLF EMISSIONS SEEN BY THE INJUN III SATELLITE ON JANUARY 14, 1963 (COURTESY OF D. GURNETT).

apparently large effective areas of some of the phenomena. As the earth rotates, a ground station moves with respect to the spatial pattern, resulting in changes in the relative intensity of a phase as the station moves closer to or away from the 'source region' of that phase.

The present study did not enable us to establish a clear picture of the day event. However, the day event often suggests a sequence analogous to that of N-1, N-2, and N-3, with emphasis on the characteristics of N-3.

A summary of the semidiurnal pattern of geophysical disturbances described in this paper was presented in Table 4.

For further work, a more detailed study of day (morning) events is recommended. The transition period between day (morning) and night (evening) should be investigated carefully. It is important to determine the relation between the temporal variation found in this work and the spatial variation found by Injun III [Gurnett and O'Brien, 1964]. To accomplish this, a careful comparison of spaced station data and of simultaneous satellite records is recommended.

IV. INSTRUMENTATION

The various data acquisition systems used at Byrd Station for this study are described in this section. The signals measured, the channel coding adopted, and the characteristics of the receiving and recording systems are listed in Table 5.

A. VLF SYSTEM

A block diagram of the vlf system is shown in Fig. 28. (For a discussion of the system see [Marks, 1962].) A loop antenna is used to detect the magnetic component of the electromagnetic wave in the frequency range of interest. The preamplifier signal is presented to a broadband vlf receiver (200 cps - 25 kc), a panoramic spectrum analyzer (200 cps - 21.5 kc), and to an eight channel frequency spectrum analyzer.

The following recording formats were available: 1) the broadband output recorded in real time on magnetic tape; 2) the panoramic spectrum analyzer output recorded on film; 3) narrowband vlf amplitude recorded on chart paper. For the panoramic display, there were two modes, log amplitude vs log frequency, and log frequency vs time. In the first mode, the sweeps (1 per second) were integrated on film for 60 seconds. A framing camera was used throughout the year to film the consecutive 60 second periods. In the second mode, the scope display of an intensity-modulated oscilloscope was filmed by a continuous motion camera.

In the narrowband format, an eight-channel spectrum analyzer (Fig. 29) recorded the absolute amplitude of vlf activity at center frequencies of 0.4, 0.75, 1.0, 1.5, 2.0, 3.0, 4.0, and 8.0 kc/s respectively. The 8 kc/s channel sampled a frequency band whose width was 150 cps wide, while the remaining seven channels sampled frequency bands which were 10 percent of the band center frequency.

The various loop antenna parameters are shown in Table 6(a). The broadband vlf receiver frequency response curve is illustrated in Fig. 30. The upper and lower 3 db points for different periods are listed in Table 6(b). To calibrate the vlf system the constant current method [Smith, et al, 1958] was used.

TABLE 5. SUMMARY OF INSTRUMENTATION

	Code	Center Freq.	Bandwidth	Time Const. (sec)	System Sensitivity *	Chart Recorder Sensitivity **	Dynamic Range (db) ***	
							In	Out
VLF vertical loop NS	V_{NS}	BB	1-25 kc/s	Rise 5 Fall .05	10^{-18} w/m^2/cps	.025 mv/m	100	30
VLF vertical loop EW	V_{EW}	BB	1-25 kc/s	Rise 5 Fall .05	10^{-18} w/m^2/cps	.025 mv/m	100	30
VLF vertical	V_V	BB	1-25 kc/s	Rise 5 Fall .05	10^{-18} w/m^2/cps		100	30
VLF horizontal loop	V_H	BB	1-25 kc/s	Rise 5 Fall .05	10^{-18} w/m^2/cps	.012 mv/m	100	30
VLF 1 kc/s	V_1	1 kc/s	100 cps	Rise 5 Fall .05	1.2×10^{-18} w/m^2/cps	10^{-17} w/m^2/cps	100	30
VLF 1.5 kc/s	$V_{1.5}$	1.5 kc/s	150 cps	Rise 5 Fall .05	1.2×10^{-18} w/m^2/cps	10^{-17} w/m^2/cps	100	30
Auroral photometer	A_λ	5577 A	50 A	.25		1 KR	60	30
Riometer	R	30 Mc/s	60 kc/s	7	.1 db	.3 db	0-∞	17
ELF Z	E_Z	BB	2-40 cps		2 μγ	60 μγ	80	30
ULF X	U_X	BB	.02-5 cps		200 μγ (at 0.5 cps)	100 mγ (at 0.5 cps)	110	30
ULF Y	U_Y	BB	.02-5 cps		200 μγ (at 0.5 cps)	100 mγ (at 0.5 cps)	110	30
ULF Z	U_Z	BB	.02-5 cps		200 μγ (at 0.5 cps)	100 mγ (at 0.5 cps)	110	30
ULF Z	U_{Zb}	BB	~dc-5 cps		200 μγ (at 0.5 cps)	100 mγ (at 0.5 cps)	110	30

*The system sensitivity is set by the minimum signal detectable above the receiver noise.

**The chart recorder sensitivity is set by the minimum resolvable deflection on the chart.

***The IN column is the dynamic range of the input signals above the system sensitivity and which are simplified without distortion. The OUT column is the dynamic range of the input signal from resolvable deflection to saturation.

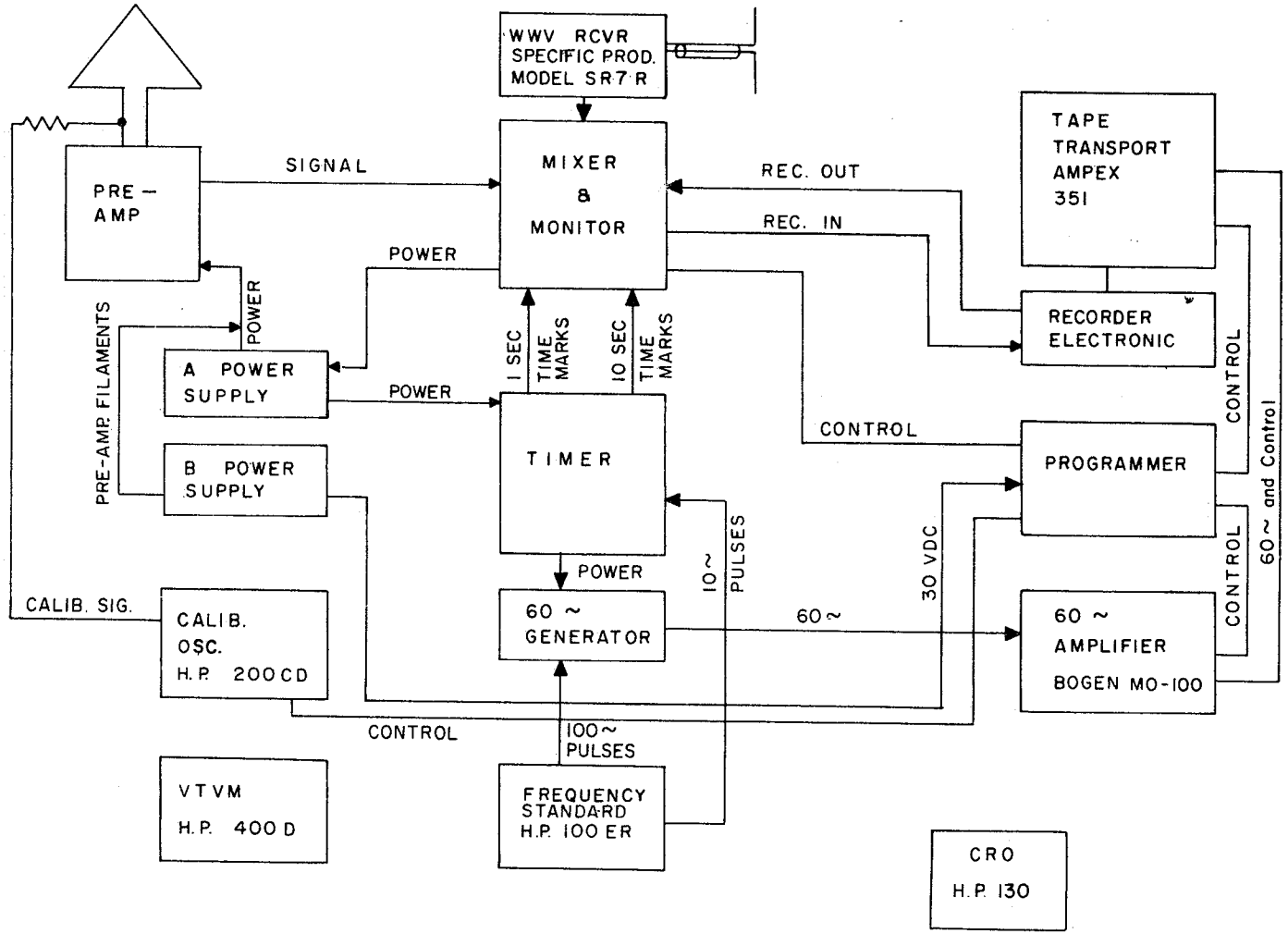

FIG. 28. BLOCK DIAGRAM OF BYRD AND SOUTH POLE WHISTLER RECORDERS.

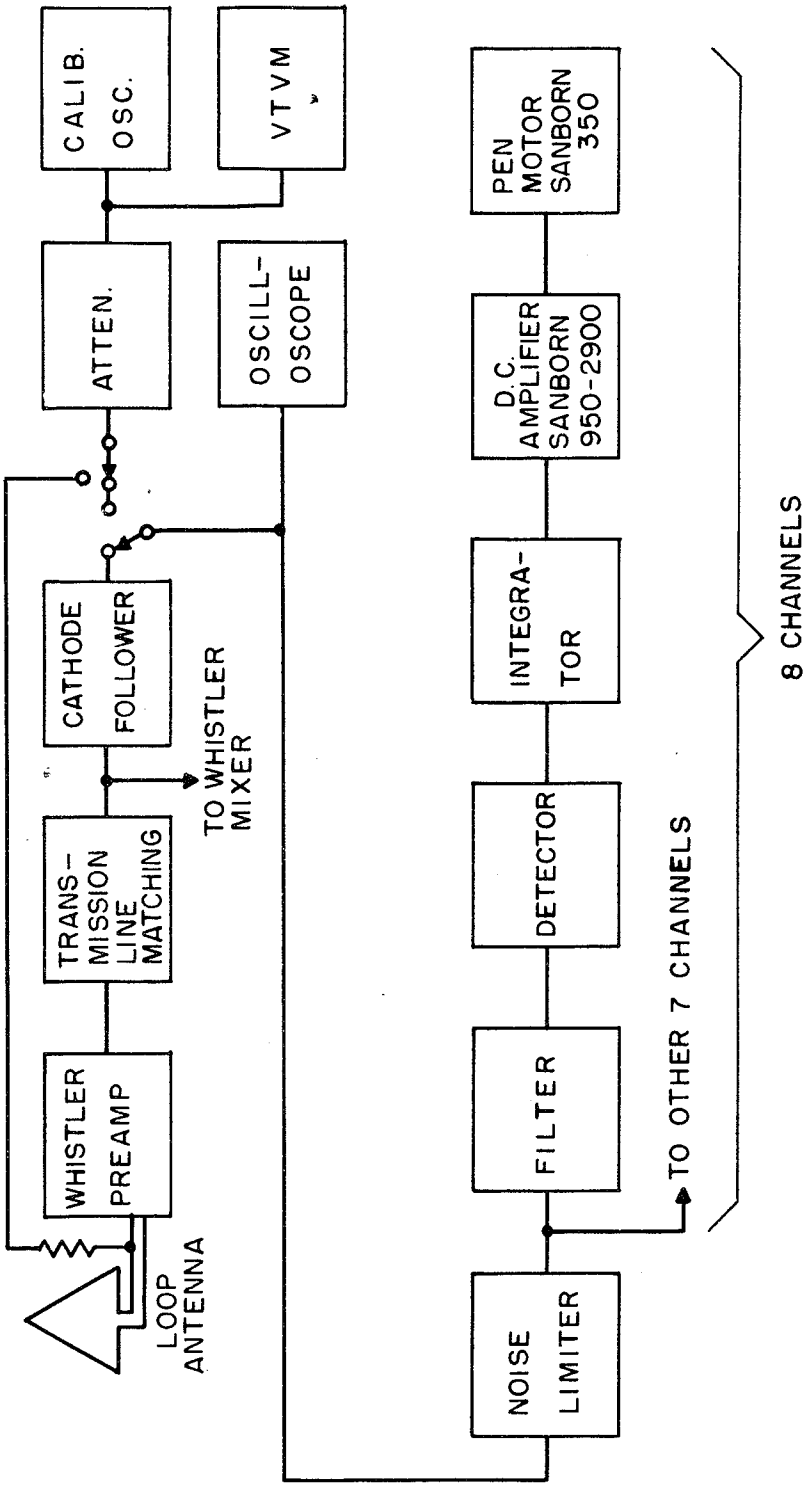

FIG. 29. BLOCK DIAGRAM OF HISS RECORDER, BYRD STATION.

TABLE 6. (a) ANTENNA PARAMETERS

	L	RDC (ohms)	Q	Cal. Factor	Antenna Orient.
IGY	70 μh	.072	6.1	12.4	N 27° E
USW*	65 μh	.058	6.4	17.5	N 27° E
USP**	51 μh	.026	11.4	22.9	N 27° E

*Under-snow wire antenna, see [Helms, 1964].

**Under-snow pipe antenna, see [Helms, 1964].

(b) MINUS 3 db POINT OF FREQUENCY BANDWIDTH OF VLF RECEIVER

NOV 1962	400 cps	-	17 kc/s
FEB 1963	200 cps	-	25 kc/s
AUG 1963	250 cps	-	25 kc/s
SEP 1963	260 cps	-	25 kc/s
OCT 1963	250 cps	-	24 kc/s

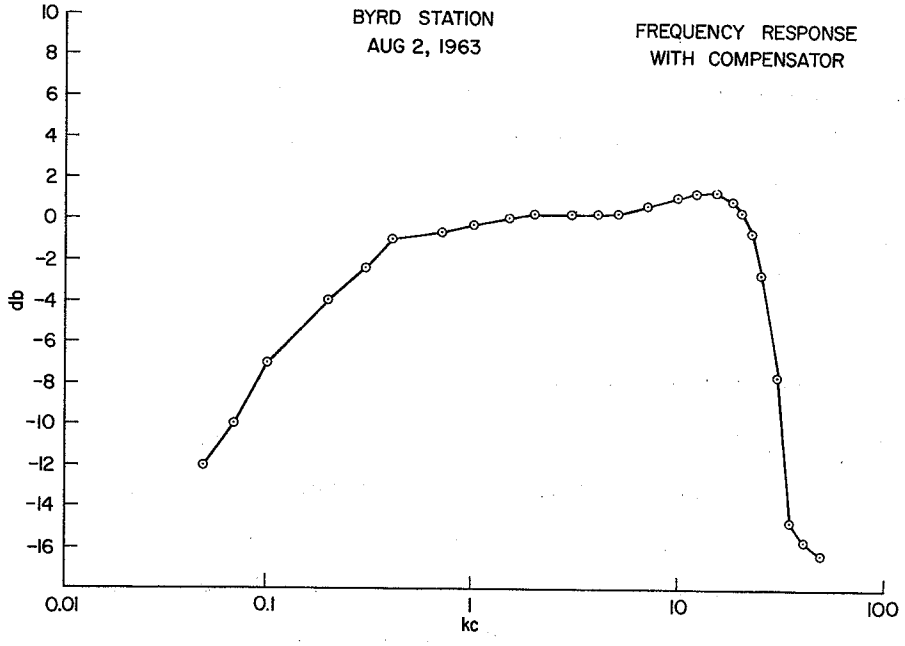

FIG. 30. FREQUENCY RESPONSE CURVE, AUGUST 1963, BYRD STATION.

B. THE ELF SYSTEM

The block diagram of the elf equipment is shown in Fig. 31. See Lokken [1964] for a detailed description of equipment and calibration techniques used for this type of measurement.

C. THE ULF SYSTEM

The block diagram of the ulf system is shown in Fig. 32. See Lokken [1964] and English, et al [1962] for a detailed description of this type of measurement.

D. THE AURORAL PHOTOMETER SYSTEM

The auroral photometer shared in this study was the property of the Arctic Institute of North America. A diagram of the optical system is shown in Fig. 33. The photometer was located atop the aurora tower, which is about 3000 feet from the vlf laboratory. The photometer dc output modulated a vco and was transmitted by a coaxial transmission line where the signal was demodulated. A low-pass filter was used to eliminate any interference, that might be picked up on the transmission line.

E. THE RIOMETER SYSTEM

The Central Radio Propagation Laboratory of the National Bureau of Standards has been measuring 30 Mc cosmic noise absorption at Byrd Station since 1963. The riometer receiver was located at the vlf laboratory during the period of this study. A signal from the riometer was made available to Stanford University by CRPL for use in the correlation study.

F. THE CORRELATION AND FM MULTIPLEX SYSTEMS

An eight-channel Sanborn recorder was used to compare various geophysical parameters simultaneously. Regular arrangement of channels are shown in Table 1. An eight-channel fm multiplex unit was used to record in real time all special events of interest. The block diagram of the FM multiplex system is shown in Figs. 34 and 35.

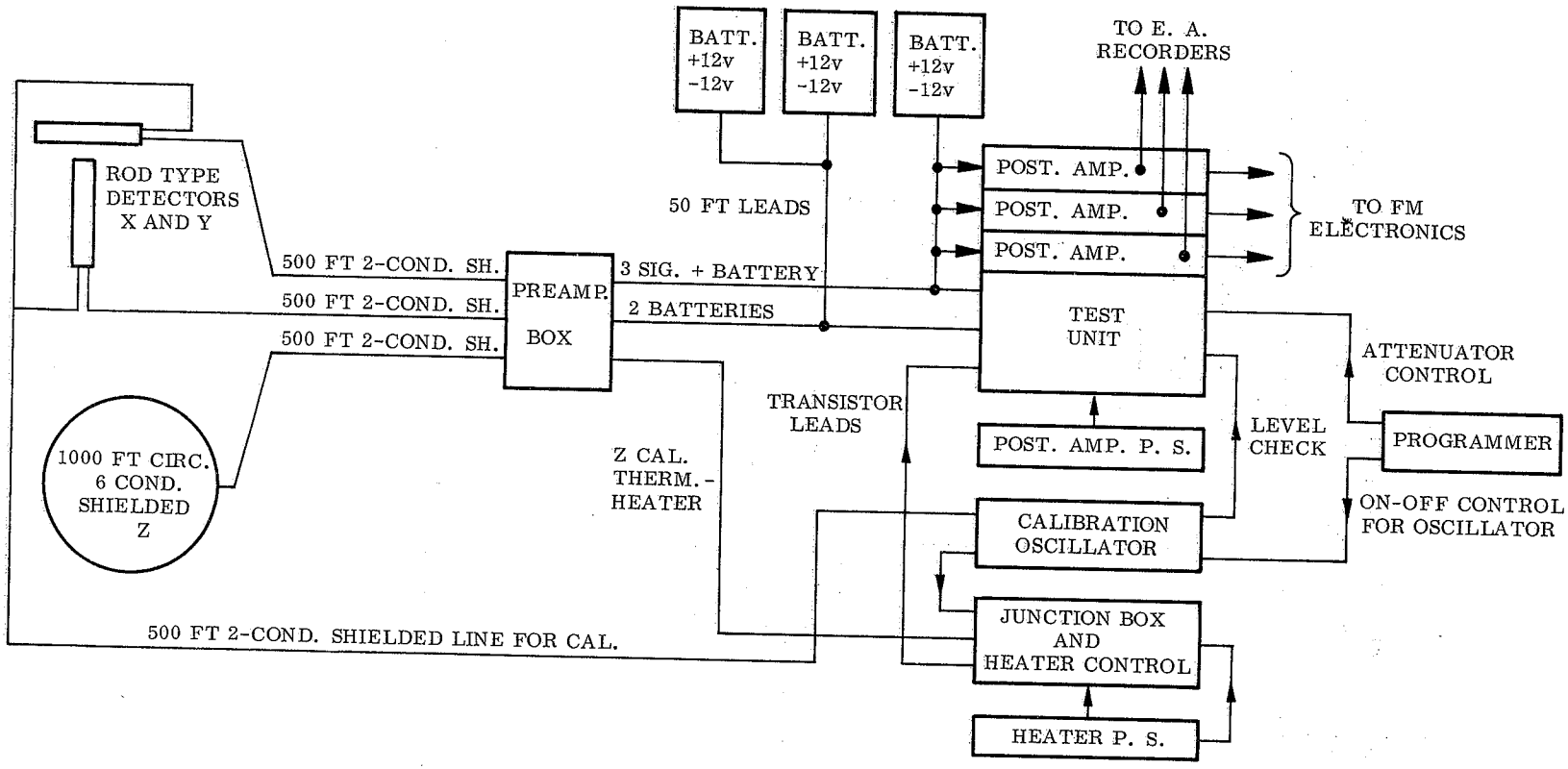

FIG. 31. BLOCK DIAGRAM OF ELF SYSTEM, BYRD STATION.

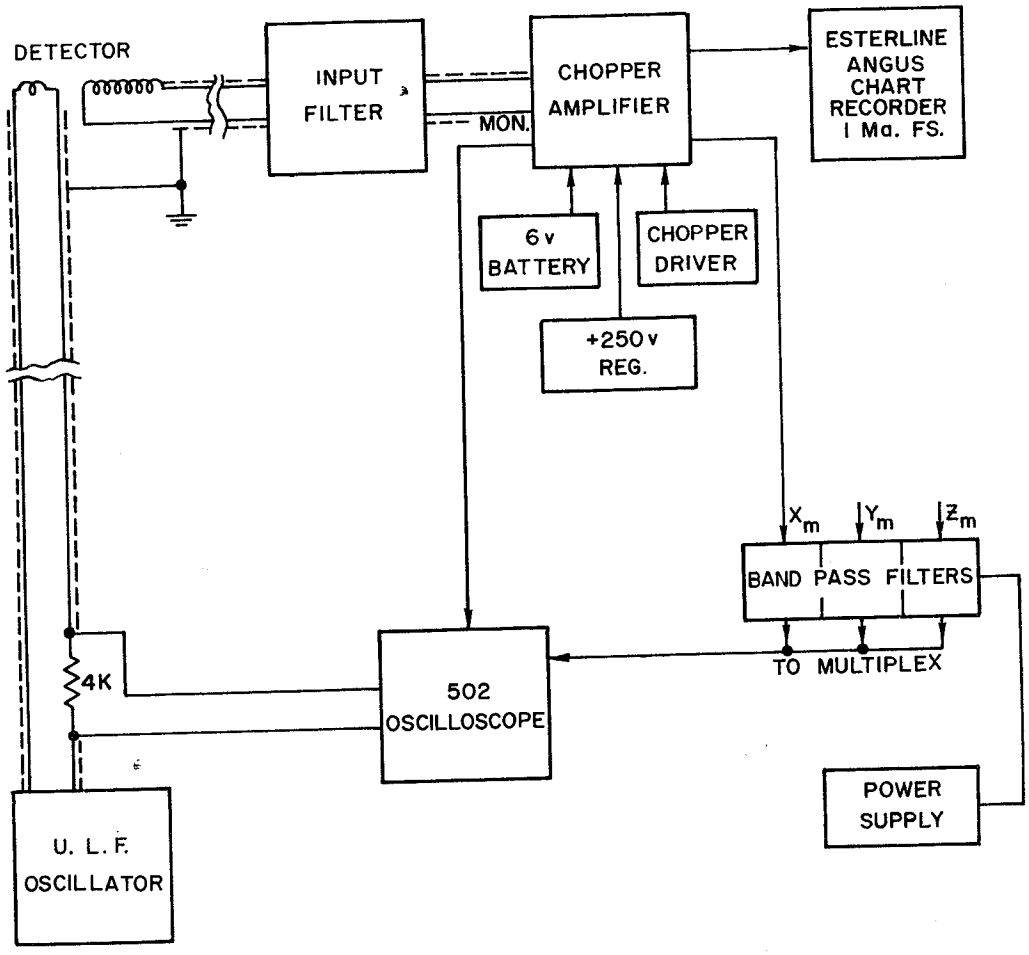

FIG. 32. BLOCK DIAGRAM OF ULF SYSTEM, BYRD STATION.

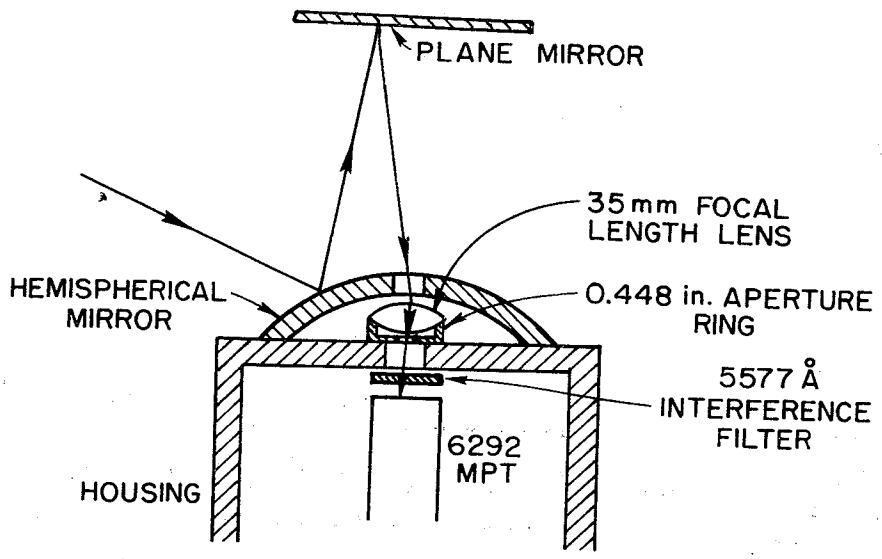

ALL SKY PHOTOMETER OPTICS

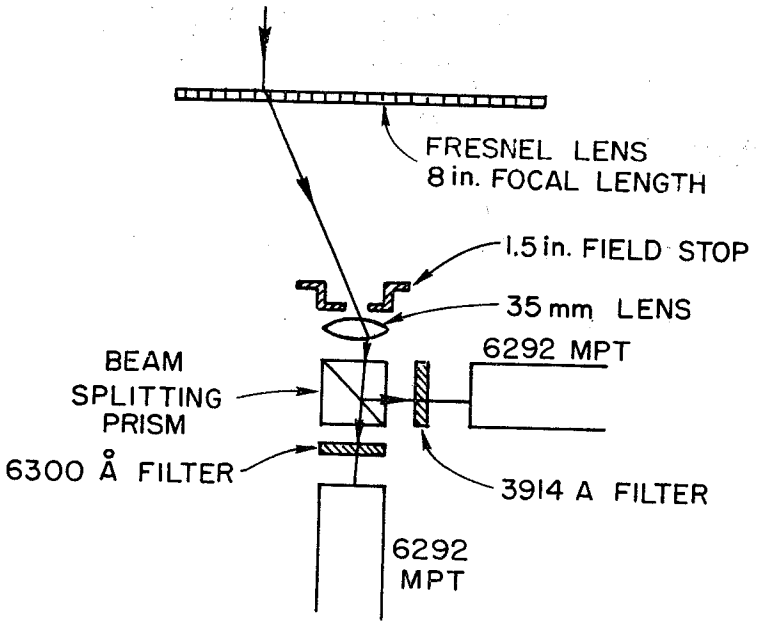

NARROW FIELD SPLIT BEAM PHOTOMETER OPTICS

FIG. 33. ALL-SKY AND NARROW-FIELD SPLIT-BEAM PHOTOMETER OPTICS, BYRD STATION.

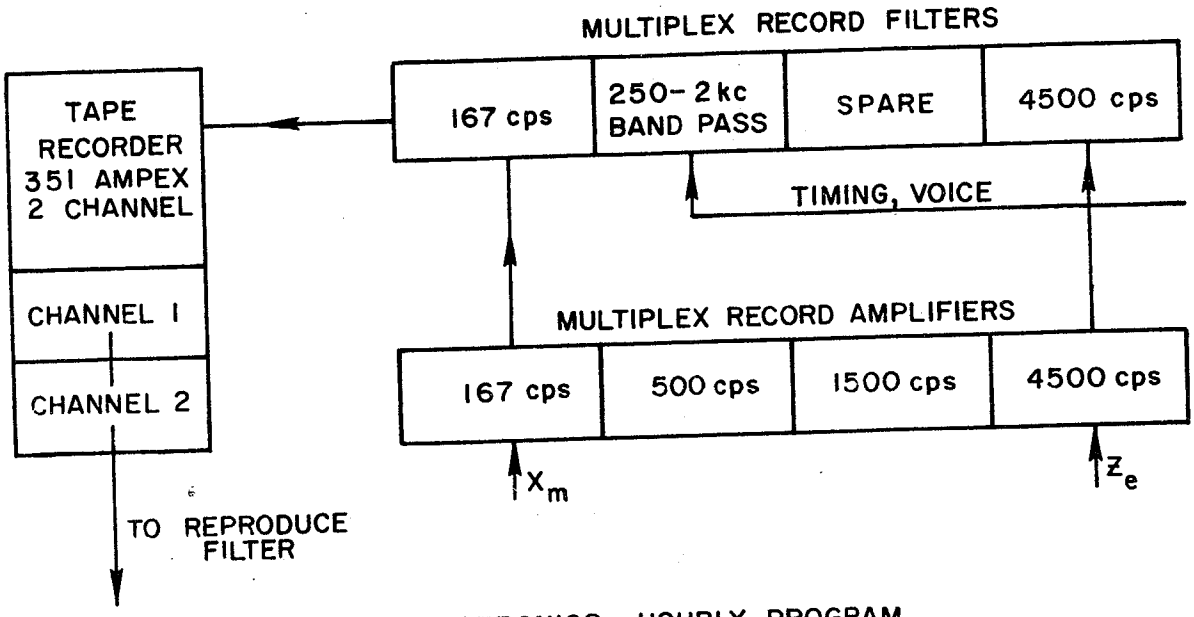

FIG. 34. FM MULTIPLEX SYSTEM 1, BYRD STATION.

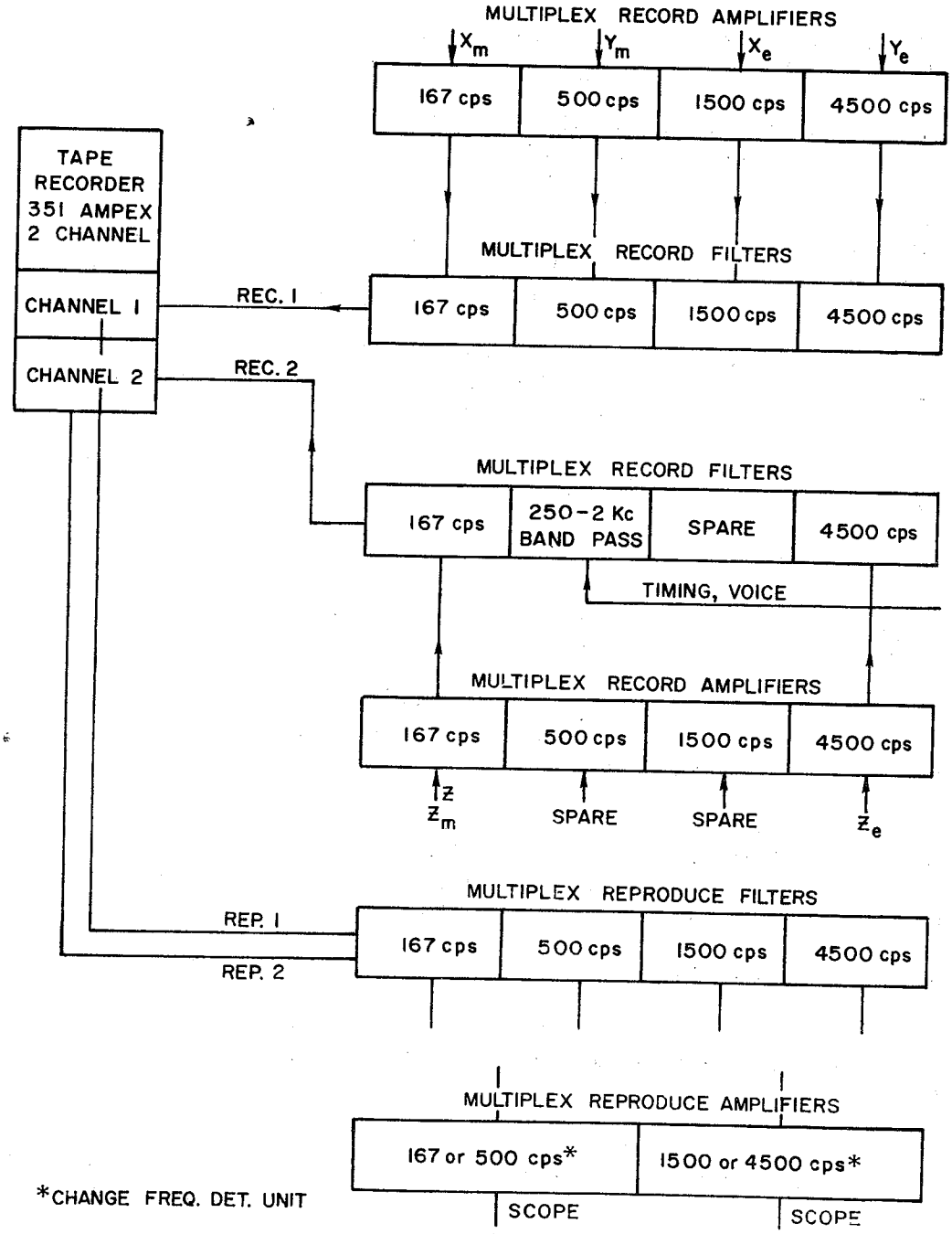

TAPE ELECTRONICS, SPECIAL RECORDING PERIODS

FIG. 35. FM MULTIPLEX SYSTEM 2, BYRD STATION.

REFERENCES

Ansari, Z. A., The aurorally associated absorption of cosmic noise at College, Alaska, J. Geophys. Res., 69 (21), 4493-4513, 1964.

Brice, N. and E. Ungstrup, Use of "local mean auroral time" for very low frequency emissions, Nature, 198 (4883), June 1, 1963.

English, W. N., D. J. Evans, J. E. Lokken, J. A. Shand and C. S. Wright, Equipment for observation of natural electromagnetic background in the frequency range 0.01 - 30 cps, Marine Sciences Instrumentation, Vol. I, ed. Roy D. Gaul, Plenum Press, New York, 1962.

Gurnett, D. A. and B. J. O'Brien, High-latitude geophysical studies with satellite Injun 3. (section) 5. Very-low-frequency electromagnetic radiation, J. Geophys. Res., 69 (1), 65-89, 1964.

Harang, L. and R. Larsen, VLF-emission observed near the aurora zone, Part I, occurrence of emissions during disturbances, Scientific Report No. 4, The Norwegian Institute of Cosmic Physics, Univ. of Oslo, Oslo, Norway, 1964.

Hargreaves, J. K., H. J. A. Chivers, and J. P. Petlock, A study of auroral absorption events at the South Pole, 1. Characteristics of the events, J. Geophys. Res., 69 (23), 5001-08, Dec. 1, 1964.

Helliwell, R. A., Whistlers and Related Ionospheric Phenomena, Stanford Press, Stanford, California, 1965.

Helms, W. J., A cooperative report on the correlation between auroral, magnetic, and elf phenomena at Byrd Station, Antarctica, Technical Report No. 3408-2, Radioscience Lab., Stanford Electronics Labs., Stanford University, Stanford, California, 1964.

Heppner, J. P., Ph.D. Thesis, California Institute of Technology, 1954.

Jacobs, J. A., Y. Kato, S. Matsushita, and V. A. Troitskaya, Classification of geomagnetic micropulsations, J. Geophys. Res., 69 (1), 180-181, 1964.

Jacobs, J. A. and C. S. Wright, Geomagnetic micropulsation results from Byrd Station and Great Whale River, Canad. J. Phys., 43, Dec. 1965.

Lokken, J. E., Instrumentation for receiving electromagnetic noise below 3,000 cps, Natural Electric Phenomena Below 30 kc/s, ed. D. F. Bleil, Plenum Press, New York, 1964.

Marks, K. E., Instruction manual for automatic whistler and hiss recorders at Byrd and South Pole Stations, Antarctica, Internal Memo No. 1108-1, Radioscience Lab., Stanford Electronics Labs., Stanford University, Stanford, California, 1962.

Morozumi, H. M., A study of aurora australis in connection with an association between vlf hiss and auroral arcs and bands observed at South Geographic Pole 1960, M. S. Thesis SUI-62-14, State University of Iowa, Iowa City, Iowa, 1962.

Morozumi, H. M., Semi-diurnal aurora peak and vlf emissions observed at the South Pole, 1960, Trans. American Geophysical Union, 44, 2 June 1963.

Morozumi, H. M., Enhancement of vlf chorus and ulf at the time of SC, Rep. Ionos. Space Res., Japan, 19 (3), 371, Sept. 1965.

Morozumi, H. M., Sudden decrease of vlf chorus intensity at the time of SC, and SI, Rep. Ionos. Space Res., Japan, 20 (3), 326, Dec. 1966.

Sandford, B. P., Aurora and airglow intensity variations with time and magnetic activity at southern high latitudes, J. Atmos. Terr. Phys., 26, 749-769, 1964.

Schneider, O., La zona auroral del hemisfero sur, Contribucion del Instituto Antarctica Argentino No. 55 Jefe del Departamento Cientifico del Instituto Antarctico Argentino, Buenos Aires, 1961.

Smith, R. L., J. H. Crary, and W. T. Kreiss, IGY instruction manual for automatic whistler recorders, IGY Project 6.10, Stanford Electronics Labs., Stanford University, Stanford, California, Jan. 1958.

Ungstrup, E., Association between vlf emissions and flickering aurora, Technical Report No. 3412-4, Radioscience Labs, Stanford Electronics Labs., Stanford University, Stanford, California, 1964.

ATLAS OF CORRELATION RECORDS

The atlas presented in this section contains examples of correlation records. Most of the cases represent moderately disturbed conditions ($10 < \Sigma K_p < 30$), and thus provide further documentation of the night and day events described in the chapter on experimental results. A special feature of the atlas is the inclusion of night-event records for 10 successive days from July 22 through July 31, 1963.

The records in the atlas are arranged chronologically. Events were scaled according to the various phases described in the text, i.e., N-1, N-2, N-3, and D. A sequence of phases apparently belonging to a single event is indicated in the figure captions by a columnar listing of start and ending times. The classification of events is tentative, and may require modification as more information is obtained. Times indicated in the descriptions are only approximated.

A few remarks need to be made about the purpose of such an extensive atlas. Many investigators, using ground methods or satellite techniques, have obtained data on specific quantities for the 1963 period represented. Important extensions of their work may become possible as the result of comparisons with the figures in the atlas. For example, observers in the northern auroral zone may obtain equivalent information on the southern zones; observers of micropulsations may obtain additional ulf data as well as corresponding data on the several other correlation phenomena recorded; satellite experimenters such as those involved in Injun III and Alouette I may obtain useful satellite-ground comparisons. Another important reason for the atlas is the opportunity to further document the analysis presented above of the night and day events.

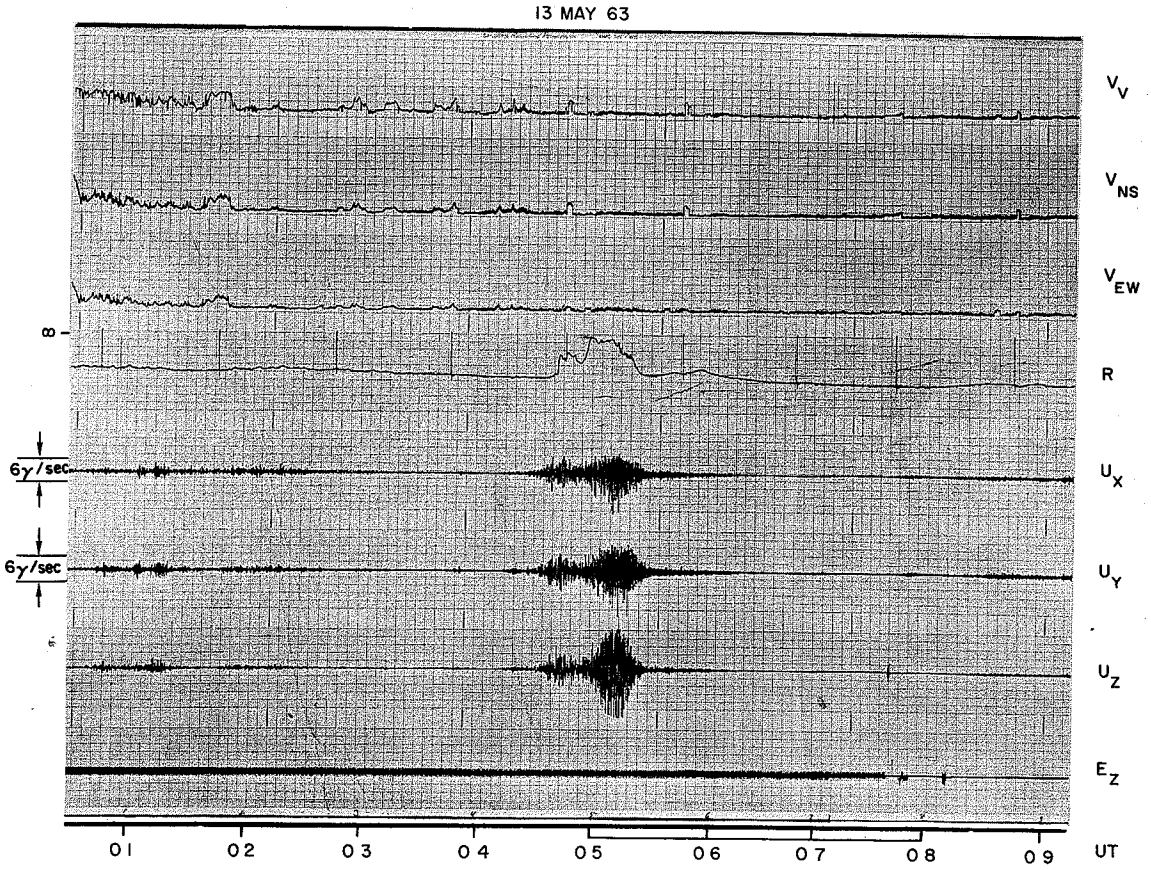

FIG. 36. MAY 13, 1963.

N-1 to 0318
N-3 0420 - 0630

Square-wavelike signals on the vlf channels represent transmissions from Navy transmitters. There appears to be a close association between the riometer event of about 14 db and ulf. Asymmetry of the X component of the ulf is due to clipping of the amplified signal.

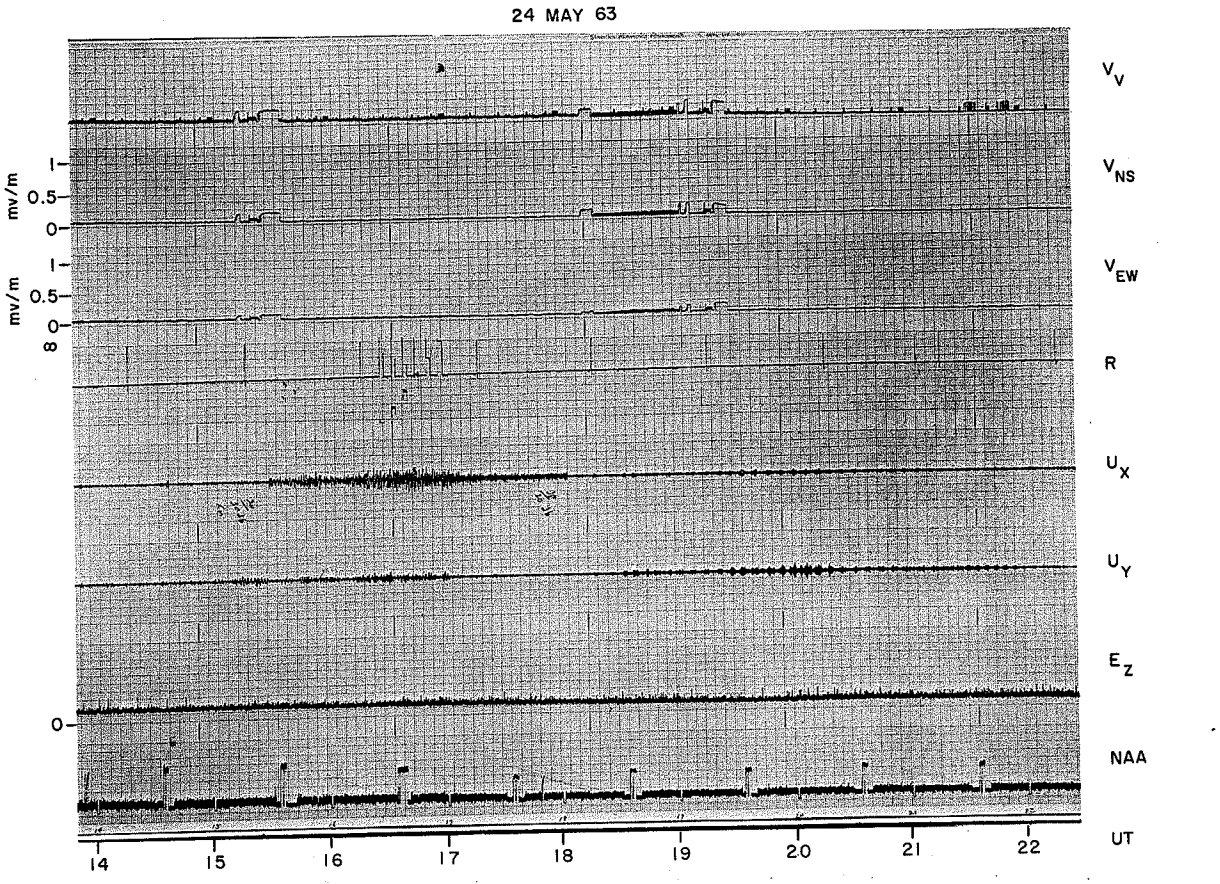

FIG. 37. MAY 24, 1963.

D 1500 ~ 2200

Signals from vlf stations are present on the upper three channels. Cosmic noise absorption is below the threshold of detection throughout the record. The ulf from about 1500 to 1800 is PC4 with period of about 1 minute. From 1800 to about 2200 the ulf is pearl-type activity. The absence of a large response on the elf channel indicates that most of the ulf activity is below a few cps.

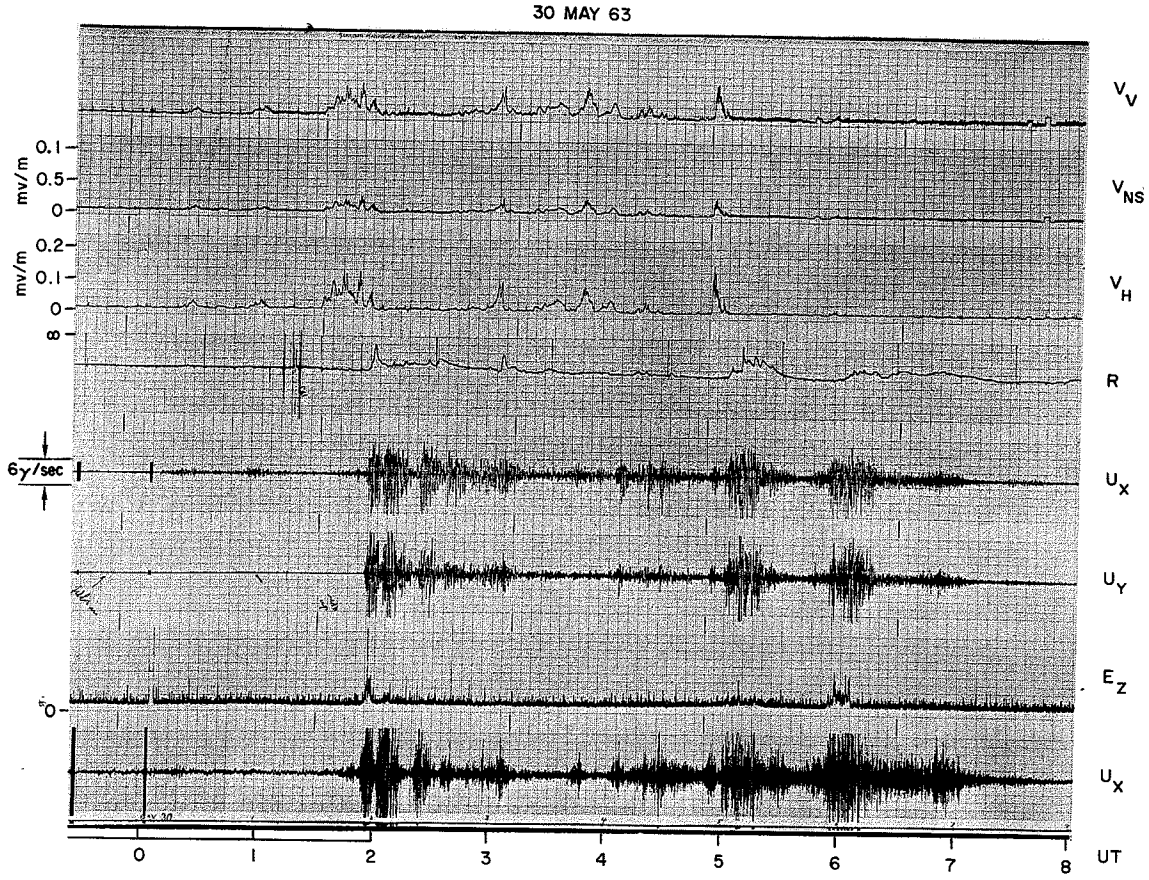

FIG. 38. MAY 30, 1963

N-1	0015 - 0150		0310 - 0451
N-2	0150 - 0203	0255 - 0310	0451 - 0530
N-3	0203 - 0255		0530 - 0717

Most of the hiss signals received by three different antennas exhibited almost simultaneous amplitude variations. Hiss stopped before the commencement of the absorption at 0501.

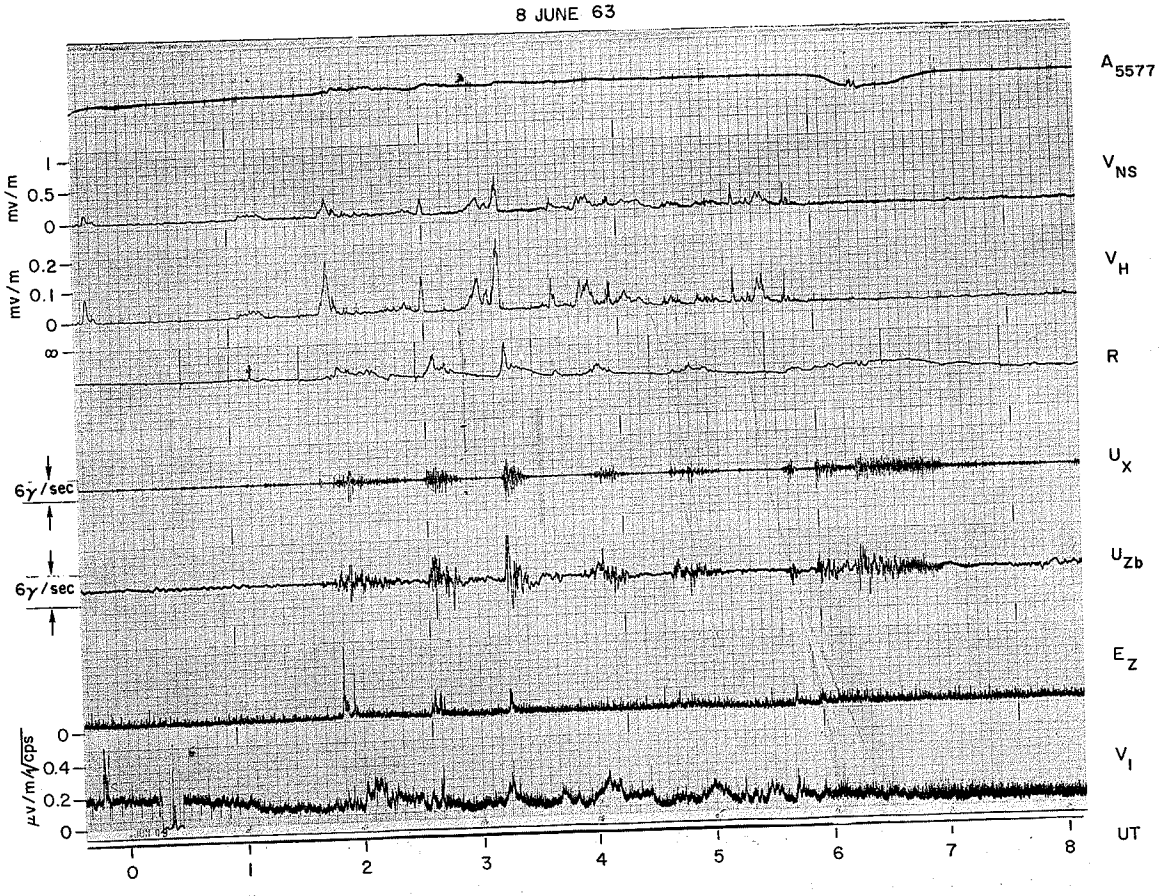

FIG. 39. JUNE 8, 1963.

N-2 0130 - 0600 (6 events)
N-3 0600 - 0800

The photometer channel is saturated by moonlight. The behavior of the vlf 1 kc/s channel differs markedly from that of the broadband vlf channels.

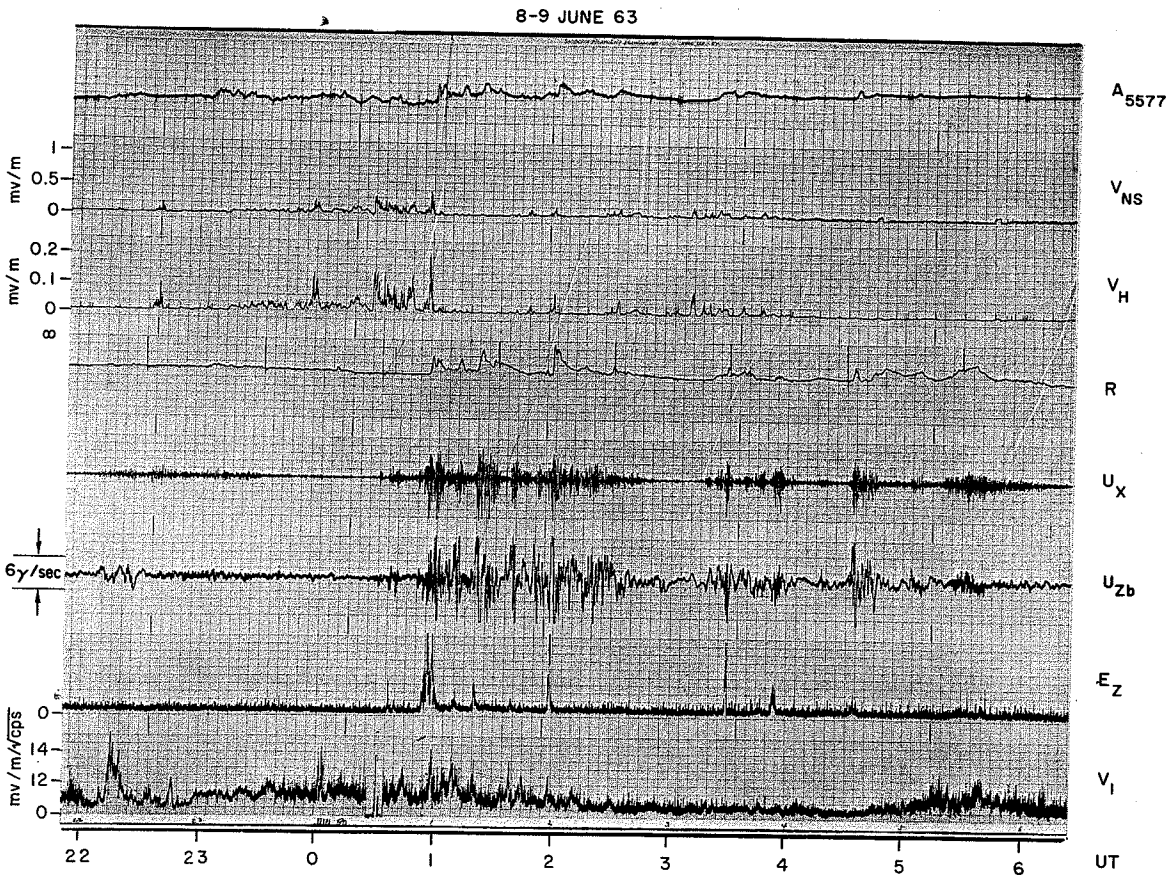

FIG. 40. JUNE 8-9, 1963.

N-1	2300 - 0035
N-2	0035 - 0410 (7 events)
N-3	0455 - 0620

The beginning of each elf burst is counted as the commencement of an N-2 event.

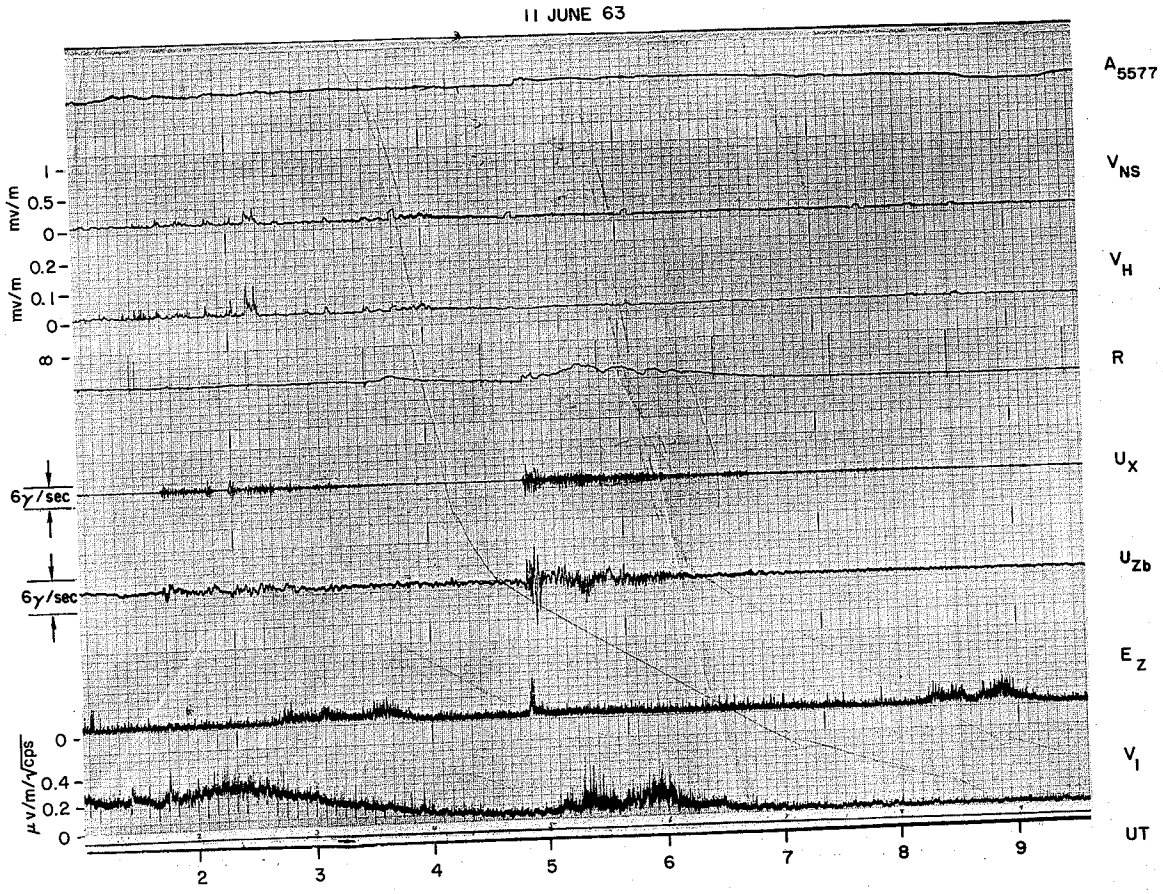

FIG. 41. JUNE 11, 1963.

N-1	0100 - 0430
N-2	0450 - 0502
N-3	0502 - 0700

The 1 kc/s vlf shows different properties between 0100 and 0400 and between 0500 and 0630. The ulf at 0450 is P_i; a P_c is superimposed on it.

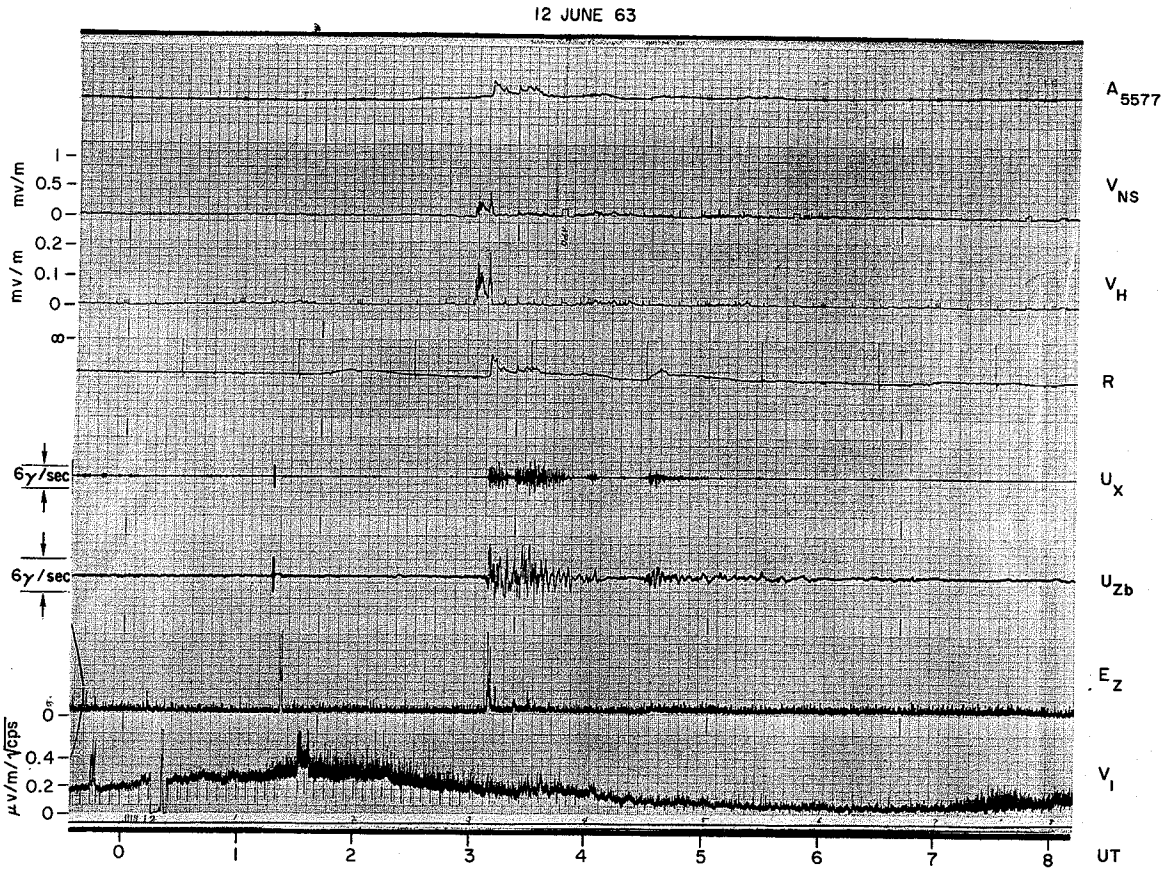

FIG. 42. JUNE 12, 1963.

N-1	0259 - 0306	
N-2	0307 - 0321	
N-3	0321 - 0412	0425 - 0600

The vlf 1 kc/s activity between 0000 ~ 0400 does not seem to be related to any other event. Note a similar amplitude variation between the photometer and the riometer record between 0258 - 0335.

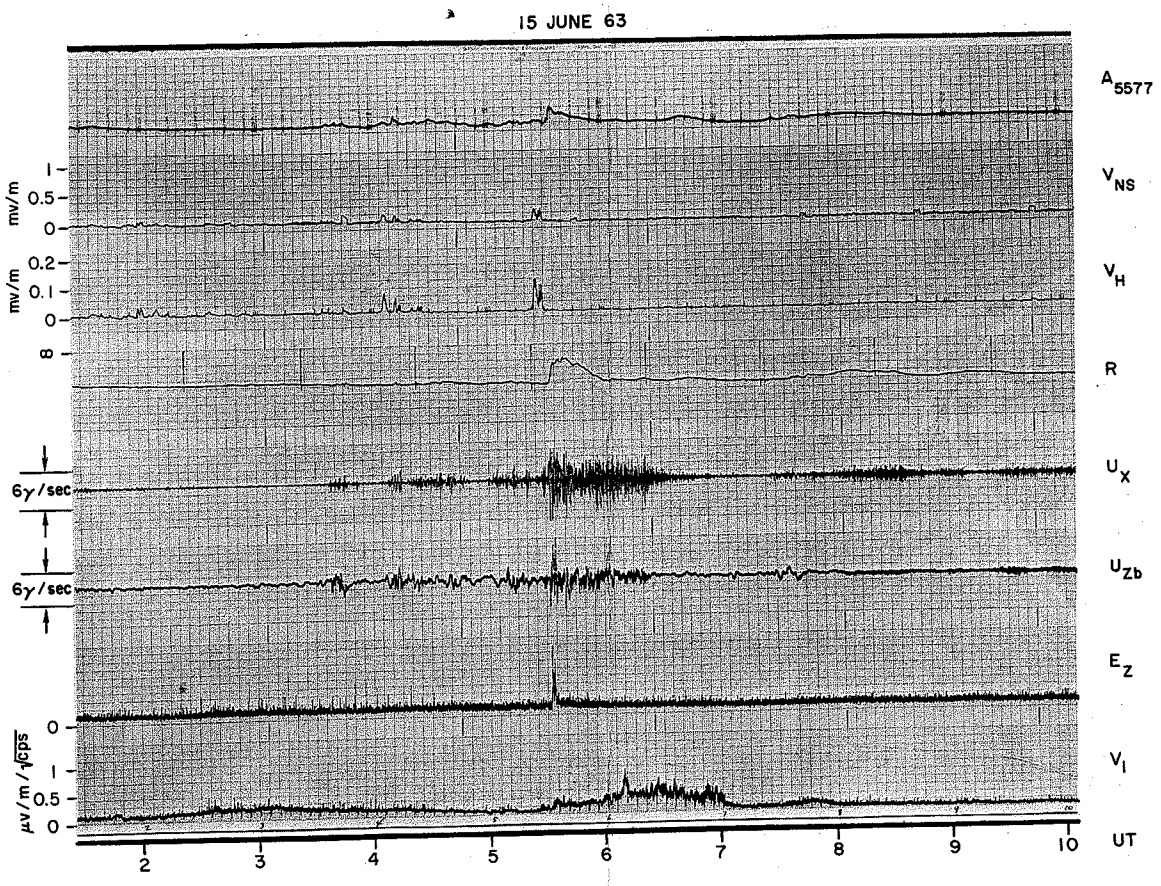

FIG. 43. JUNE 15, 1963.

N-1	0300 ~ 0524	
N-2	0525 ~ 0538	
N-3	0538 - 0710	0730 - 0930

The vlf 1 kc/s activity commenced after the cessation of vlf hiss (~ 0530).

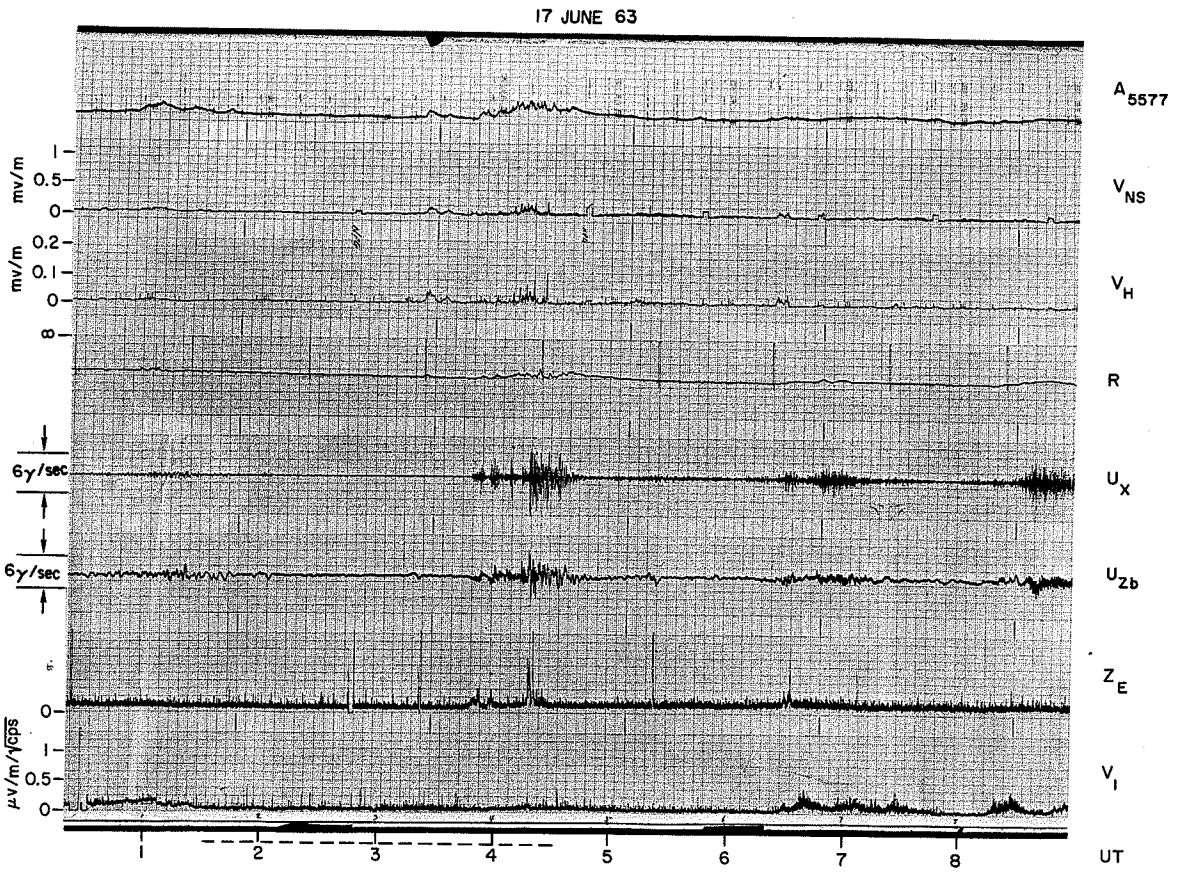

FIG. 44. JUNE 17, 1963.

N-1	0052 - 0400	
N-2	0416 - 0422	
N-3	0422 - 0450	0625 - 0810

The N-2 event resembles the regular N-1 event.

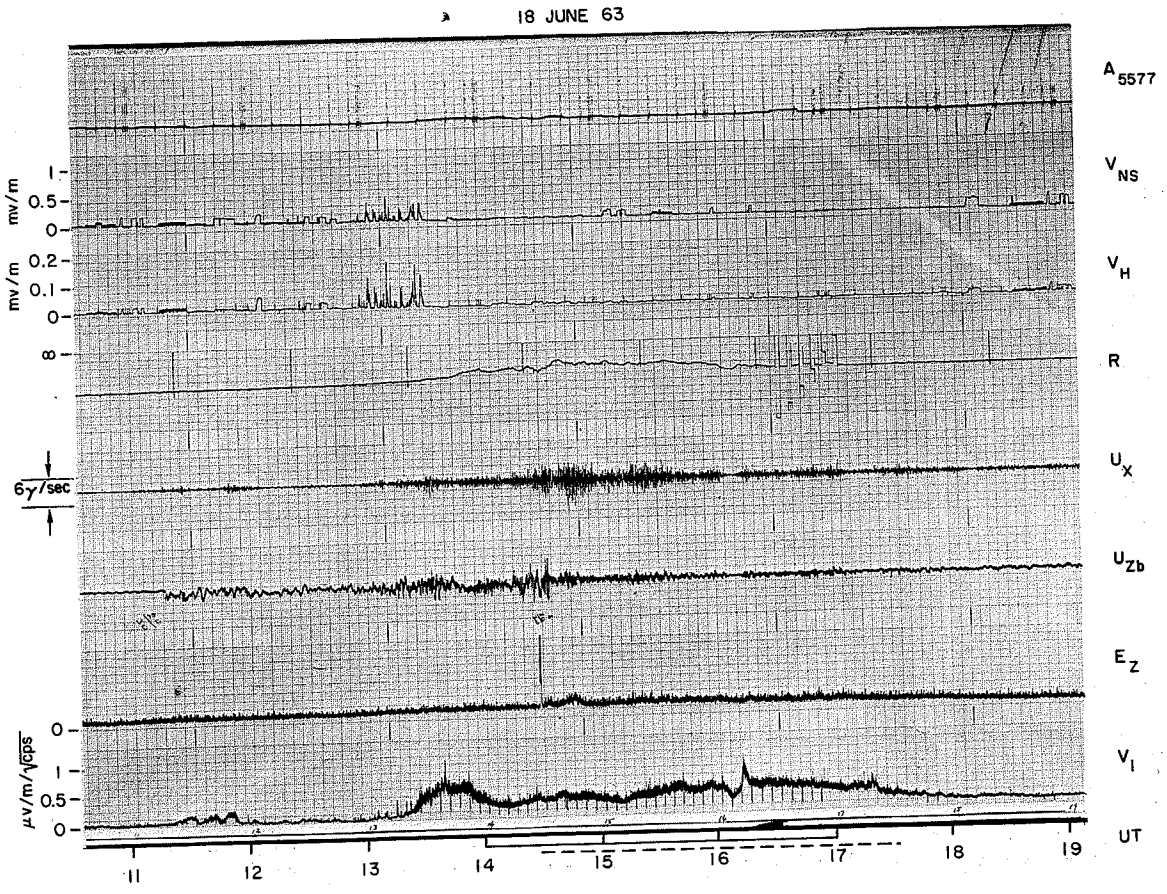

FIG. 45. JUNE 18, 1963.

D 1258 - 1800

Hiss bursts are observed at about 1300 and are followed by vlf chorus. This sequence is analogous to the sequence of night events. Although the absorption level was high, very little auroral activity was recorded.

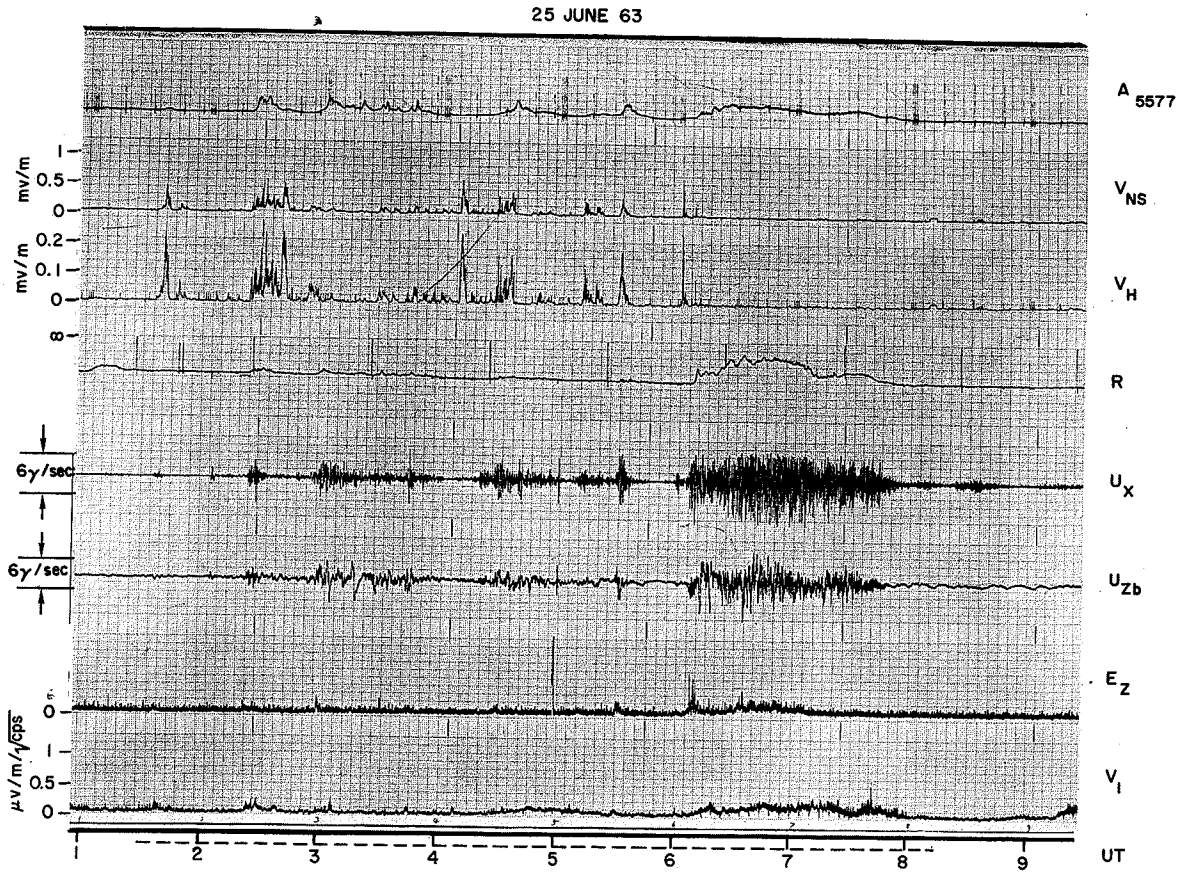

FIG. 46. JUNE 25, 1963.

N-2	0559 - 0620
N-3	0620 - 0800

Events between 0130 - 0600 are mixtures of N-1 and N-2. It is very difficult to make a clear cut distinction here. Note a simultaneous increase in 1 kc/s vlf amplitude and cosmic noise absorption between 0610 and 0800.

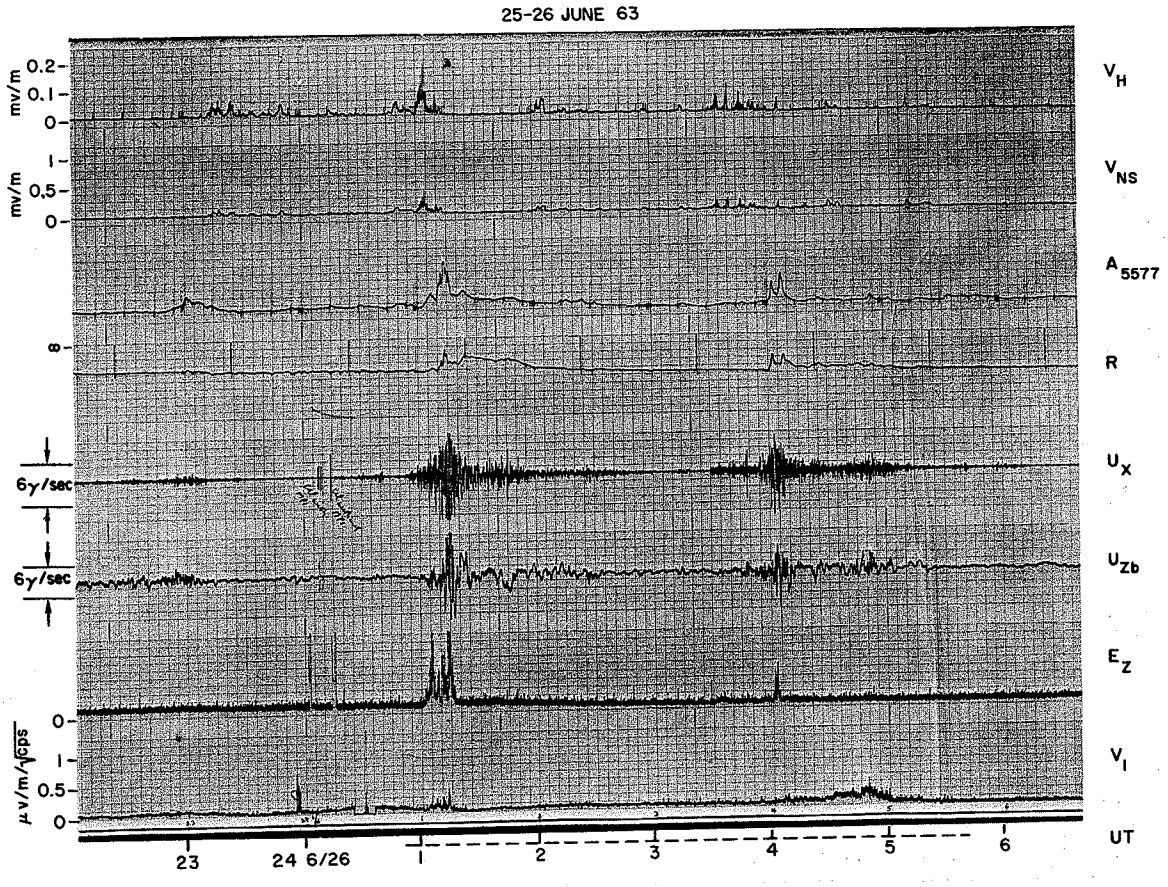

FIG. 47. JUNE 25-26, 1963.

N-1	2310 - 0030		0335 - 0359
N-2		0050 - 0120	0359 - 0415
N-3		0120 - 0230	0415 - 0530

There are two sets of night disturbances, both of which follow a regular sequence of development.

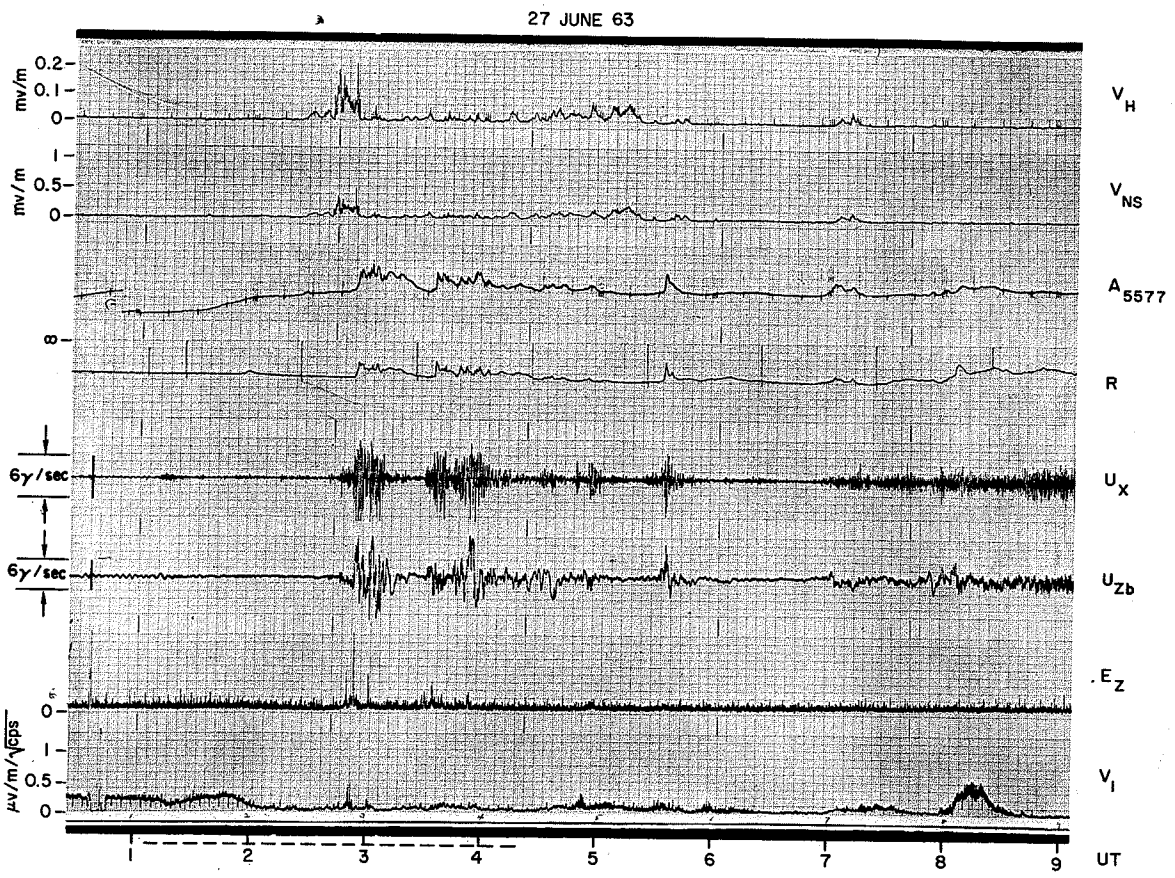

FIG. 48. JUNE 27, 1963.

N-1	0227 - 0248		0655 - 0730
N-2	0252 - 0308	0327 - 0400	
N-3			0730 on

Events between 0200 and 0600 are a mixture of N-1 and N-2. Note the presence of vlf hiss throughout this period.

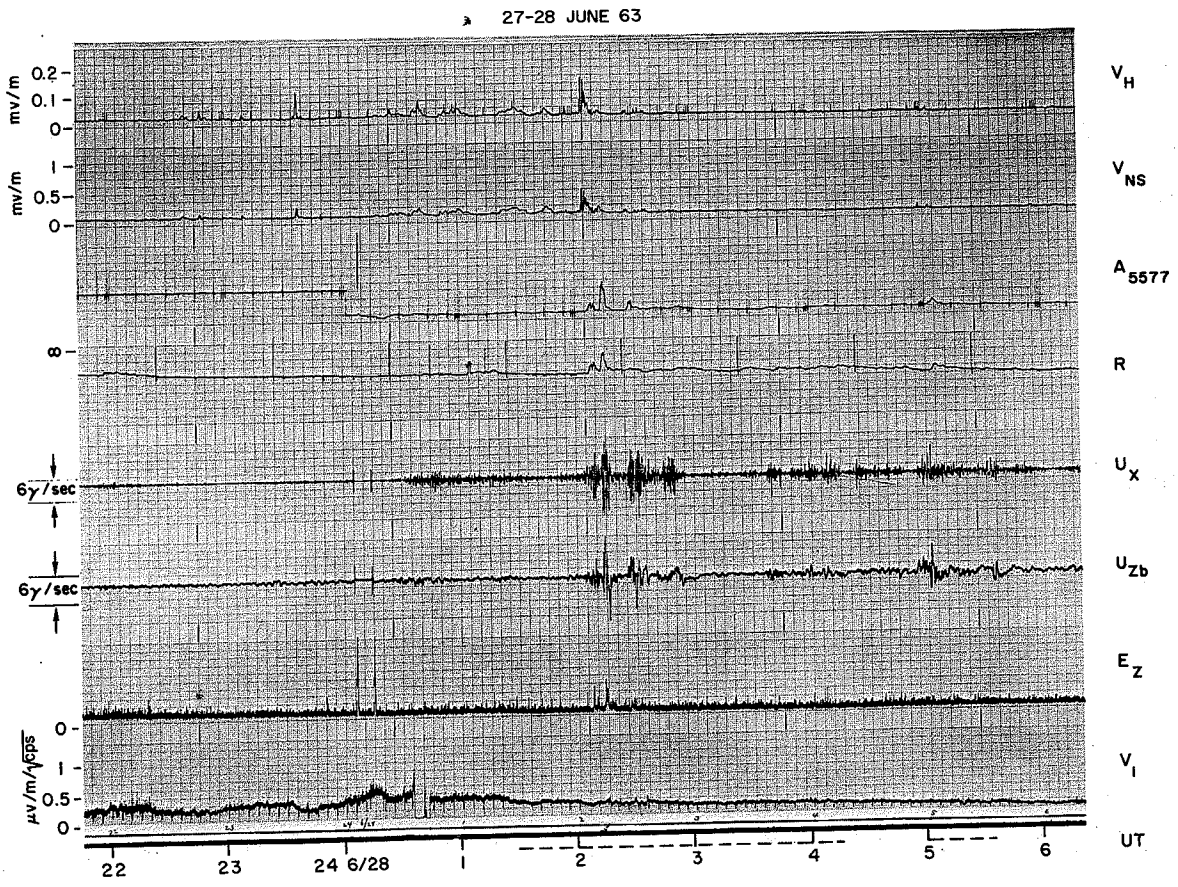

FIG. 49. JUNE 27-28, 1963.

N-1	0000 - 0200
N-2	0203 - 0220
N-3	0220 - 0300

The N-3 event is not well defined.

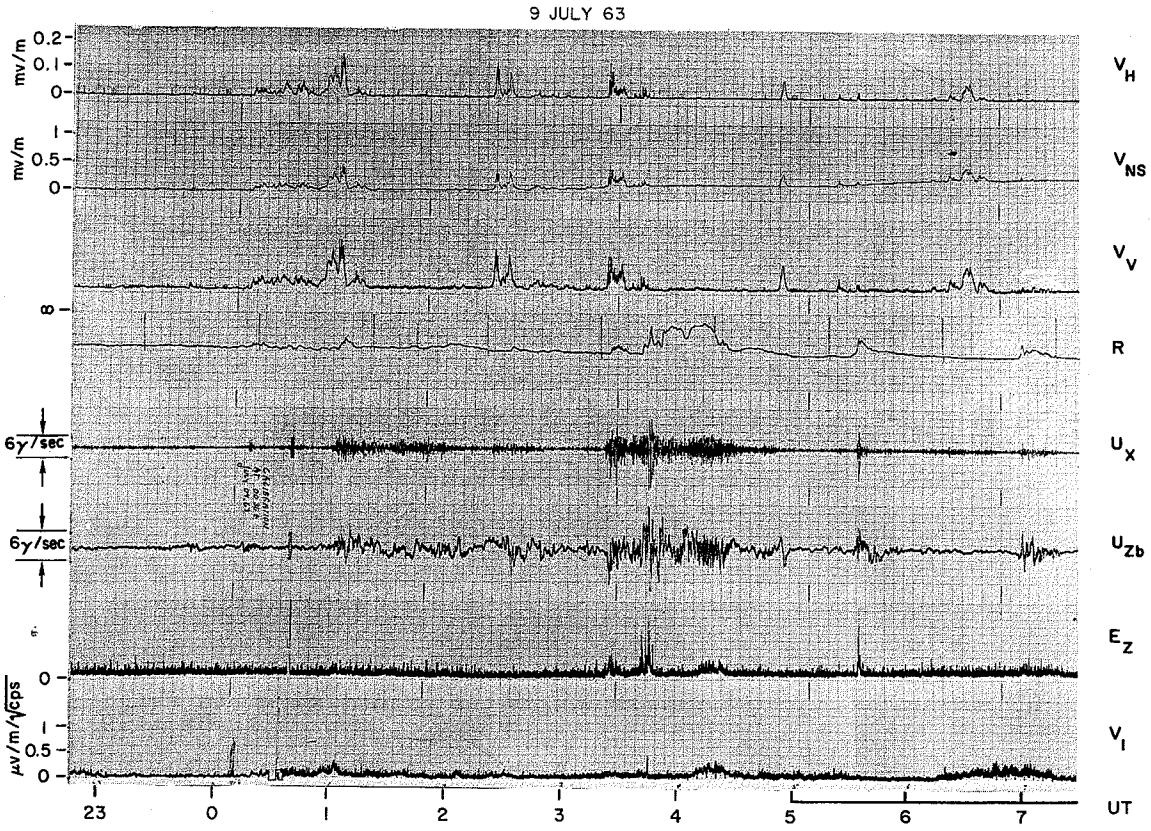

FIG. 50. JULY 9, 1963.

N-2	0320 - 0332
N-3	0332 - 0440

The events between 0000 - 0300 exhibit characteristics of N-1, although the events commencing at about 0100 and 0230 are suggestive of the N-2 stage.

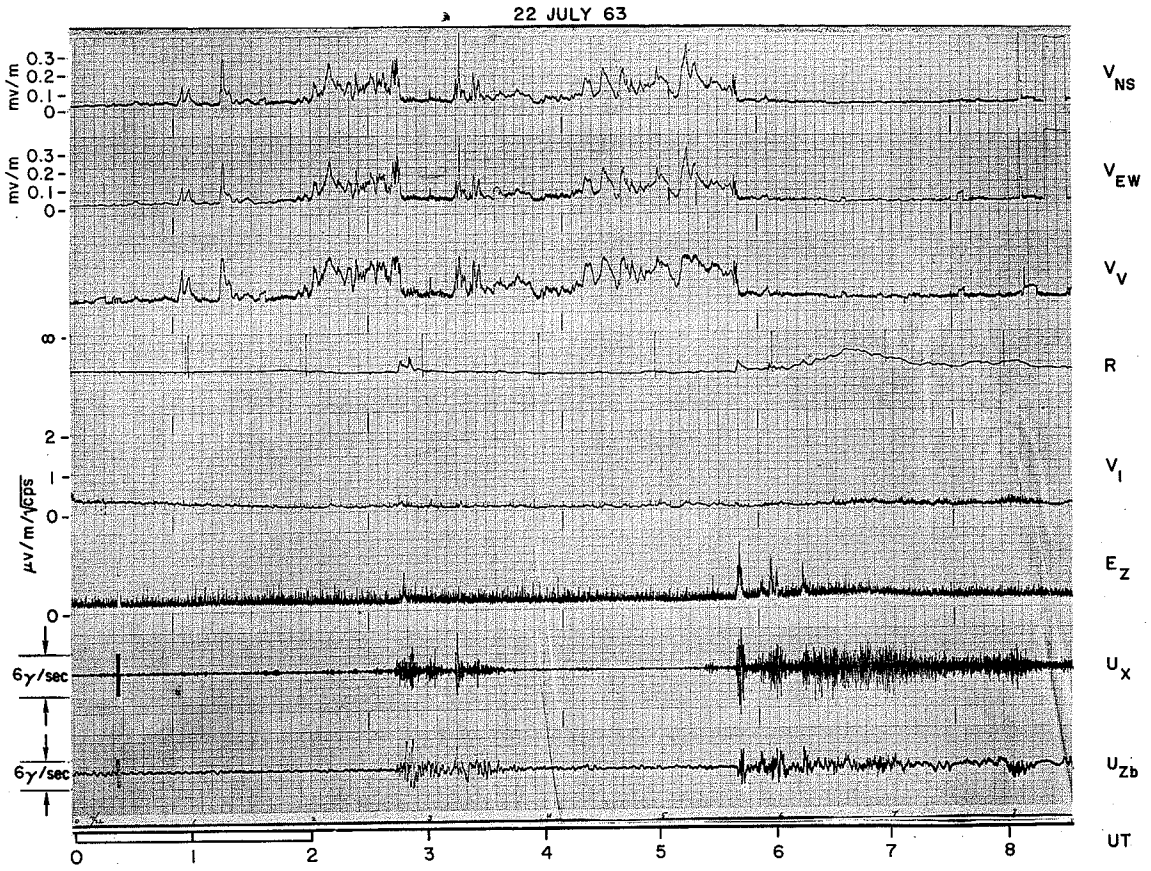

FIG. 51. JULY 22, 1963.

N-1	0050 - 0242	0330 - 0535
N-2	0246 ~ 0257	0537 ~ 0545
N-3		0545 ~ 0820

Hiss intensity variations recorded by the NS and EW antennas are almost the same at all times.

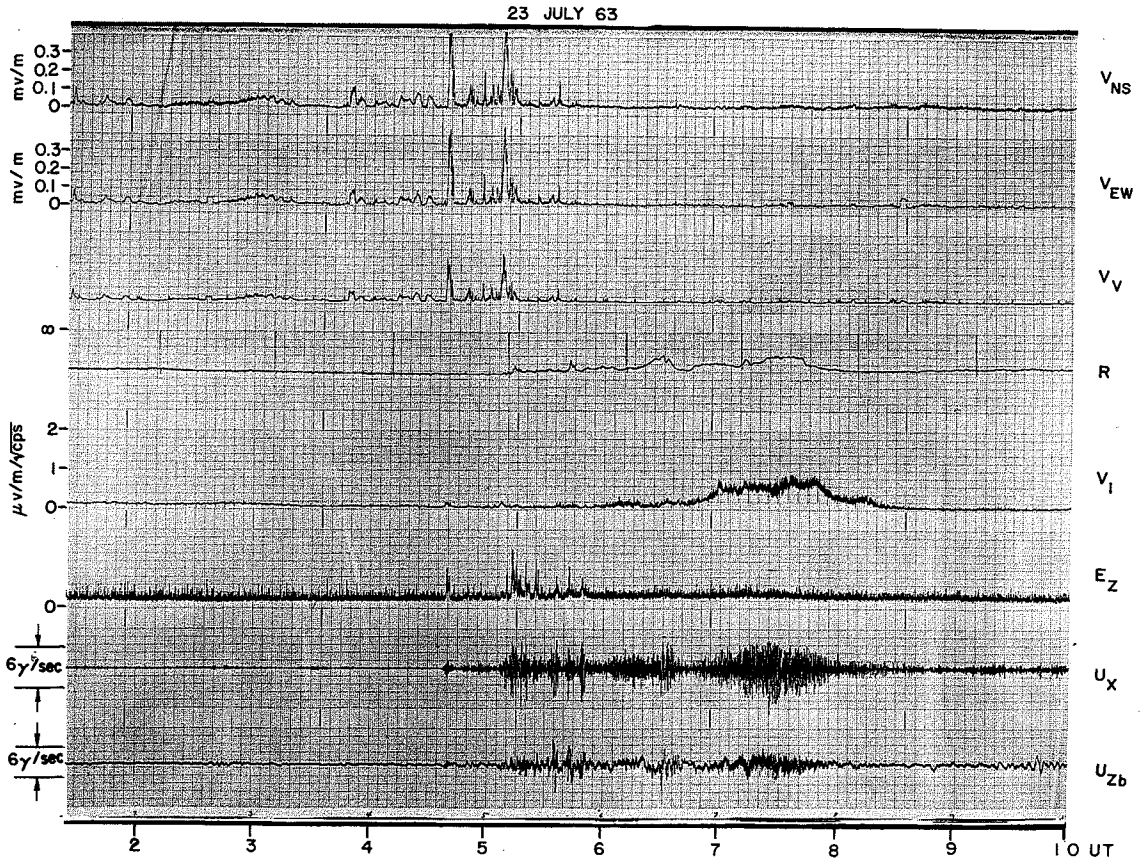

FIG. 52. JULY 23, 1963.

N-1	0345 - 0507
N-2	0508 - 0600
N-3	0600 - 0830

Several small N-2 events occur between 0508 and 0600. Vlf 1 kc/s activity is pronounced during the N-3 stage.

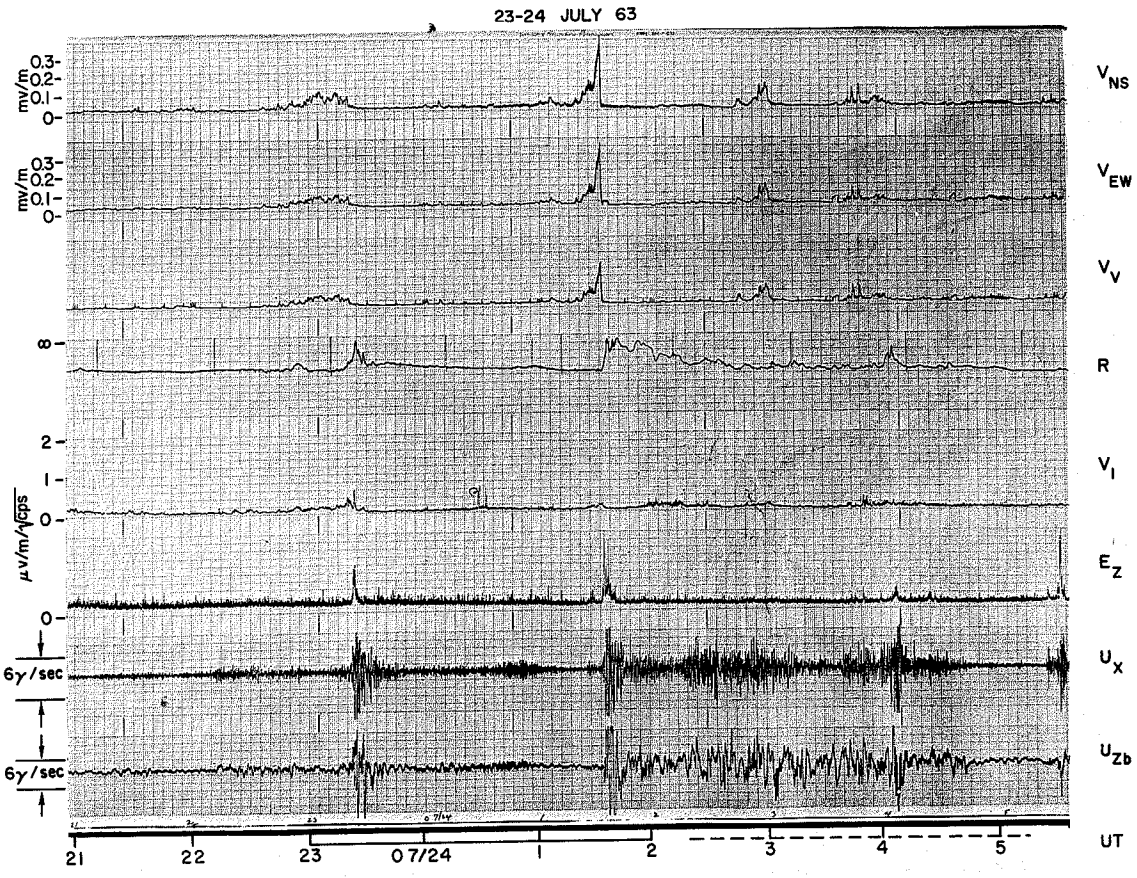

FIG. 53. JULY 23-24, 1963.

N-1	2208 - 2312	0100 - 0125
N-2	2313 - 2330	0127 - 0148
N-3		0148 - 0430

There are two small N-2 events between 0148 and 0430. Note the gradual buildup of hiss and following decay near 0130.

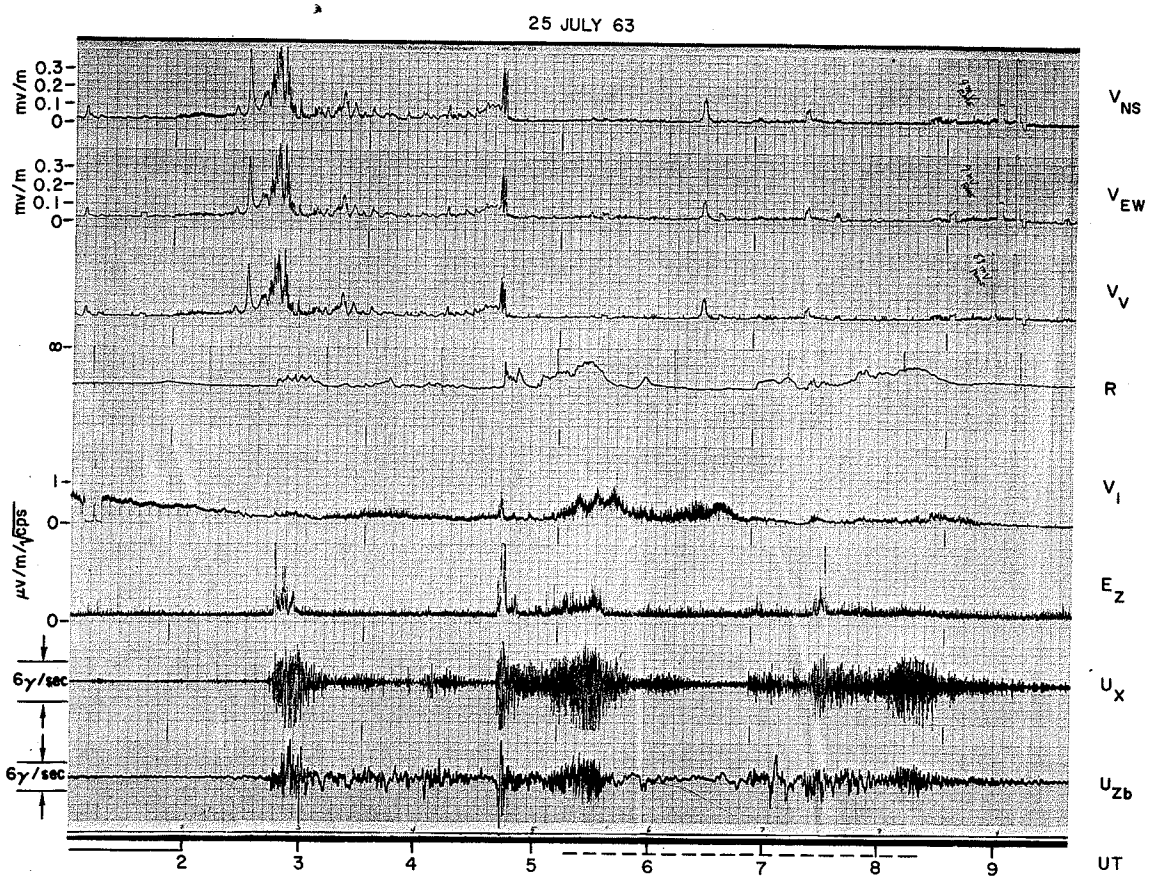

FIG. 54. JULY 25, 1963.

N-1	0222 - 0245	0310 - 0439	
N-2	0246 - 0309	0440 - 0458	
N-3		0459 - 0610	0650 - 0900

Vlf hiss persisted until 0443, when absorption suddenly increased. Vlf hiss did not recover its intensity in spite of a large decrease in absorption at 0548. (See also Fig. 2.)

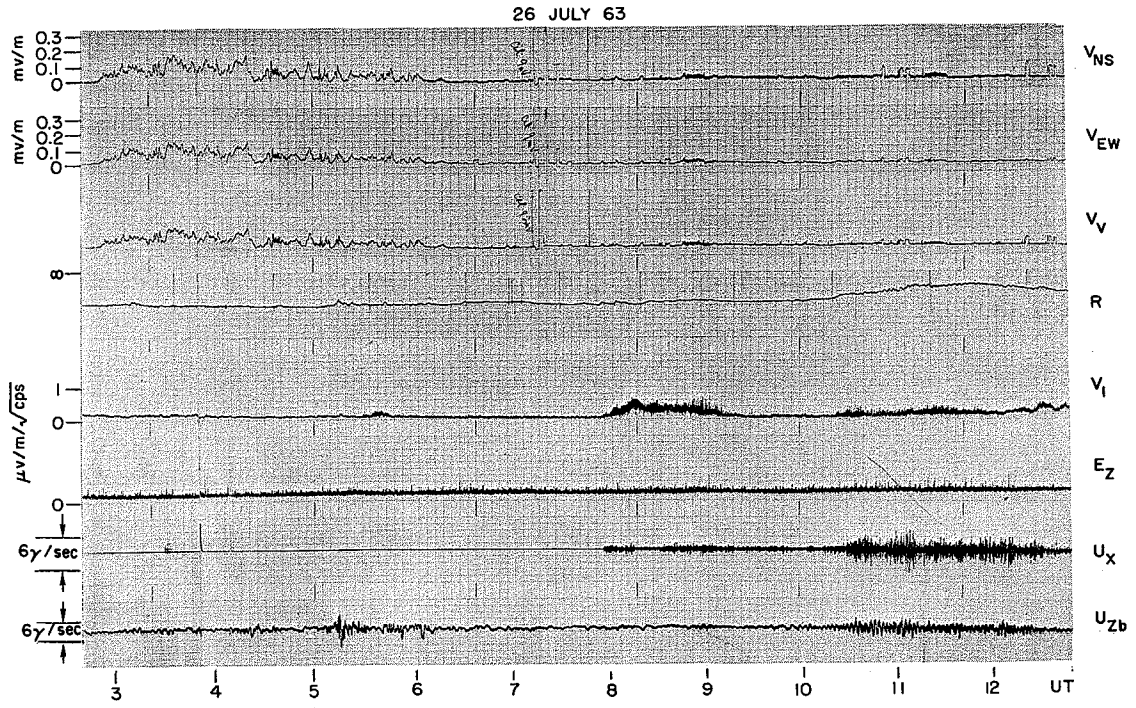

FIG. 55. JULY 26, 1963.

N-1 0252 - 0615
N-3 0950 on

There is a slight suggestion of an N-2 event at 0515. Vlf 1 kc/s from 0755 to 0914 may belong to N-3.

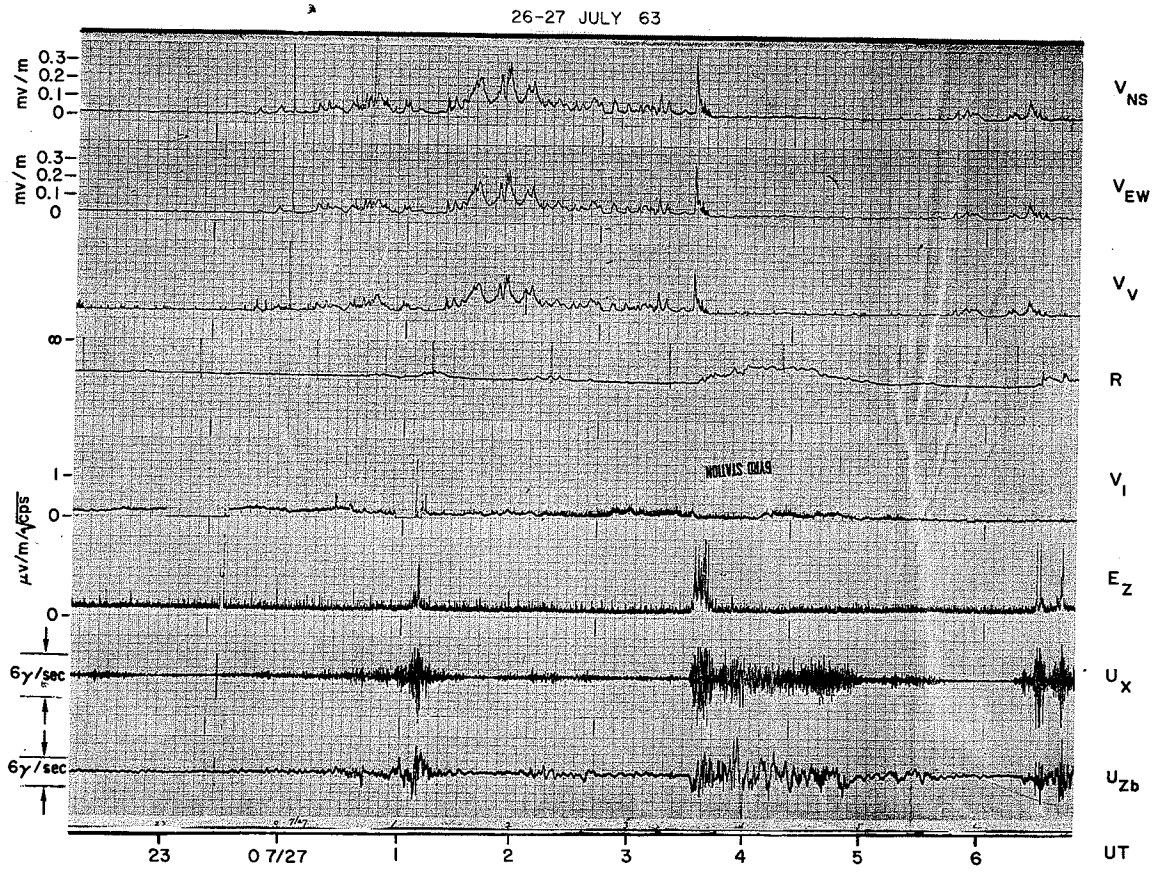

FIG. 56. JULY 26-27, 1963.

N-1	2340 - 0055	0120 - 0330
N-2	0056 - 0120	0331 - 0344
N-3		0345 - 0550

Vlf hiss commenced at about 2340 and was terminated by a commencement of absorption at 0334.

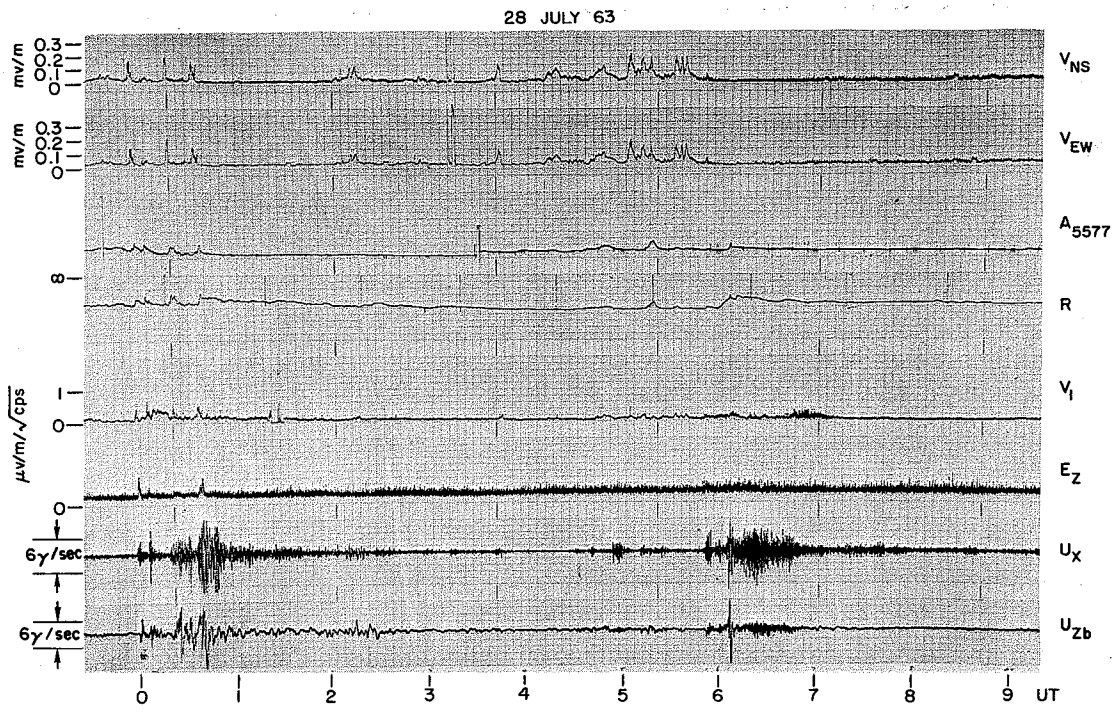

FIG. 57. JULY 28, 1963.

N-1	0412 - 0553
N-2	0553 - 0604
N-3	0604 - 0730

The events between 0000 - 0200 are difficult to classify. However, N-3 may be present in the period 0032 - 0200.

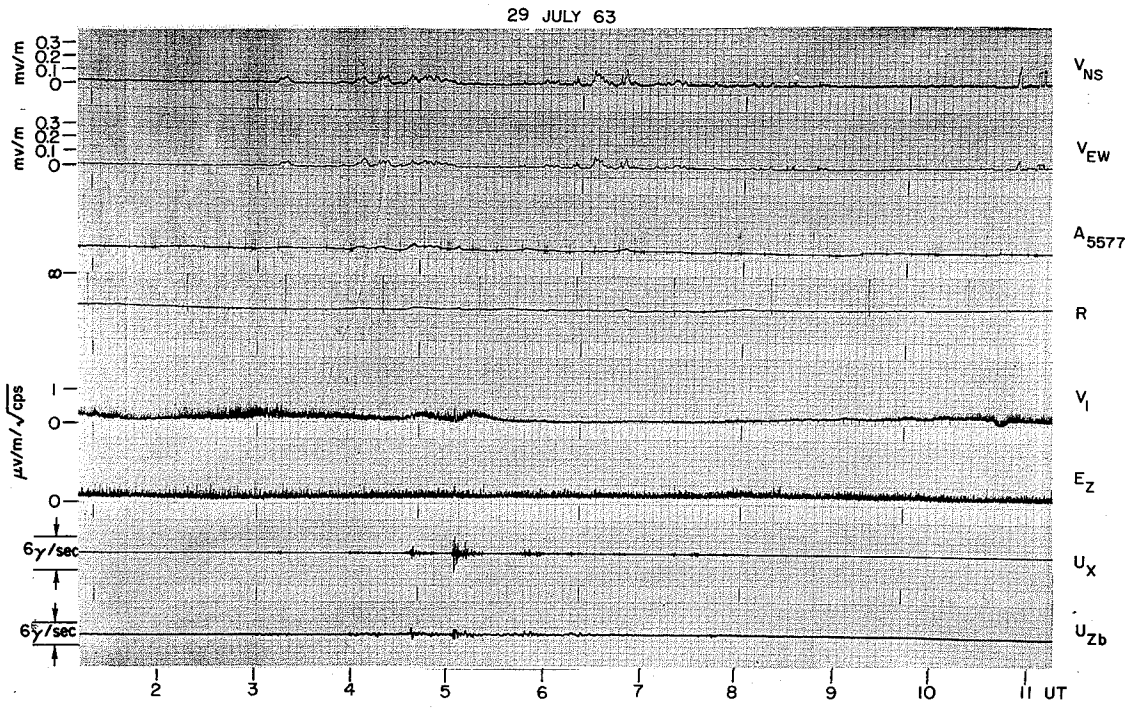

FIG. 58. JULY 29, 1963.

N-1 0312 - 0725

A very quiet day. There is a slight suggestion of N-2 at 0505.

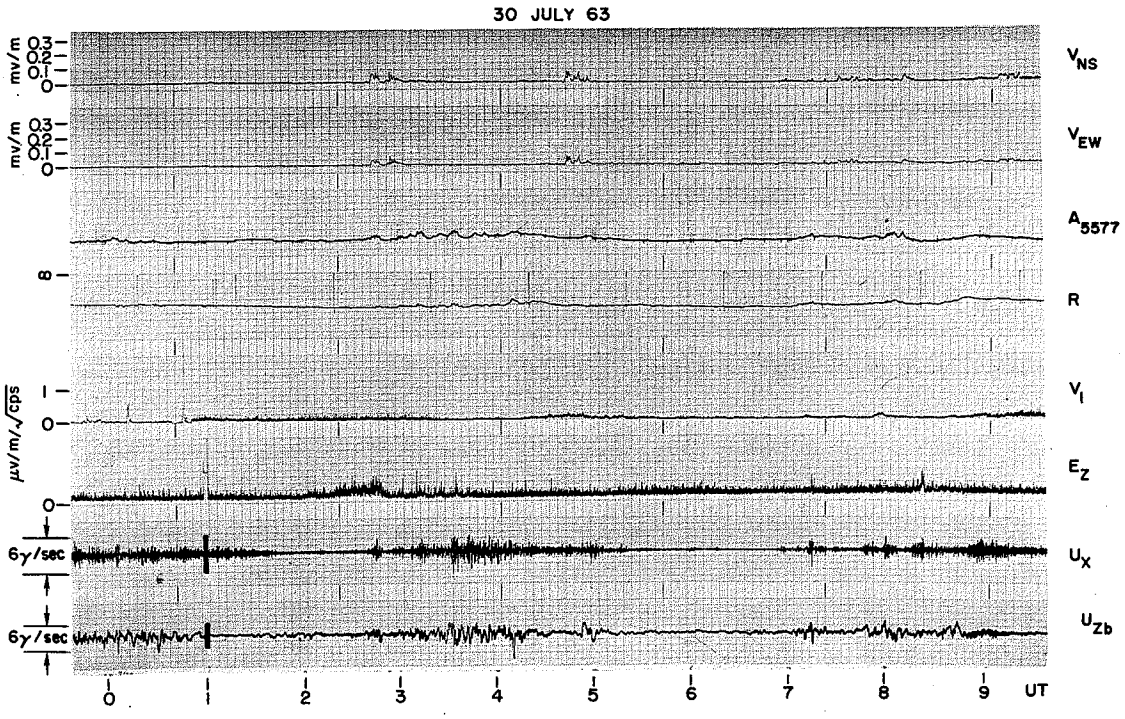

FIG. 59. JULY 30, 1963.

N-1 0243 - 0500

A quiet day. Phase relations are not clearly evident on either quiet days or severely disturbed days.

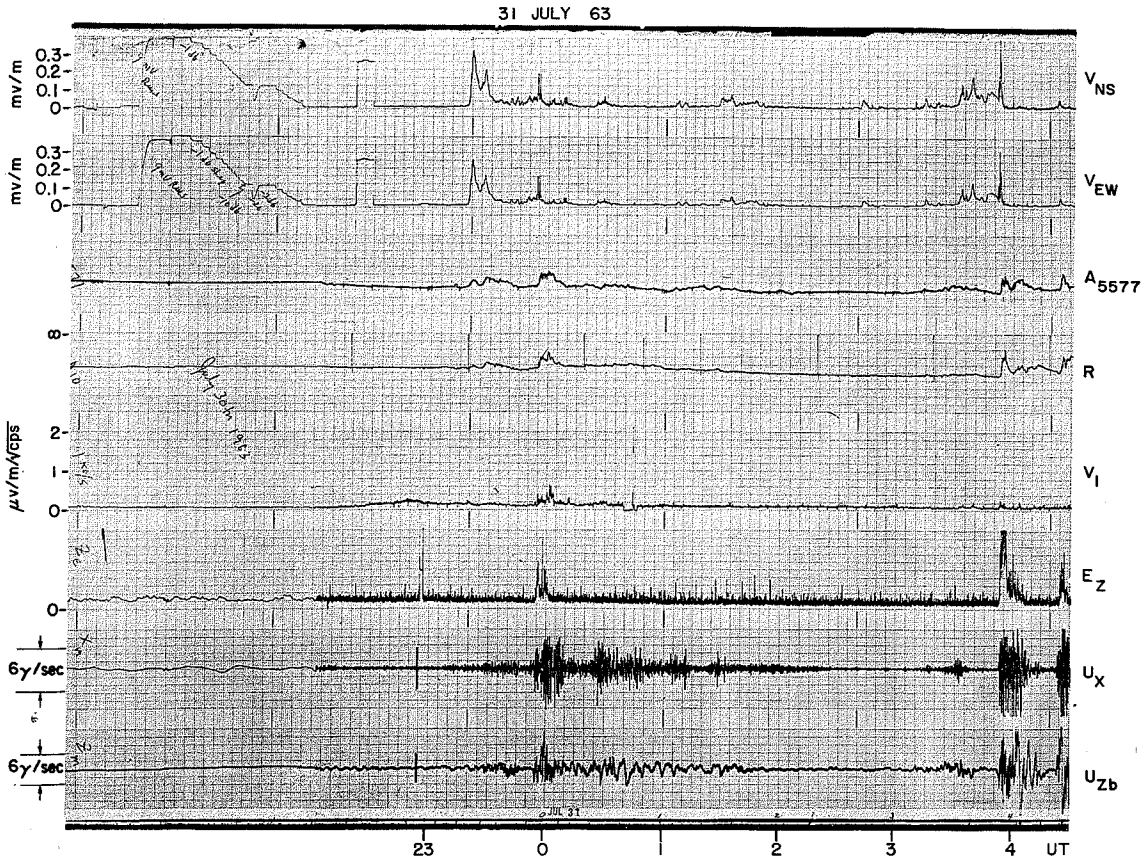

FIG. 60. JULY 31, 1963.

N-1	2317 - 2343	0310 - 0346
N-2	2352 - 0016	0354 - 0415
N-3	0016 - 0200	

A linearity calibration of the vlf broadband channels shows that the channels have approximately equal sensitivity. The 9-mv rms calibration voltage was attenuated in 1 db steps. The records indicate that during most of the period 2330 to 0400 the signal received by the NS antenna was larger than that of the EW antenna.

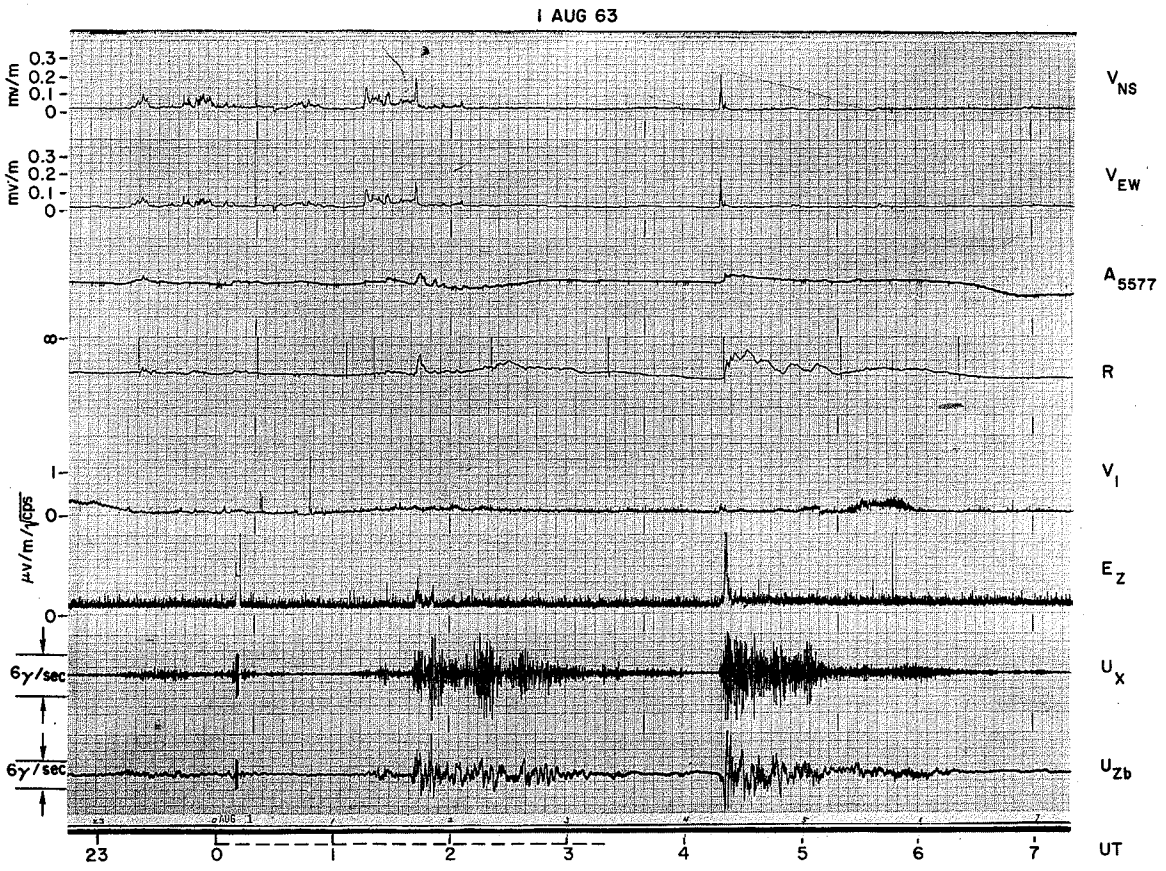

FIG. 61. AUGUST 1, 1963.

N-1	2310 - 0105	0113 - 0138	
N-2		0140 - 0200	0415 - 0448
N-3		0200 - 0330	0448 - 0630

The photometer amplitude variation is inaccurate due to moonlight interference.

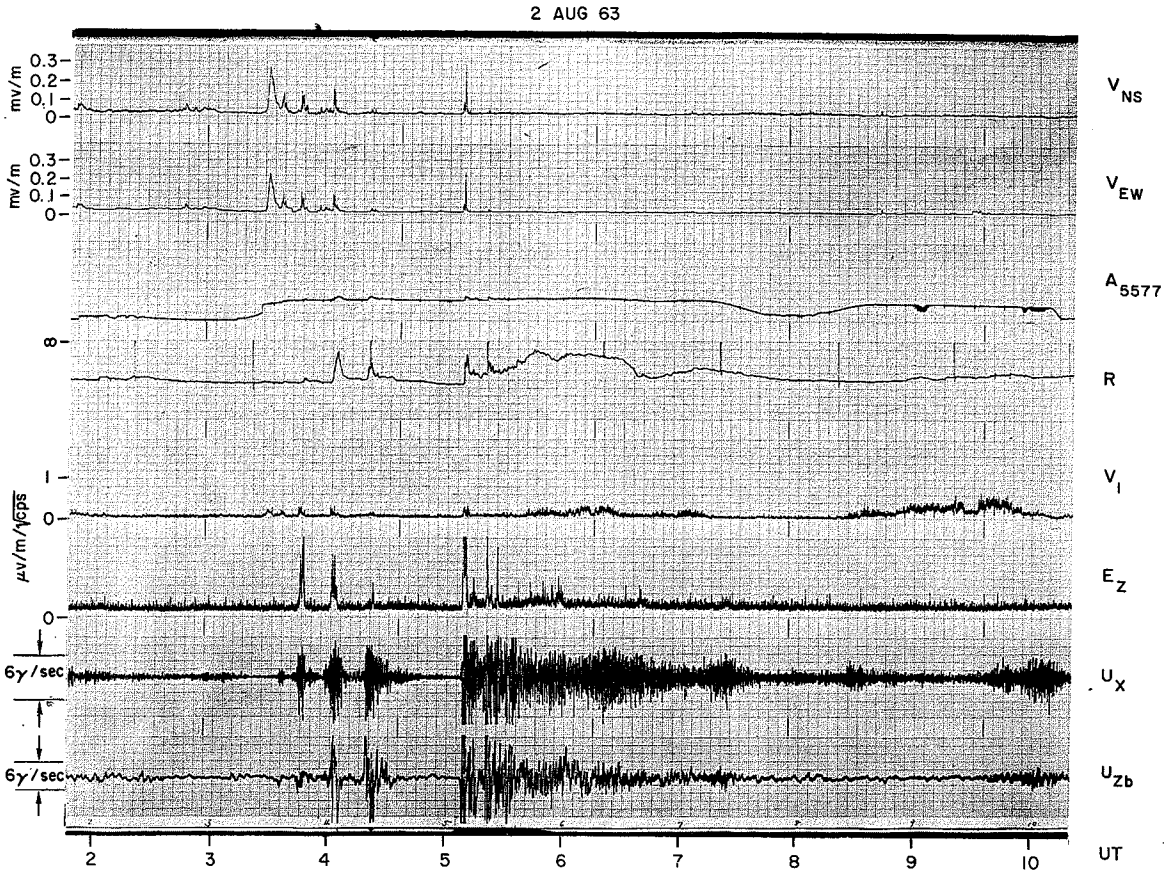

FIG. 62. AUGUST 2, 1963.

N-1	0325 - 0340	
N-2	0340 - 0425	0506 - 0515
N-3	0425 - 0450	0516 - 0800

There are three N-2 events between 0340 and 0425. The photometer output is saturated by moonlight. While the sign of dHz/dt is usually negative at the onset of N-2 (see Fig. 11), it may sometimes be positive at the beginning of an event. An example is shown at 0417.

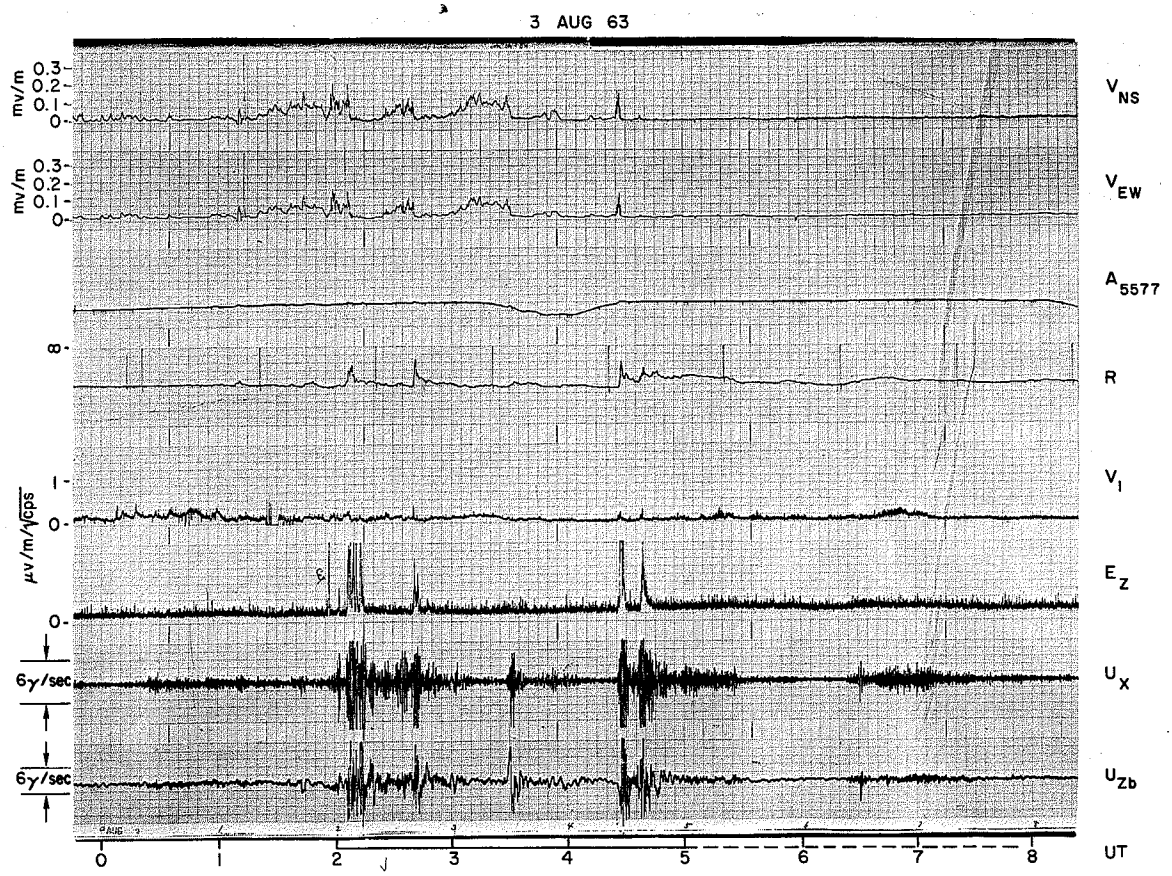

FIG. 63. AUGUST 3, 1963.

N-1	0055 - 0153			
N-2	0200 - 0219	0238 - 0250	0425 - 0434	
N-3			0455 - 0530	0620 - 0735

The entire photometer record is saturated by moonlight.

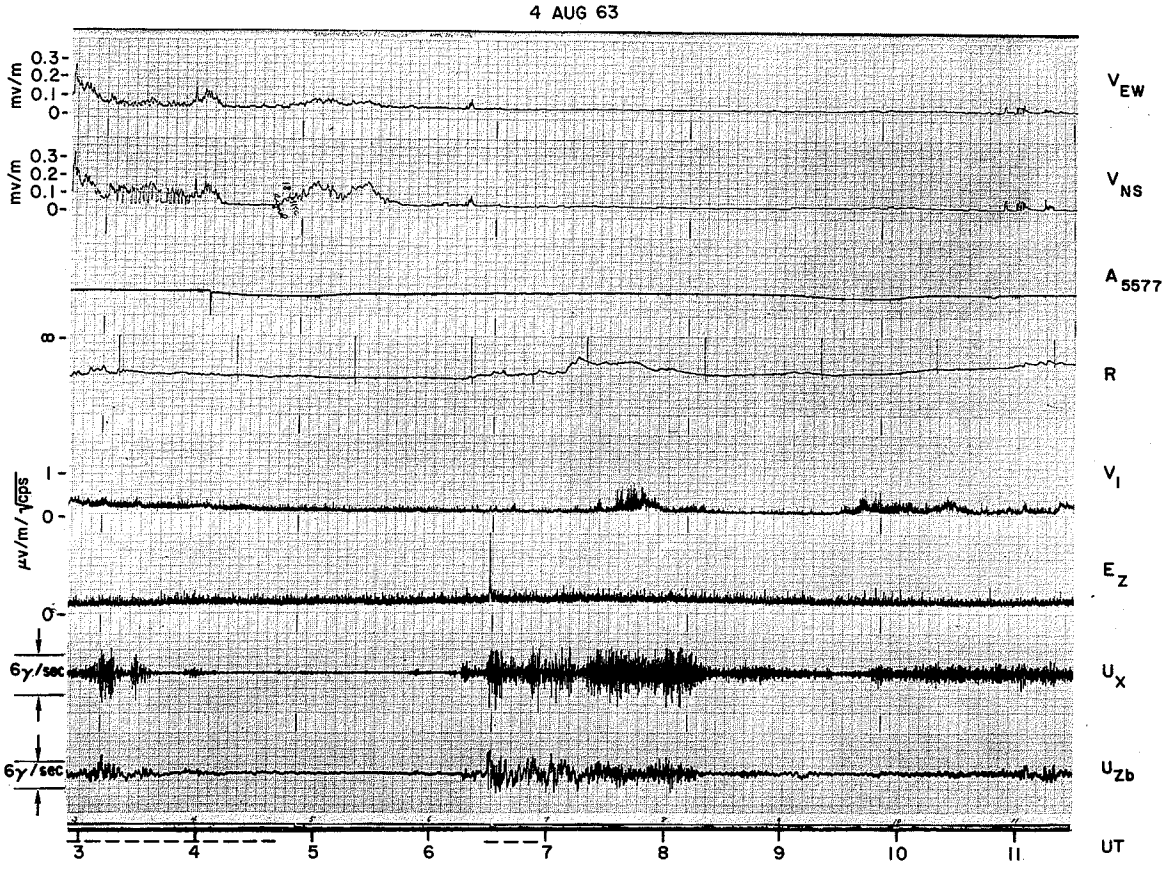

FIG. 64. AUGUST 4, 1963.

N-3 0613 - 0825

The N-3 event here is difficult to classify. The onset of this event is similar to N-2. Note a hiss burst at about 0620.

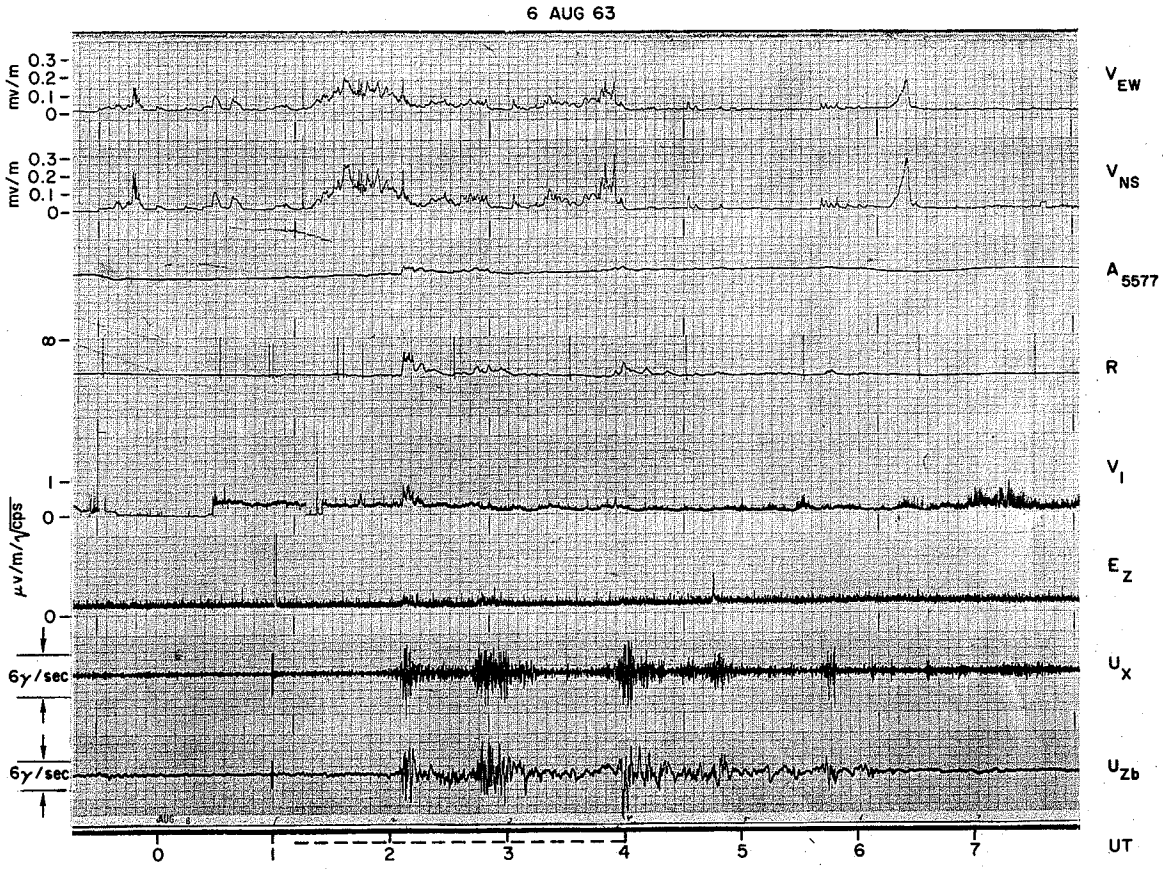

FIG. 65. AUGUST 6, 1963.

N-1	0108 - 0202	
N-2	0203 - 0220	0353 - 0425

Vlf hiss started at about 0108 and stopped at 0400.

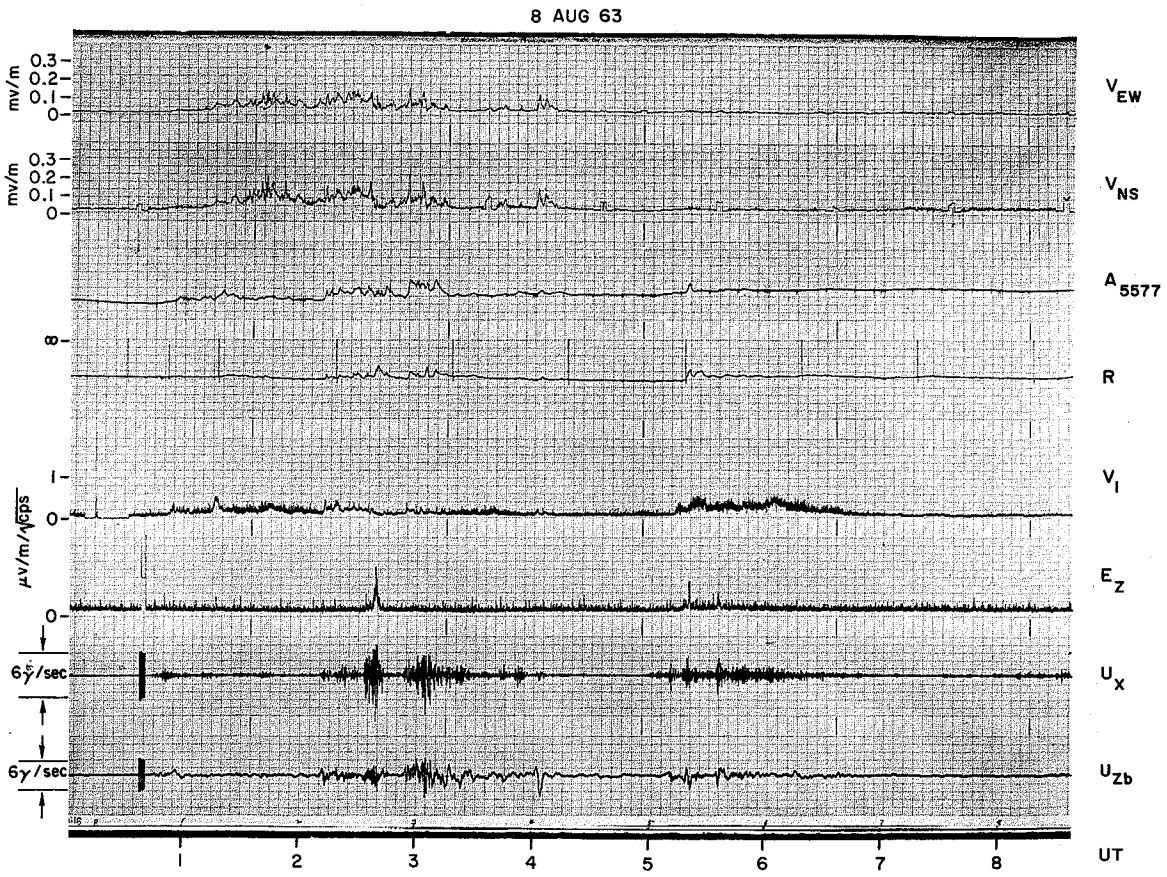

FIG. 66. AUGUST 8, 1963.

N-1 0045 - 0315
N-3 0500 - 0700

The event at 0240 exhibits some of the features of N-2. The polarity of dHz/dt is positive at 0255.

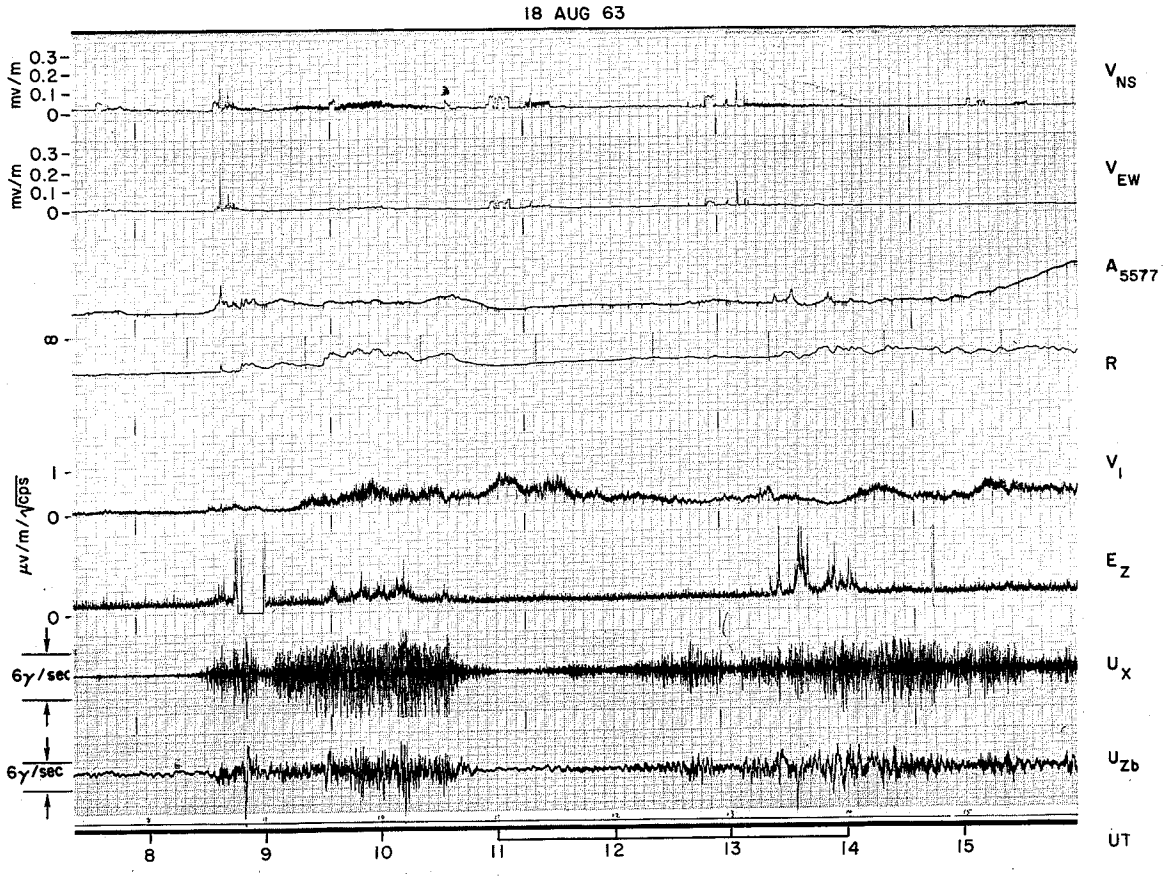

FIG. 67. AUGUST 18, 1963.

N-2	0830 - 0859	
N-3	0859 - 1100	
D		1300 on

After the hiss burst of 0837, the amplitude of the vlf transmitter signal received by the NS antenna increased. This record is unusual because aurora is still observable at about 1300 and even later. Sunlight interference begins near 1500 (0700 LMT). Auroral pulsations of periods less than 30 sec are seen between 1450 and 1520 UT.

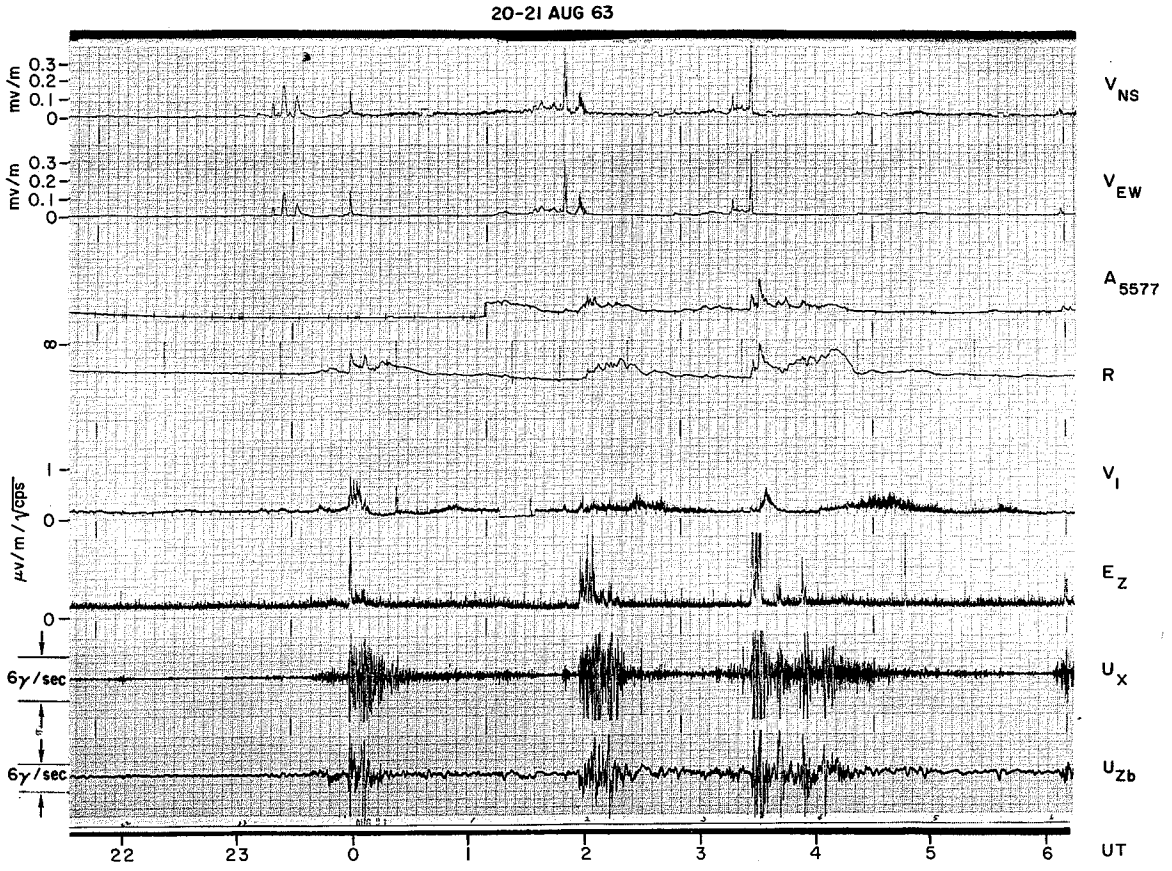

FIG. 68. AUGUST 20-21, 1963.

N-1	2310 - 2350	0130 - 0145	0255 - 0320
N-2	2355 - 0010	0145 - 0210	0321 - 0340
N-3	0010 - 0035	0210 - 0250	0340 - 0500

The amplitude variations of vlf 1 kc/s and the riometer channel are similar from about 2355 to 0005. The difference in behavior of vlf 1 kc/s and the broadband vlf hiss suggests that these two emissions are generated by different mechanisms. Note an increase in vlf 1 kc/s intensity after the cessation of vlf hiss.

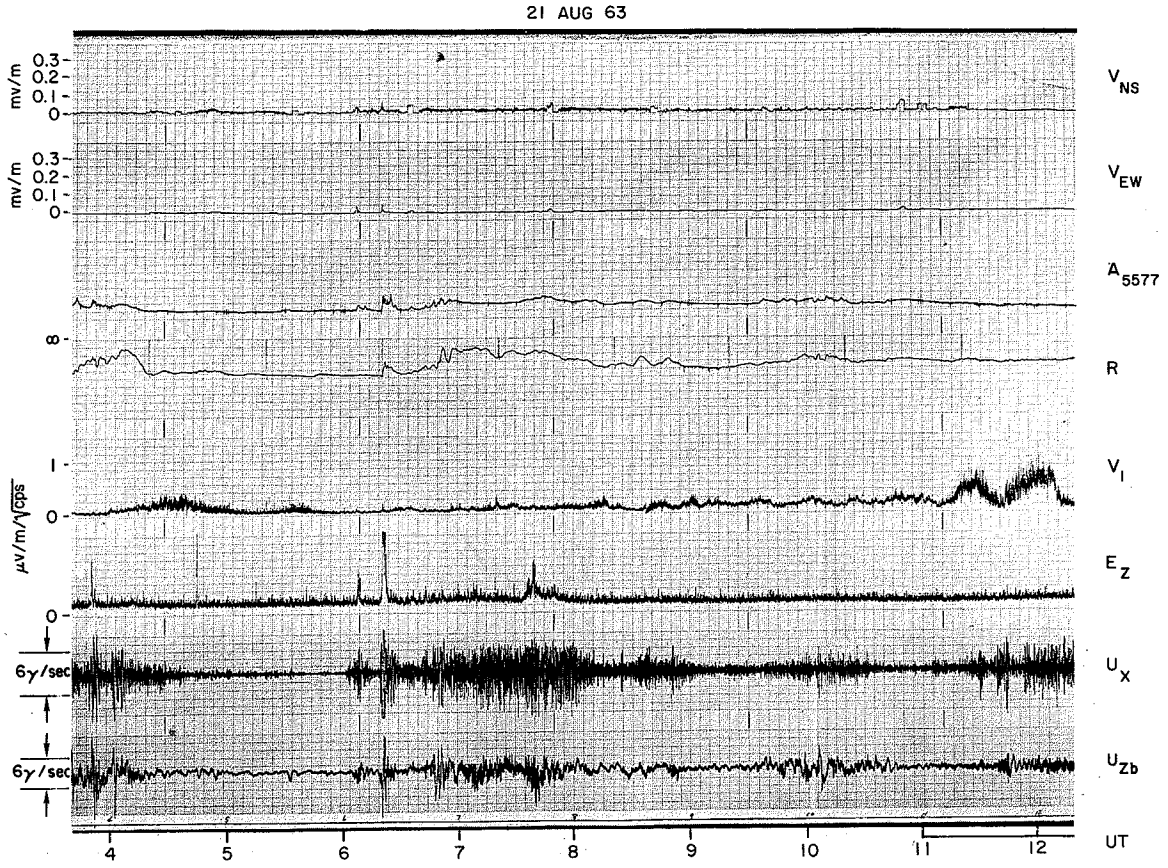

FIG. 69. AUGUST 21, 1963.

N-1	0600 - 0617
N-2	0618 - 0632
N-3	0633 - 0930

The magnitude of absorption in N-3 is much higher than in N-2. However, the auroral luminosity is relatively greater in N-2 than in N-3. In general, high frequency components of ulf, often up to the elf range, are observed more frequently in N-2 than in N-3.

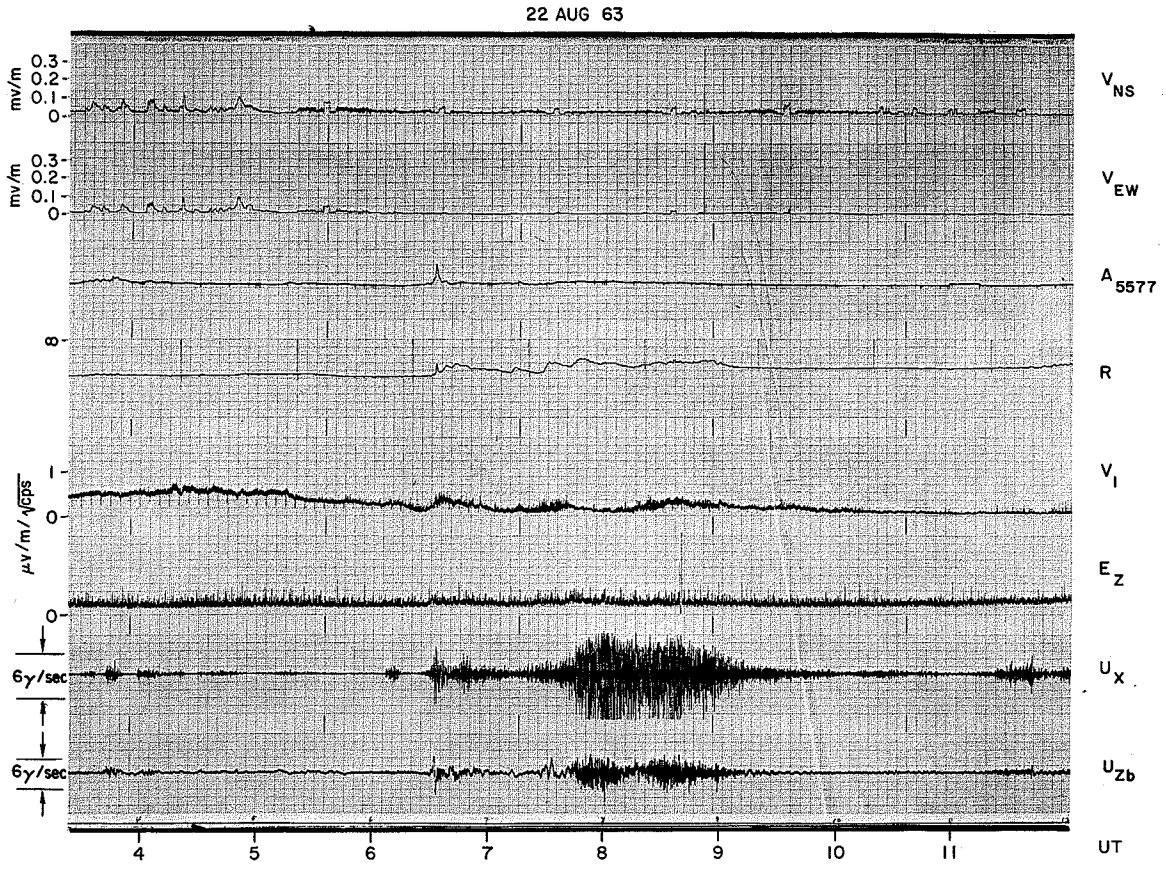

FIG. 70. AUGUST 22, 1963.

N-1	to ~ 0600	
N-2		0625 - 0700
N-3		0700 - 1000

N-2 and N-3 are well illustrated here.

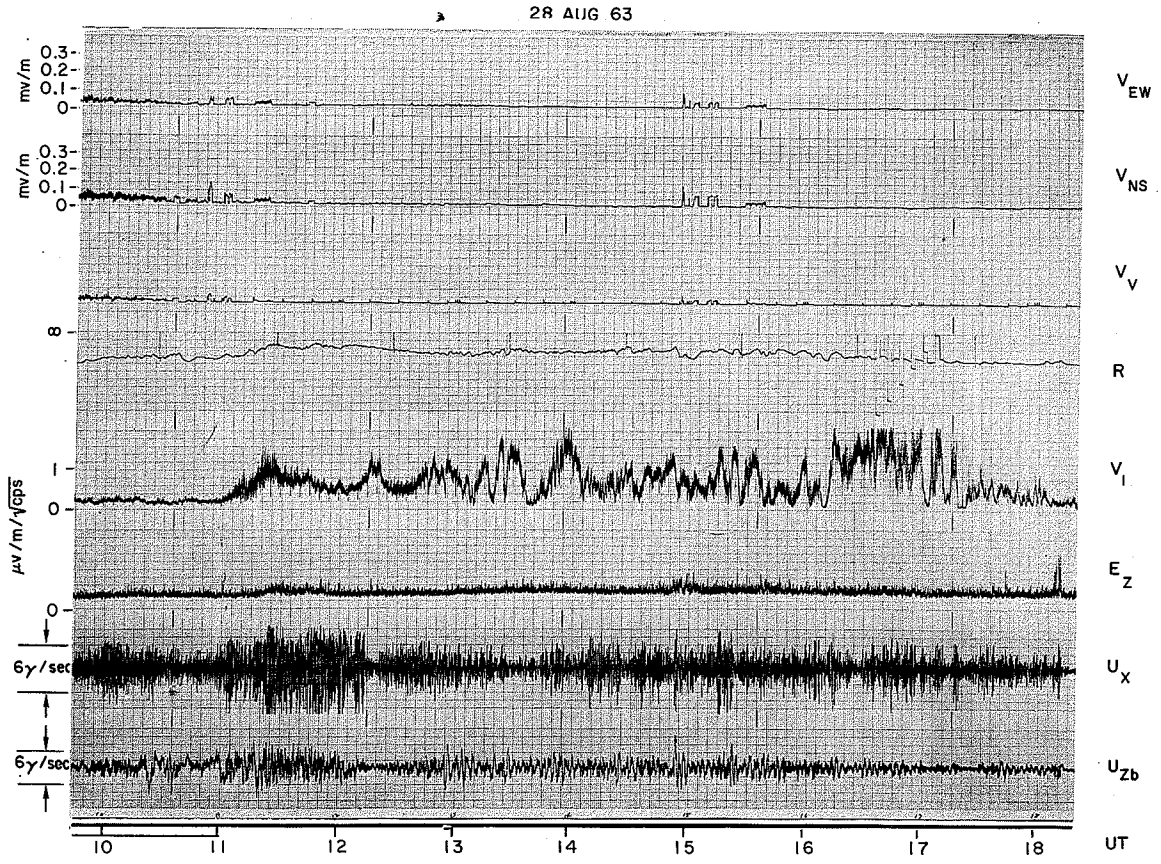

FIG. 71. AUGUST 28, 1963.

D throughout

A detailed examination indicated a high correlation between the phases of vlf 1 kc/s amplitude variations and riometer absorption. The magnitudes of the two types of events are not as highly correlated.

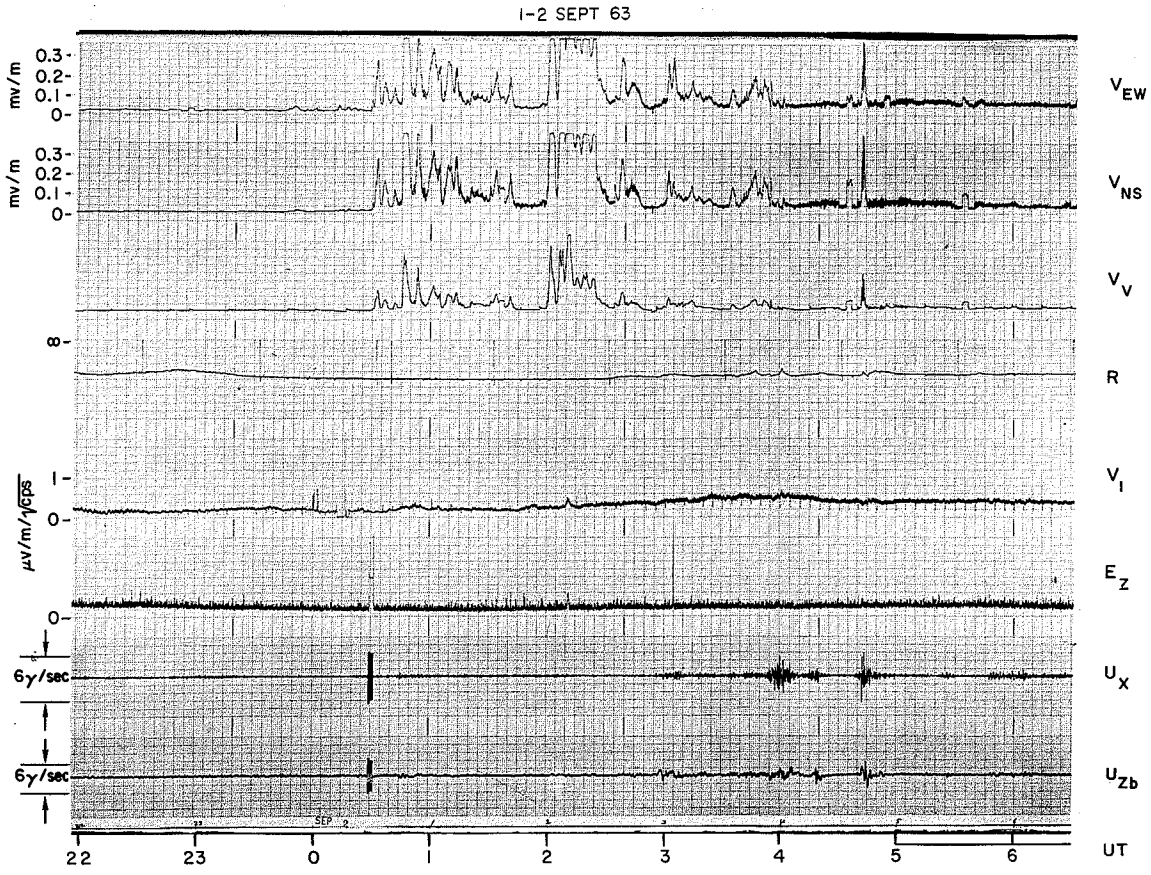

FIG. 72. SEPTEMBER 1-2, 1963.

N-1 0030 - 0430

Unusually intense hiss lasted for several hours. A peak power spectral density of 10^{-13}w/m^2/cps was recorded. Vlf transmitter signal strength increased with the onset of hiss.

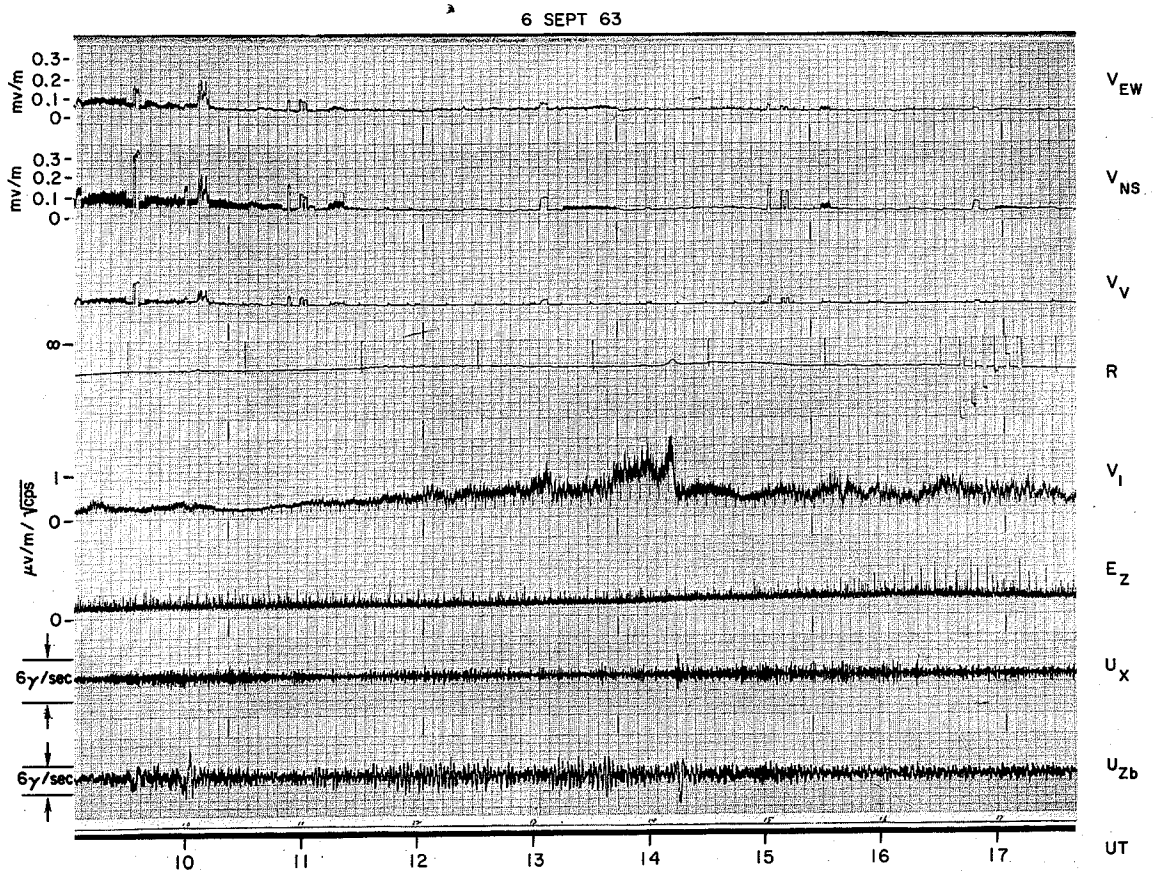

FIG. 73. SEPTEMBER 6, 1963.

D throughout

Note a sudden decrease of 1 kc/s vlf at about 1414. This type of decrease frequently occurs after about 1300 UT.

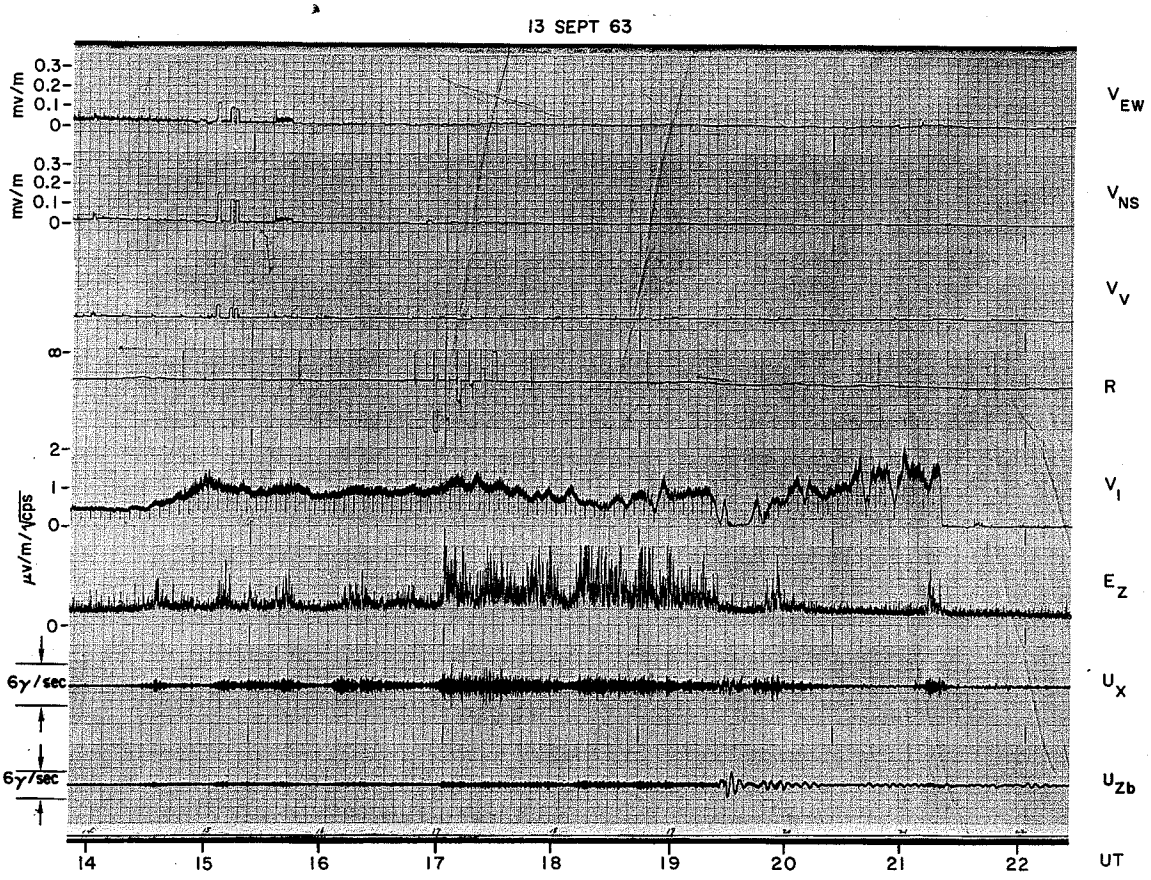

FIG. 74. SEPTEMBER 13, 1963.

D 1420 - 2122

Ionospheric absorption is low throughout. The elf bursts are unusual for this time of the day. Note a sudden decrease of vlf 1 kc/s at about 2120.

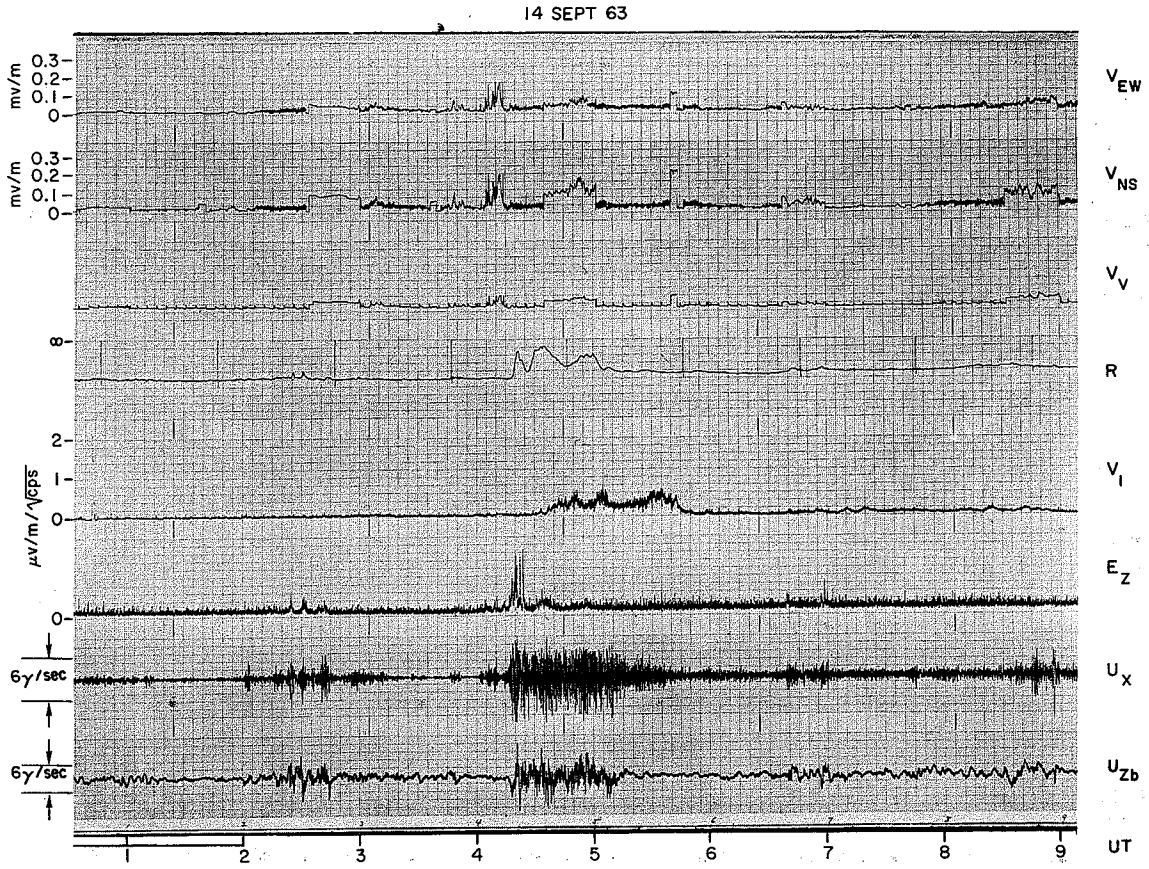

FIG. 75. SEPTEMBER 14, 1963.

N-1	0200 - 0310	0402 - 0413
N-2		0413 - 0430
N-3		0430 - 0550

Square-wavelike behavior on the broadband vlf channels represents vlf transmitter signals.

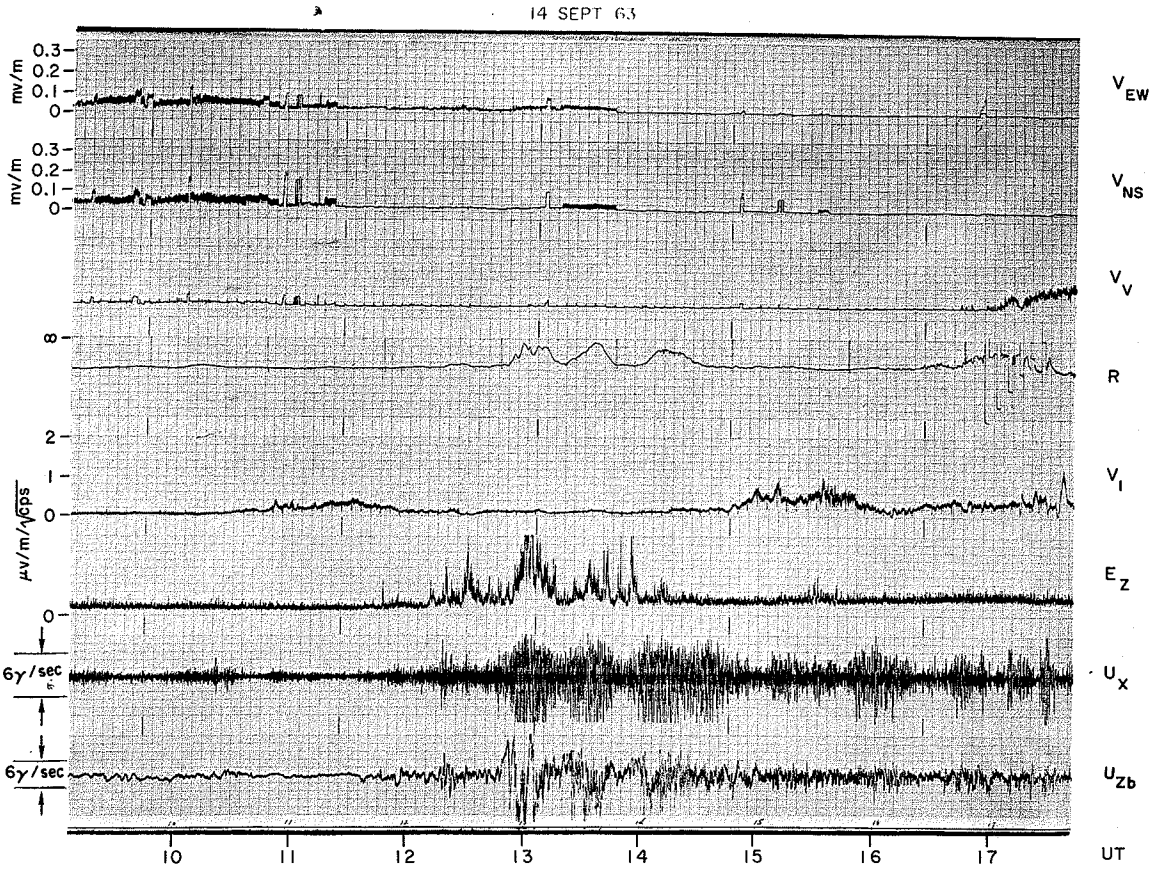

FIG. 76. SEPTEMBER 14, 1963.

D ~ 1200 on

The increase in vlf vertical signal strength at about 1650 is due to blowing snow. This phase D exhibits many properties which, during nighttime hours, would be classified as N-2 or N-3.

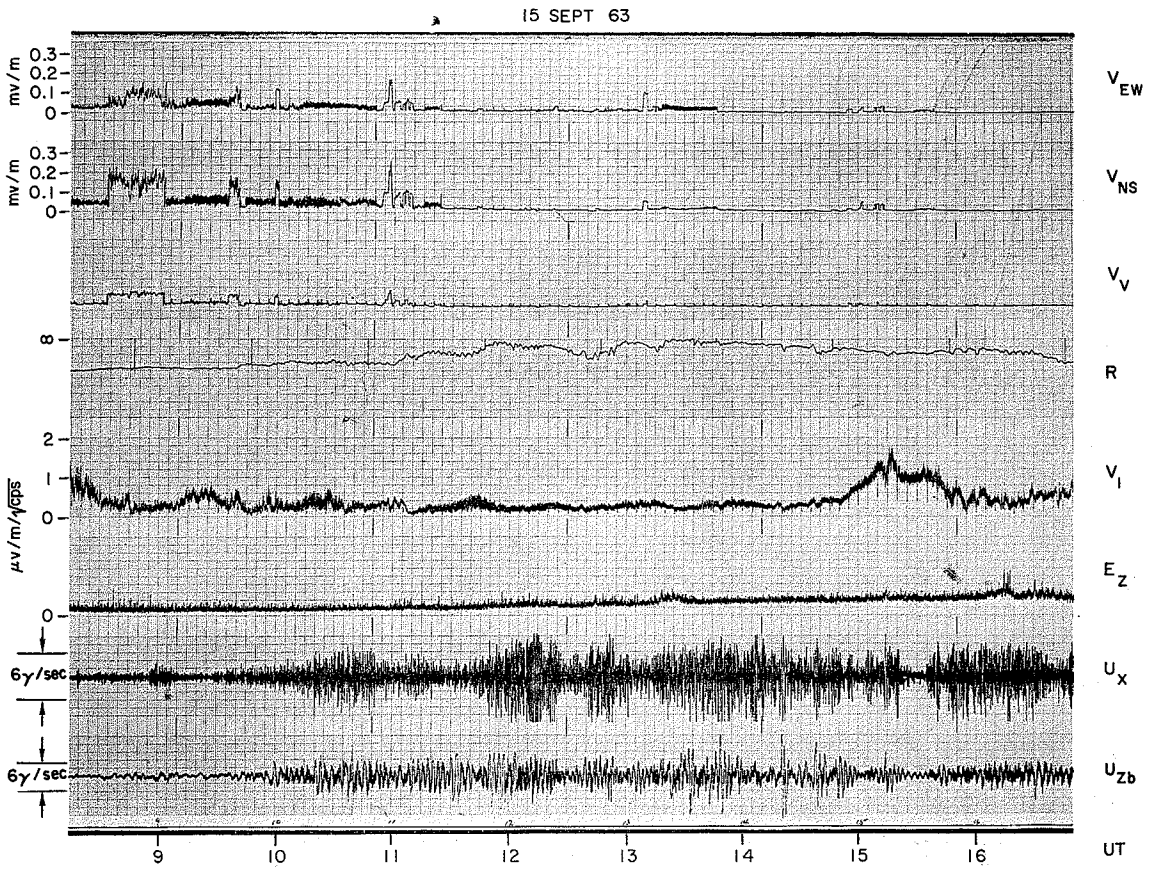

FIG. 77. SEPTEMBER 15, 1963.

D throughout

Ionospheric absorption was extremely high between 1100 and 1500. Very little association between this absorption and vlf chorus is seen here.

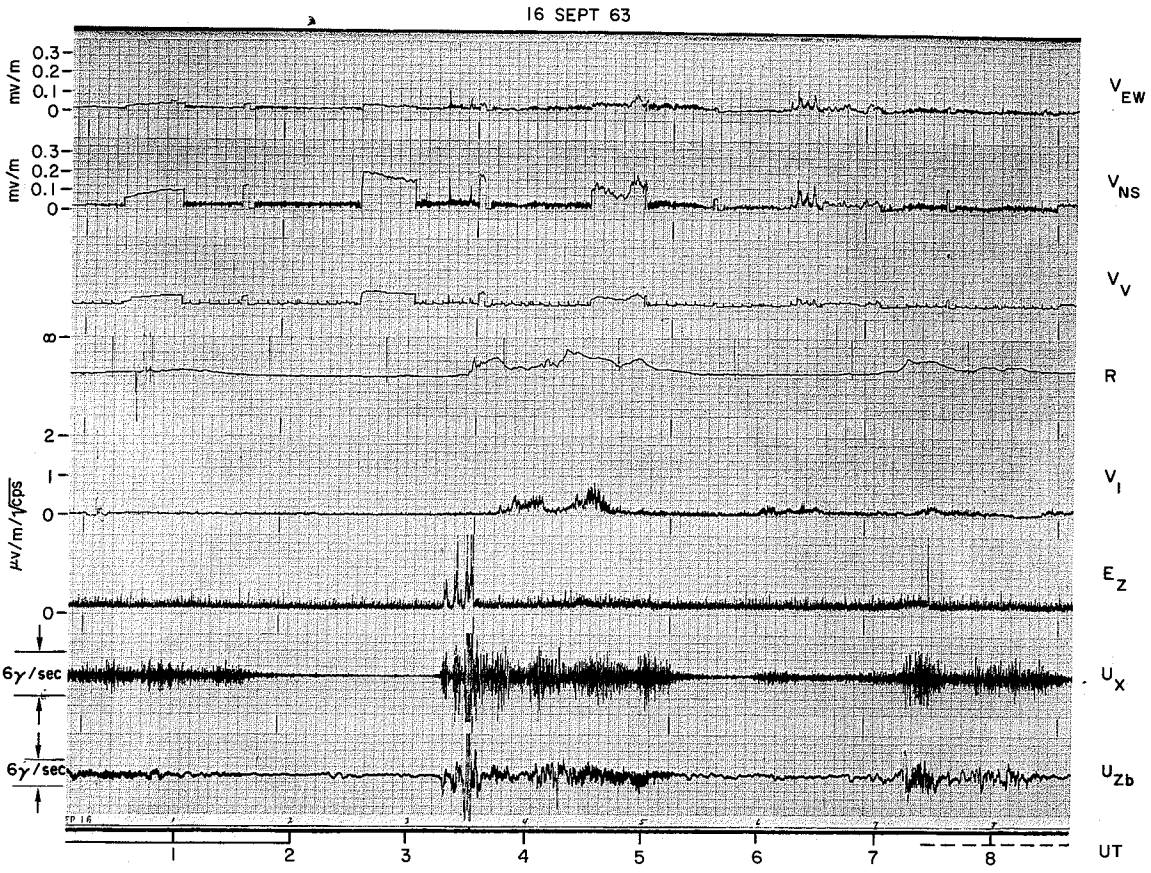

FIG. 78. SEPTEMBER 16, 1963.

N-2	0316 - 0350	
N-3	0350 - 0520	0712 - 0840

Square-wavelike signals represent fixed-frequency transmissions. Vlf 1 kc/s vlf and ionospheric absorption exhibit some similarities.

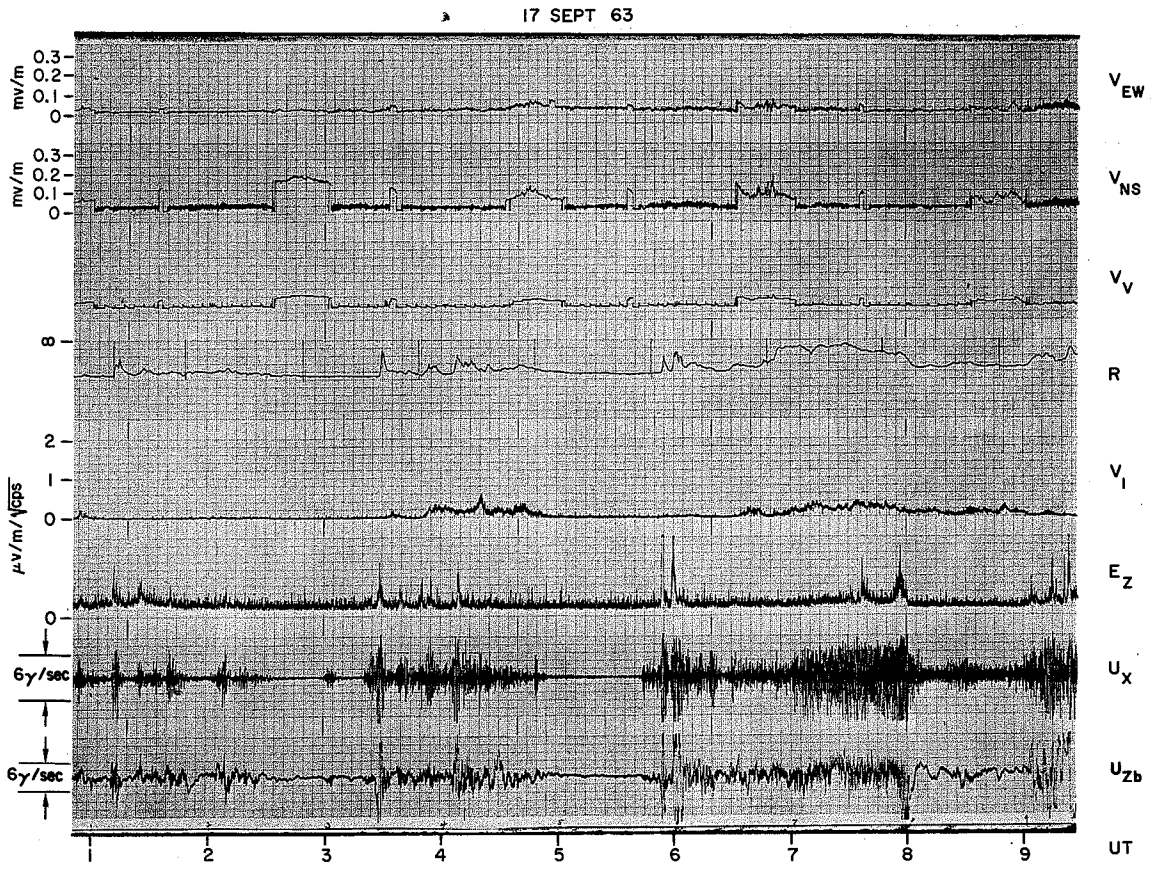

FIG. 79. SEPTEMBER 17, 1963.

N-2	0108 - 0118	0320 - 0334	0540 - 0625
N-3		0335 - 0500	0630 - 0810

A complex series of events.

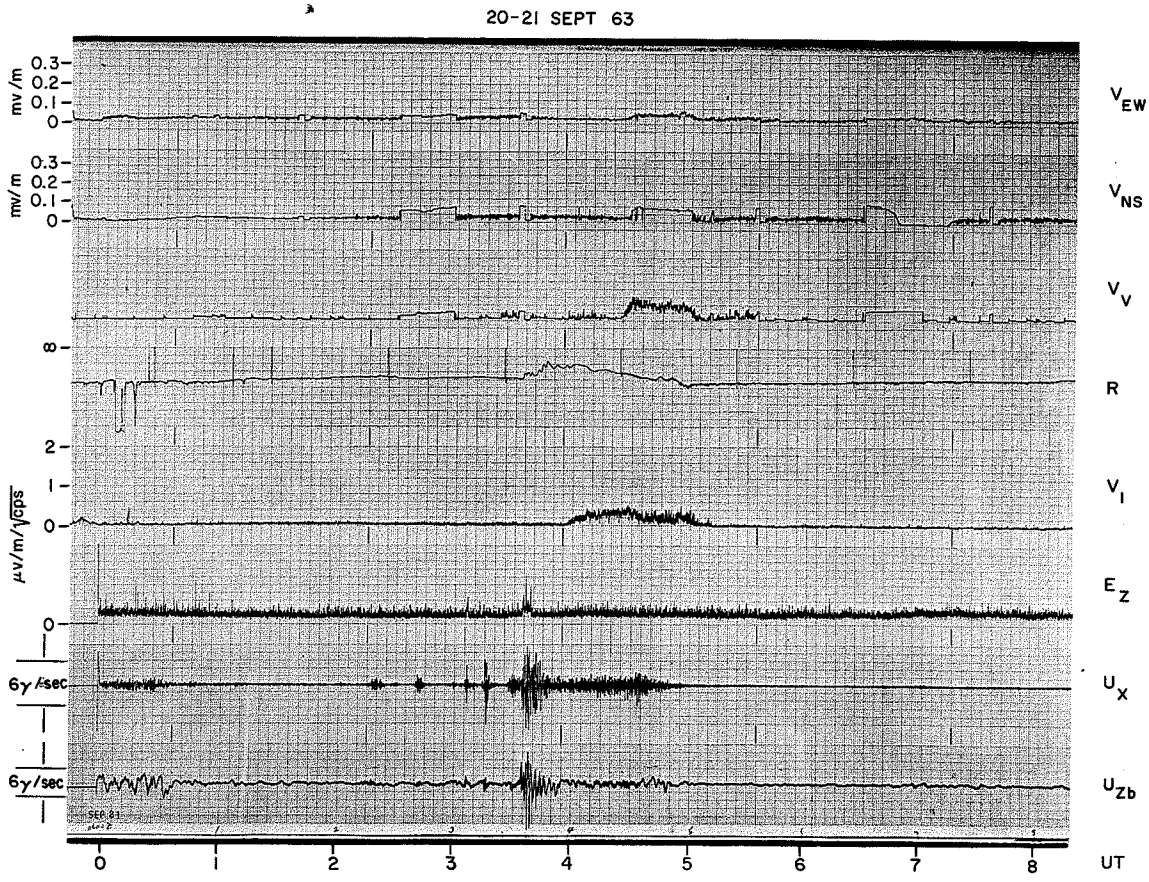

FIG. 80. SEPTEMBER 20-21, 1963.

N-1	0215 - 0330
N-2	0334 - 0345
N-3	0345 - 0515

The spike in the riometer channel at 0006 is probably due to a solar flare. A similar spike is observed at 0016.

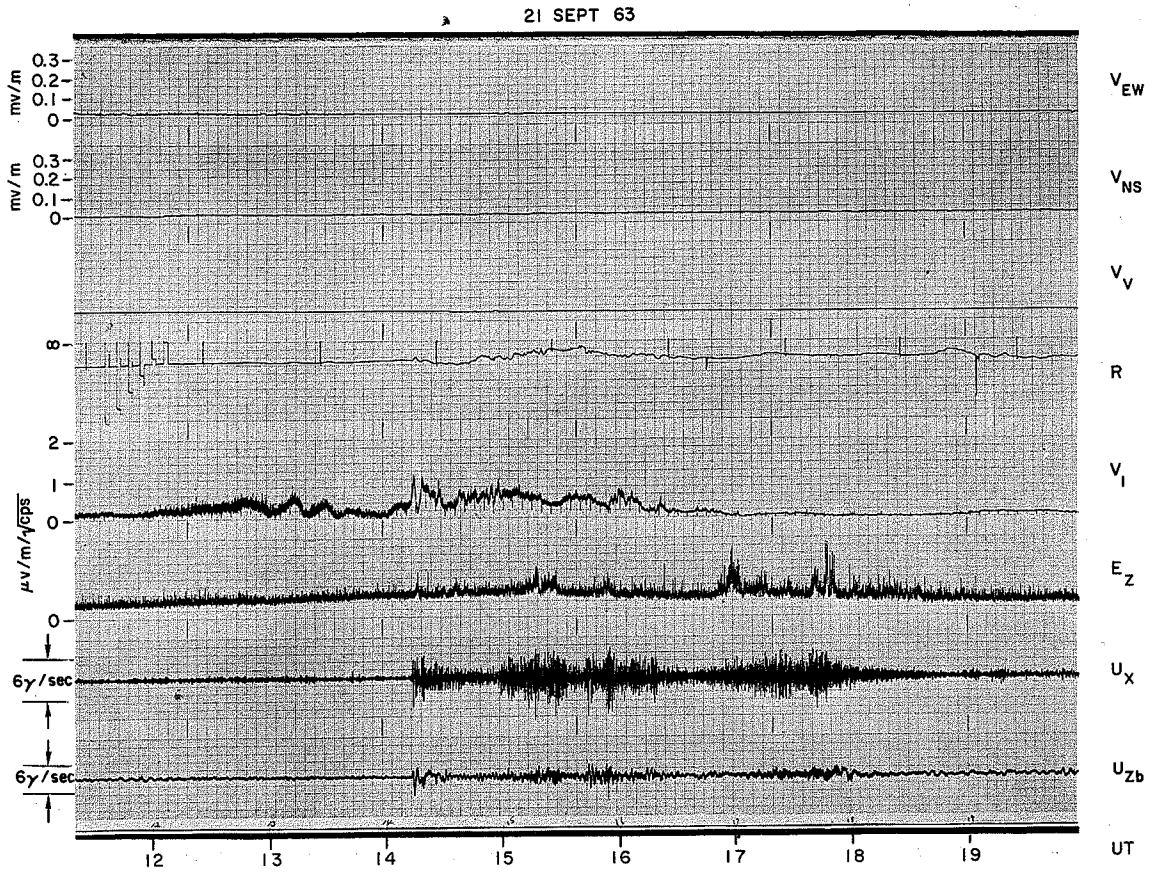

FIG. 81. SEPTEMBER 21, 1963.

D 1410 - 1850

A close phase relation is exhibited between the 1 kc/s vlf and riometer absorption. This phenomenon was also observed at Eights simultaneously. This event is an SC.

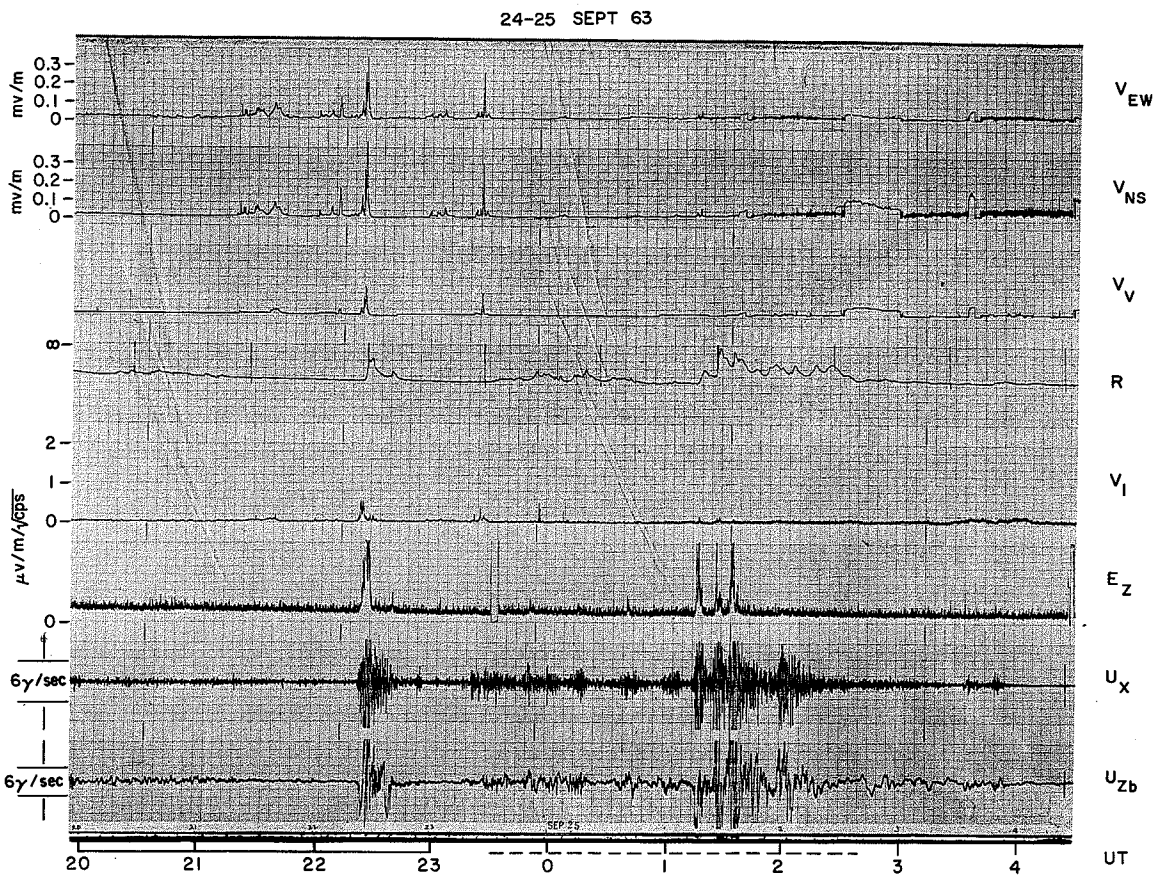

FIG. 82. SEPTEMBER 24-25, 1963.

N-1	2118 - 2219		
N-2	0220 - 2245	2320 - 2348	0112 - 0140
N-3			0140 - 0240

There are three N-2 events in the period 0012 - 0140.

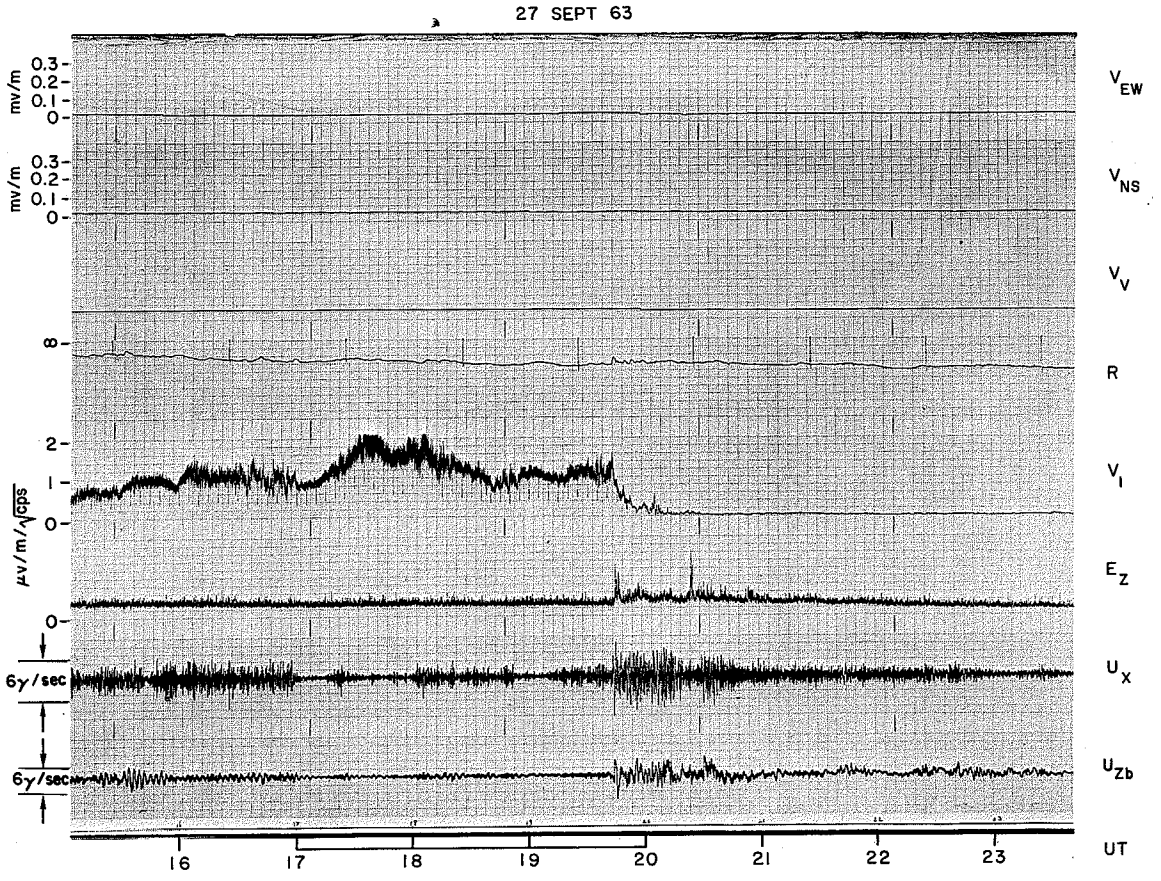

FIG. 83. SEPTEMBER 27, 1963.

D throughout

One of the interesting features of D events is an abrupt end vlf 1 kc/s chorus. An example of this occurs at 1942. After the cessation of chorus, elf, ulf, and riometer events are frequently observed [Morozumi, 1966].

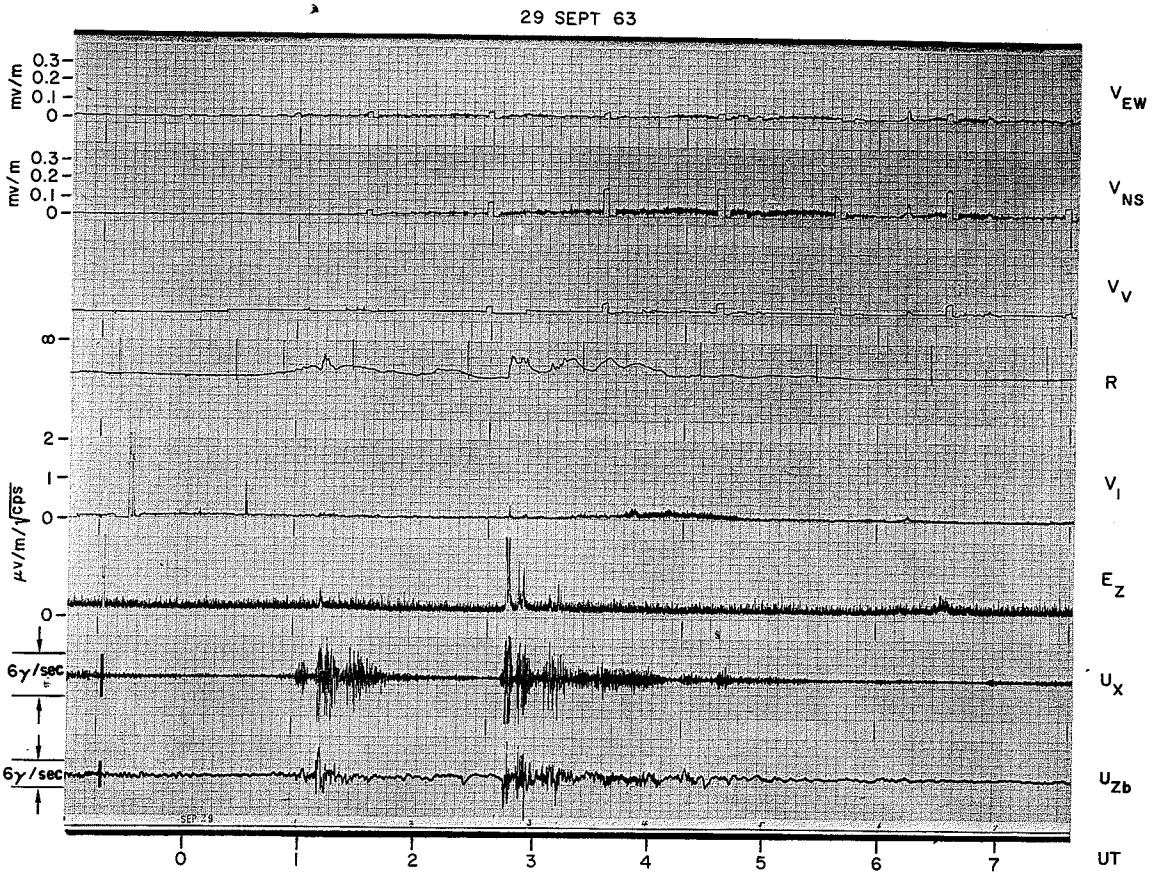

FIG. 84. SEPTEMBER 29, 1963.

N-1	0055 - 0108	
N-2	0108 - 0122	0143 - 0330
N-3	0122 - 0145	0330 - 0455

Note an increase in vlf transmitter signal strength after the onset of the N-1 event.

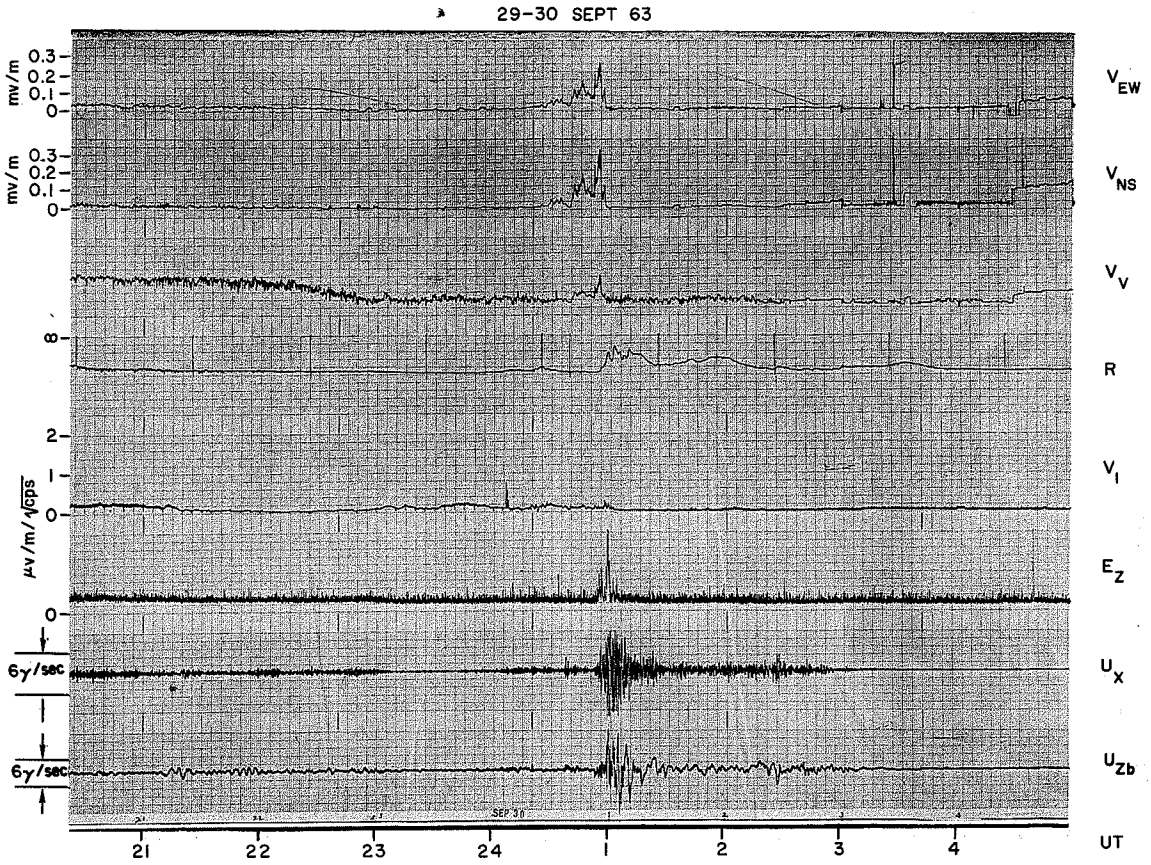

FIG. 85. SEPTEMBER 29-30, 1963.

N-1	2355 - 0052
N-2	0052 - 0123
N-3	0123 - 0300

The fluctuating signal seen on the vertical vlf channel is wind noise.

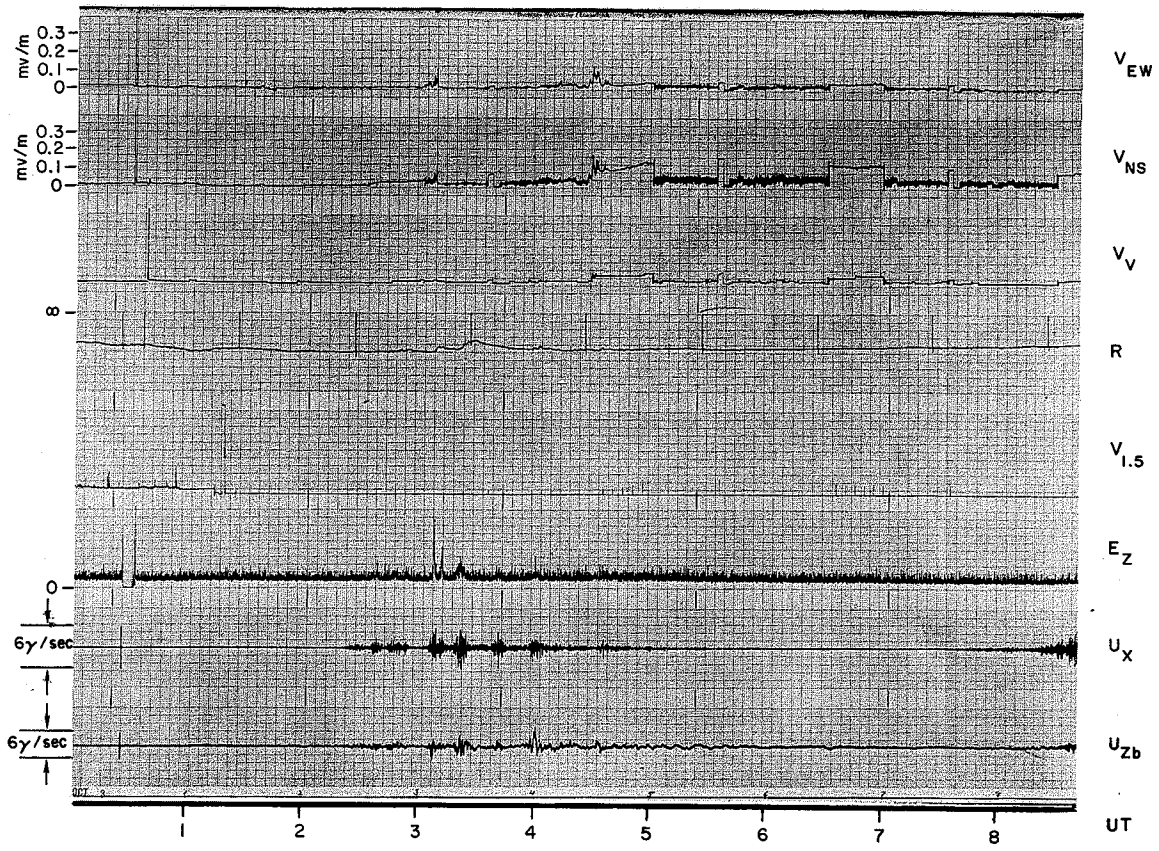

FIG. 86. OCTOBER 3, 1963.

N-1 0225 - 0255
N-2 0307 - 0500

Several N-2 events occurred between 0307 and 0500. Note an increase in the vlf transmitter signals after the hiss at 0307.

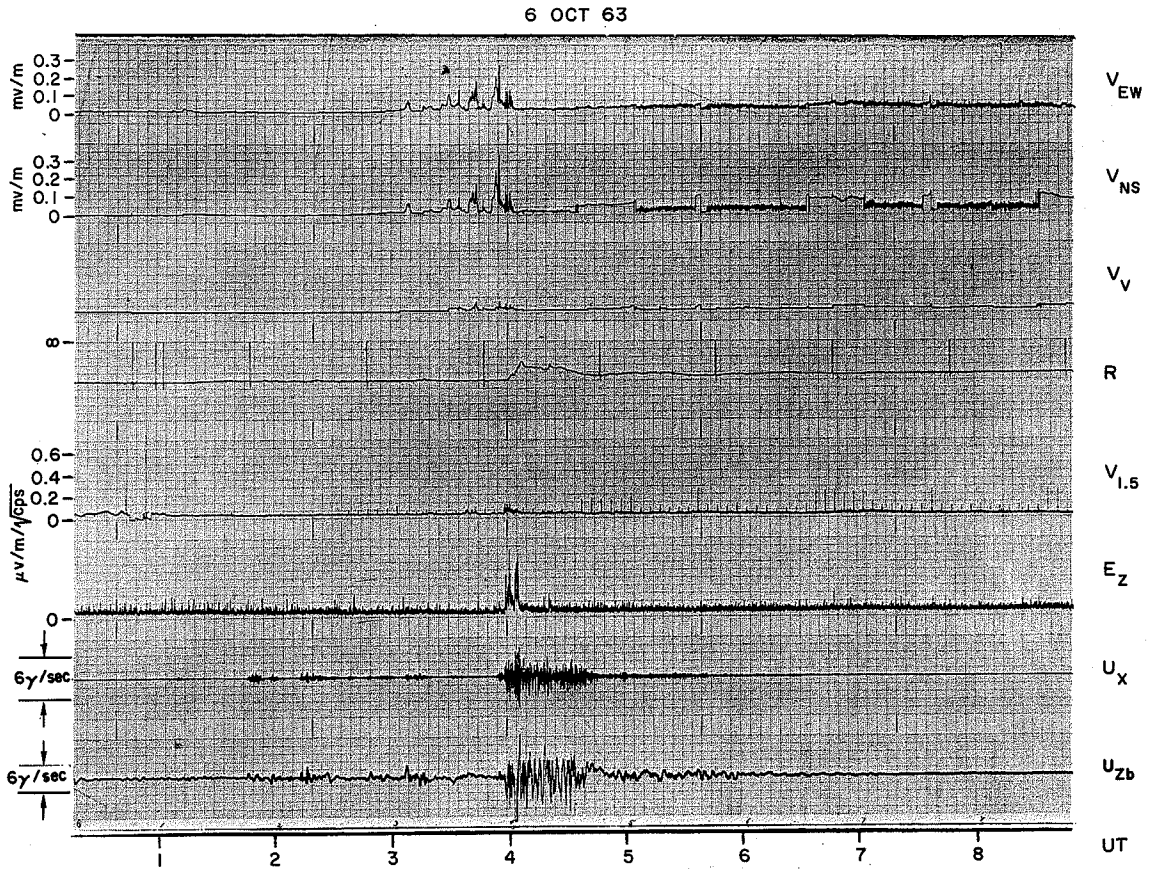

FIG. 87. OCTOBER 6, 1963.

N-1	0142 - 0345
N-2	0352 - 0407
N-3	0407 - 0530

An increase in vlf transmitter signals is seen after the N-2 event.

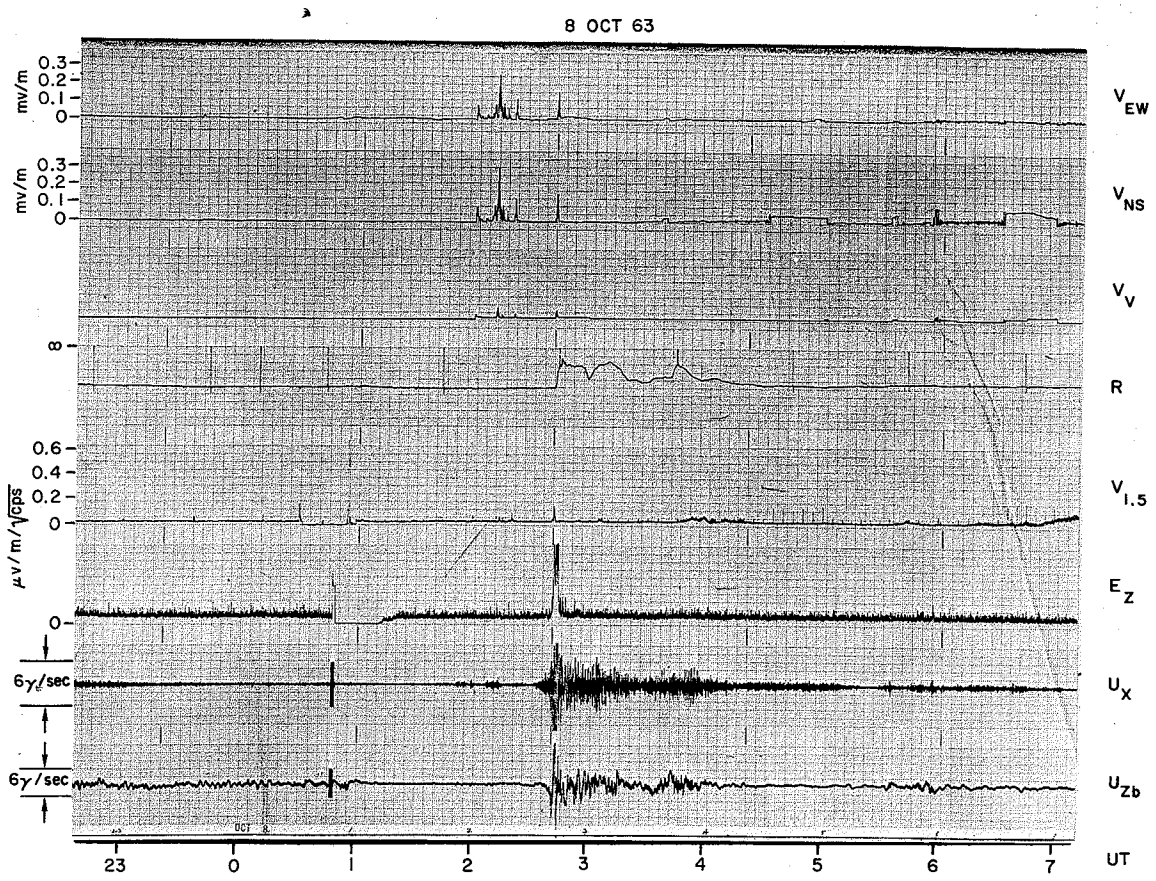

FIG. 88. OCTOBER 8, 1963.

N-1	0155 - 0215	
N-2		0232 - 0247
N-3		0247 - 0430

Ulf shows a gradual commencement about 10 minutes prior to the onset of hiss bursts and riometer absorption at 0241.

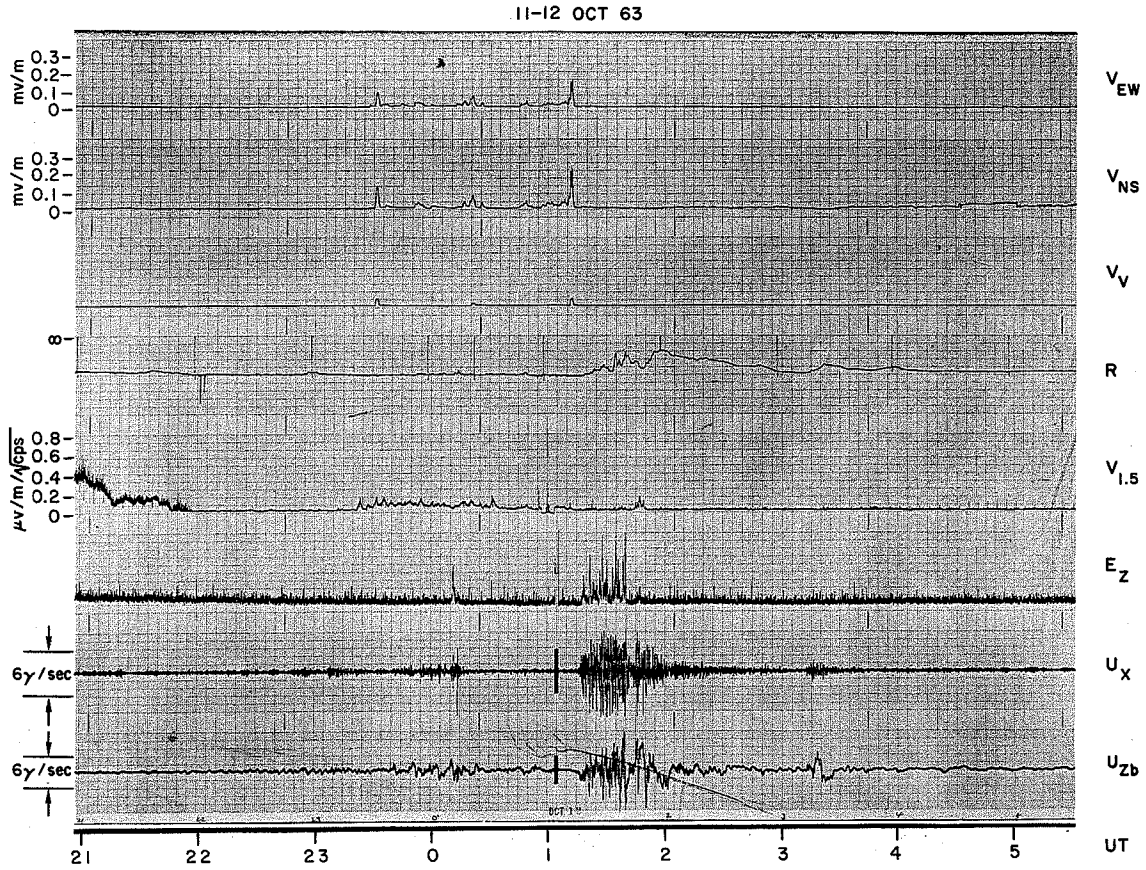

FIG. 89. OCTOBER 11-12, 1963.

N-1	2328 - 0108
N-2	0109 - 0143
N-3	0143 - 0300

The ulf activity during N-2 has an entirely different spectrum than that observed in N-3 (compare E_z and U_x).

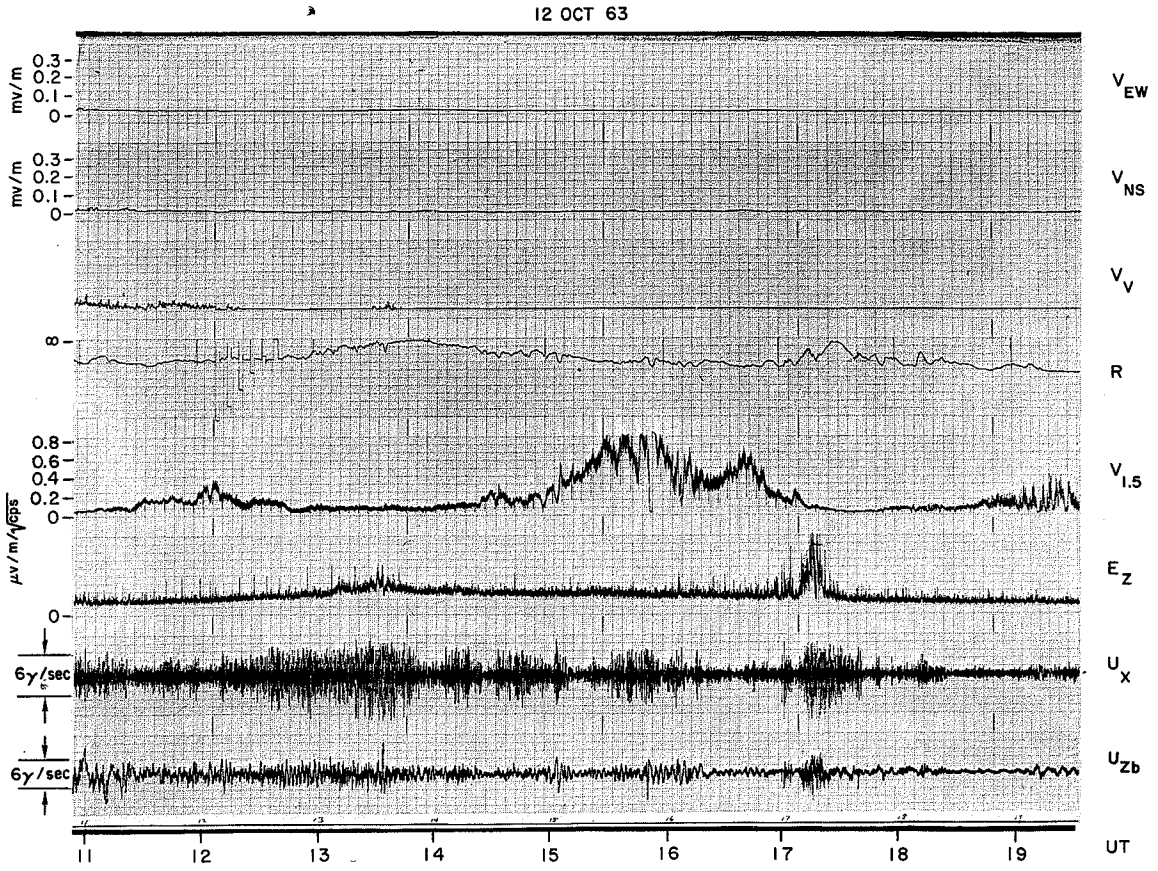

FIG. 90. OCTOBER 12, 1963.

D throughout

Many of the small variations in 1.5 kc/s vlf are in phase with riometer absorption. The best example is seen at 1549.

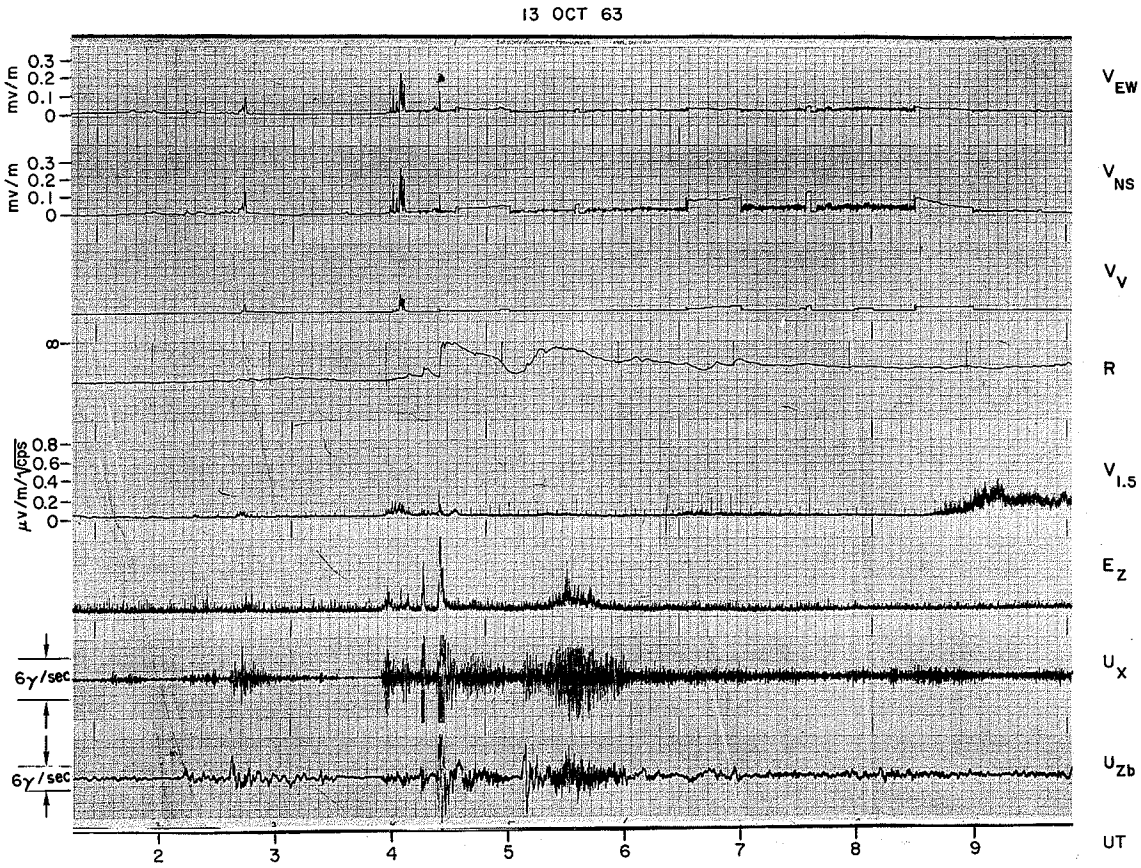

FIG. 91. OCTOBER 13, 1963.

N-1	0212 - 0330*
N-2	0352 - 0500
N-3	0508 - 0710

There are several small N-2 events during the time interval between 0352 - 0500. The polarity of dHz/dt near the beginning of the N-3 event is positive.

*Not a duration of a single N-2.

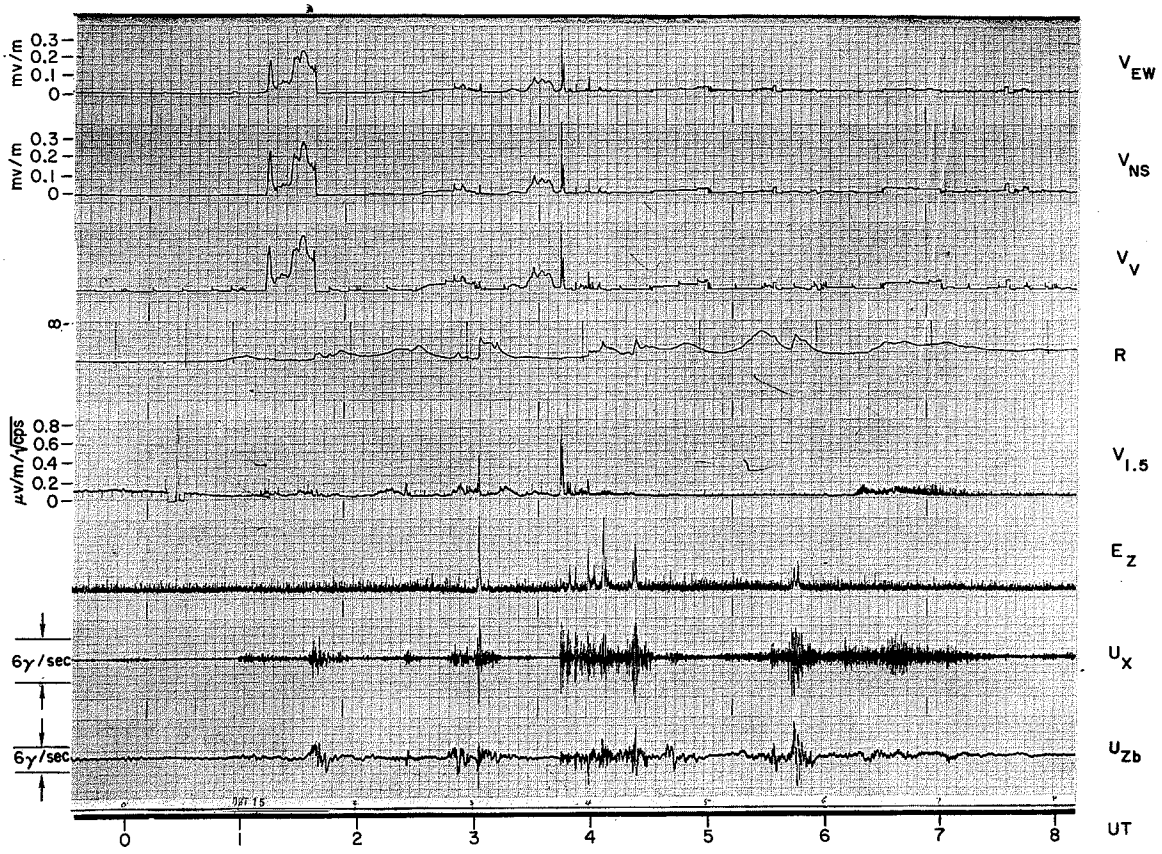

FIG. 92. OCTOBER 15, 1963.

N-1	0112 - 0138		
N-2	0130 - 0150	0301 - 0315	0342 - 0500
N-3			0500 - 0730

The sudden decrease of hiss intensity at 0130 is very closely associated with the commencement of riometer and ulf events. The magnitudes of the signals received by the EW and NS antennas are about the same for the impulsive event.

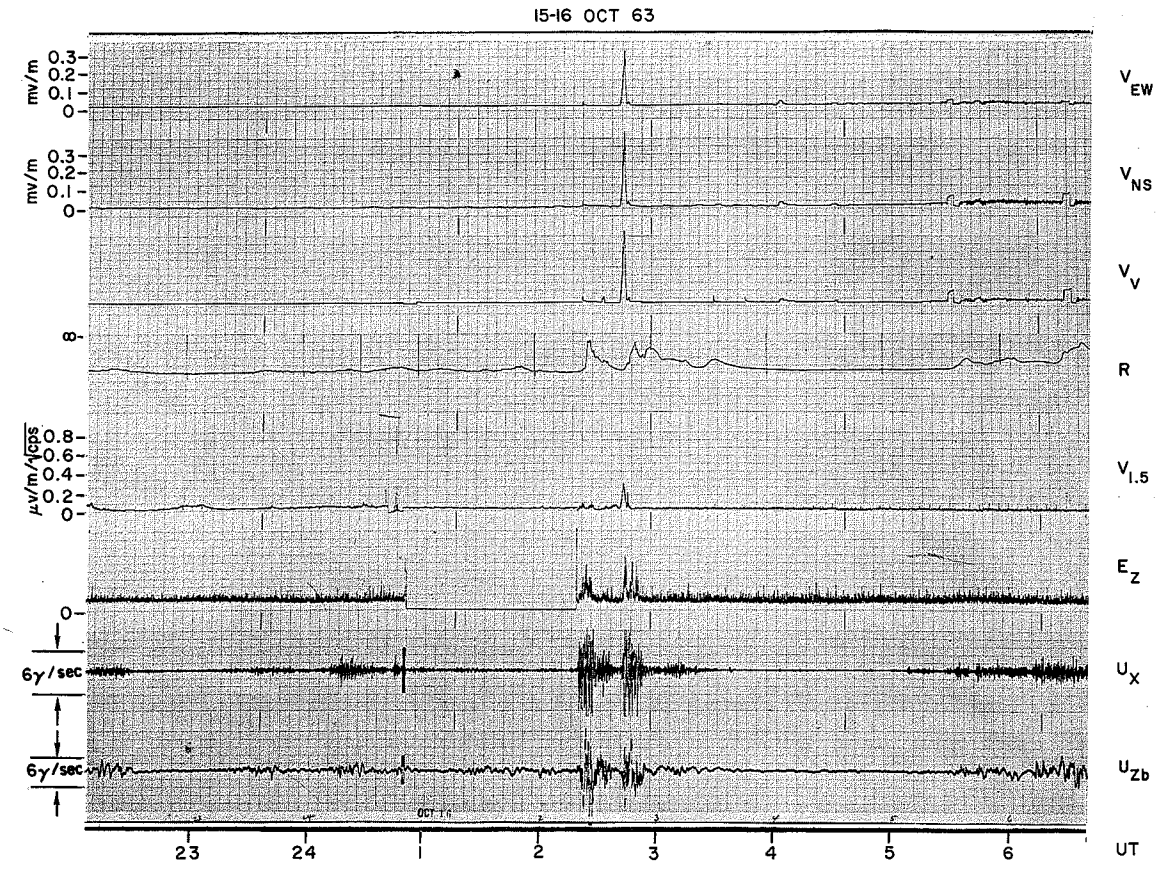

FIG. 93. OCTOBER 15-16, 1963.

N-2	0217 - 0237	0237 - 0254	
N-3		0300 - 0345	0530 on

There are two N-2 events between 0200 and 0300. During these events the ulf, elf, and riometer channels exhibit similar trends. There is a great difference in the magnitude of vlf hiss in the two events.

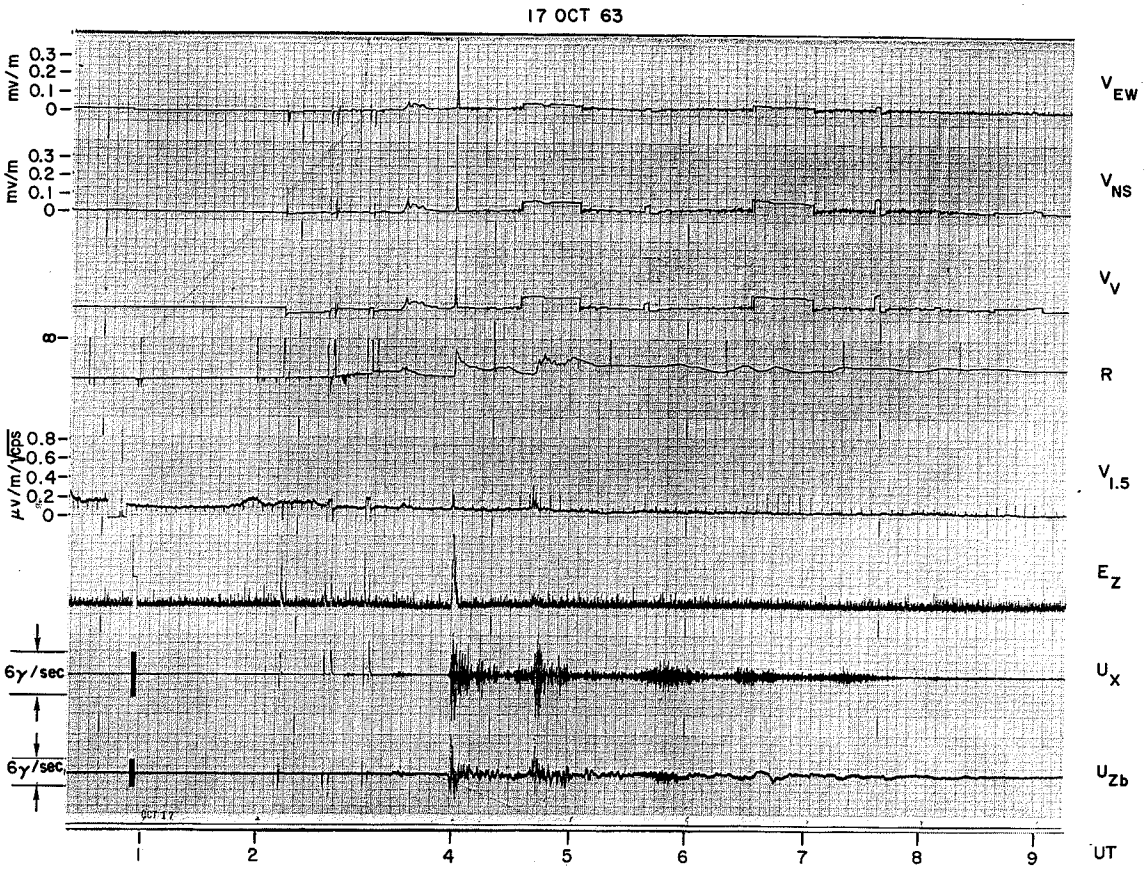

FIG. 94. OCTOBER 17, 1963.

N-1	0327 - 0345
N-2	0356 - 0410
N-3	0435 - 0800

A series of power failures made time marks between 0200 and 0320 uncertain.